UNIVERSITÀ DEGLI STUDI DI URBINO CARLO BO

Department of Biomolecular Sciences (DISB)

Ph.D. programme in: Biomolecular and Health Sciences

CYCLE: XXXVIII

Characterization of POXAPy-macrocycle molecule activity in acute promyelocytic leukemia NB4 cells

ACADEMIC DISCIPLINE: MEDS-26/A

Coordinator: Prof. Ferdinando Mannello

Supervisor: Prof. Stefano Amatori

Co-Supervisor: Prof. Mirco Fanelli

Ph.D. student: Enrica Sordini

ACADEMIC YEAR

2024/2025

TABLE OF CONTENTS

ABSTRACT

In the last years, macrocyclic polyamines gained attention as anticancer agents in consequence of their unique properties such as improved bioavailability, binding affinity, and favorable pharmacokinetics profiles. Similarly, compounds containing 1,3,4-oxadiazole rings showed main biological properties, including potential antitumor activities. Based on this evidence, new polyamine macrocycle molecules containing 1,3,4-oxadiazole rings were synthesized, leading to the selection of a molecule named POXAPy-macrocycle, showing the ability to reduce the survival of cancer cells at micromolar concentrations.

The molecule was tested against a panel of 60 cell lines encompassing tumors of different origins, indicating a selectivity against hematopoietic tumors, with the promyelocytic leukemia NB4 cell line being the most sensitive. Thus, the effects of the molecule were investigated at the molecular level by integrating transcriptome and proteome profiling of POXAPy-macrocycle-treated NB4 cells. This approach led to the identification of mTOR signaling as the most significantly affected pathway. mTOR signaling inhibition plays a main role in autophagy and has been recently proposed as a new potential target in different kinds of tumors. mTOR inhibition was confirmed by analyzing its phosphorylation by Western blotting, and the activation of autophagy was also evaluated, confirming the increased expression of main autophagic markers such as LC3B and p62. Due to its role in autophagy and its interplay with mTOR signaling, the MAPK/ERK pathway was also investigated, showing the reduction of ERK phosphorylation. Transmission electron microscopy (TEM) showed mitochondria alteration and their engulfment in autophagic vesicles, suggesting the activation of mitophagy and indicating the mitochondrion as a target of POXAPy-macrocycle activity.

Finally, in a preliminary attempt to elucidate the mechanism through which POXAPy macrocycle exerts its biological activity, and considering the known ability of structurally related molecules to interact with DNA G-quadruplex (G4) structures, the interaction between the POXAPy macrocycle and specific G4-forming DNA sequences was investigated. In cell-free assays, POXAPy displayed a strong and selective affinity for specific G4 structures. However, this observation was not confirmed in cell-based models, leaving open the possibility that such interaction may occur in the cellular context and suggesting that additional mechanisms of action might be involved. Although further

studies are required to elucidate the molecular mechanisms underlying its activity, the present findings identify POXAPy macrocycle as a promising antitumor candidate.

ABBREVIATIONS

AML	Acute Myeloid Leukemia
FBS	Fetal Bovine Serum
GSEA	Gene Set Enrichment Analysis
NCI	National Cancer Institute
NIH	National Institute of Health
RCF	Relative Centrifugal Force
PCA	Principal Component Analysis
SD	Standard Deviation
WB	Western Blot
TEM	Transmission Electron Microscopy
ROS	Reactive Oxygen Spices
FDA	Food and Drug Administration
MDS	Multidimensional Scaling
MSigDB	Molecular Signatures Database
DEG	Differentially Expressed Genes
DEP	Differentially Expressed Proteins
FDR	False Discovery Rate
DCFDA	Dichlorofluorescin Diacetate
G4	G-quadruplexes
PDS	Pyridostatin
IF	Immunofluorescence
PCR	Polymerase Chain Reaction

INTRODUCTION

For almost a century, cytotoxic chemotherapeutics together with surgical operation, radiotherapy and biotherapy constitute the main approaches to cancer treatment. Over the past two decades, there has been a tremendous shift in cancer treatment, from broad-spectrum cytotoxic drugs to targeted drugs (Bedard et al., 2020). Among them, the Food and Drug Administration (FDA) has approved a bunch of macrocyclic drugs to treat cancer patients. The importance of such molecules in cancer drug development remains underestimated, although studies support that macrocyclic molecules can also serve as an effective strategy to overcome drug resistance in cancer treatment (Song et al., 2023). Heterocyclic scaffolds, particularly oxadiazoles, have emerged as promising bio-isosteres in medicinal chemistry due to their favorable physicochemical properties such as electronic stability, metabolic resilience, hydrogen-bonding capability, and synthetic flexibility (Sethi G et al., 2024). The oxadiazole moiety, encompassing isomers like 1,2,4- and 1,3,4-oxadiazoles, has demonstrated notable anticancer potential by modulating critical oncogenic pathways, including EGFR, PI3K/Akt/mTOR, and p53 (V. Kumar et al., 2025). The broad and potent activity of these molecules has established them as important pharmacological scaffolds especially in the treatment of cancer disease. Several di-, tri-, aromatic, and heterocyclic substituted 1,3,4-oxadiazole derivatives have been reported to possess potent anticancer activity (Ahsan, 2022; Bajaj et al., 2015; G. Kumar et al., 2024; V. Kumar et al., 2025; Vaidya et al., 2021).

For this reason, the present study was undertaken to explore the biological activity of the POXAPy-macrocycle, a supramolecular compound incorporating two 1,3,4-oxadiazole rings and synthesized in the laboratory of Prof. Vieri Fusi, which had previously been selected for its ability to reduce the survival of cancer cells (Ambrosi et al., 2020), in light of the growing body of evidence indicating the antitumor potential of this class of molecules.

1. Cancer

Cancer is a major global health problem with huge economic, social, and demographic impacts. In 2022, an estimated 20 million people worldwide had cancer, which accounted for approximately 9.7 million deaths from cancer (Bray et al., 2024; Y. Liu & Zheng, 2024). The burden of the disease will

grow exponentially, with an estimated 35 million cases in 2050, primarily due to population aging and increased risk factors like smoking, physical inactivity, and obesity (Bizuayehu et al., 2024). However, early diagnosis, universal access to health care and developments in cancer therapies has resulted in a significant improvement of cancer survival (Urruticoechea et al., 2010).

1.1 The hallmarks of cancer

It is necessary to consider several crucial points that establish a way to define the required steps for normal cellular transformation, also known as hallmarks of cancer. Cancer is a very complex disease, in terms of phenotypes and genotypes among different subtypes and it could be promoted by different factors. It is considered a multistep disorder rising from a defective event, as genetic mutations or epigenetic aberrations, and subsequently followed by a cascade of abnormal events leading to malignant cell transformation. These biological changes are not only related with intrinsic factors and other external agents can be involved as ionizing agents (e.g., gamma rays, X-rays, UV radiation), chemical agents (e.g., arsenic, tobacco, benzene, nickel, radon) and biological agents (e.g., some viral agents, parasites, bacteria) (S. Wu et al., 2016).

The hallmarks of cancer (Figure I) —distinctive and complementary capabilities that enable tumor growth and metastatic dissemination— continue to provide a solid foundation for understanding the biology of cancer (Hanahan, 2022):

- self-sustaining proliferative signaling by deregulating this signaling, cancer cells acquire the ability to sustain their growth in complete autonomy. They become able to produce their own mitogenic signals or, alternatively, inducing other non-tumor cells to produce it;
- evading growth suppressors activities: in order to sustain their ability to proliferate, cancer cells activate ways to negatively regulate tumor suppressive programs (as RB or TP53);
- resisting cell death: cancer cells master cell death by avoiding apoptotic programs. In this sense they negatively regulate expression of anti-apoptotic proteins (ex. Bcl-2 family), autophagy machinery component (TGF-β) and inducing necrosis factors to promote tumor (e.g., releasing IL-1);

- enabling replicative immortality: to sustain tumor growth, cancer cells acquire limitless replicative potential, through the telomere maintenance, by telomerase activity, and by suppressing cellular senescence pathways;
- inducing angiogenesis: upregulation of factors involved in inducing angiogenesis, as vascular endothelial growth factor-A (VEGF-A), and preventing expression of those inhibiting it, as thrombospondin 1 (TSP-1). By this, cancer cells sustain growth with the sufficient afflux of nutrient and oxygen, mimicking a normal tissue;
- activating invasion and metastasis: cancer cells acquire the ability to invade, enhance cell motility, express protease to degrade extracellular matrix and disseminate from a primary tumor to another site in the body. This, mainly, is associated with downregulation of E-cadherin expression, a well-established protein involved in cell-to-cell junctions;
- deregulating cellular energetics: to fuel cell growth and division, cancer cells need to push their proliferation by glycolytic switch, that allows for a generation of different intermediates of biosynthetic pathway, facilitating production of macromolecules;
- genome instability and mutation: this step is fundamental, both for acquisition and progression of tumor capabilities. Defects in "DNA caretakers" result in loss of their function by inactivating mutation or epigenetic repression;
- avoiding immune destruction: immune evasion represents one of many forms of cancer cells to conceal eradication by disabling component of the immune system (e.g., secretion of immunosuppressive factors, as TGF-β);
- tumor-promoting inflammation: inflammatory response is a way by which cancer cells can achieve hallmarks and evade suppression by the immune system. Moreover, immune response cells can release some reactive oxygen species (ROS), that are actively mutagenic with nearby cells (Hanahan & Weinberg, 2011).

Recently, new feature have been added by Hanahan D., such as:

- unlocking phenotypic plasticity: critical component to bypass terminal differentiation. Cancer cells can "unlock" this capability by three different ways: de-differentiation (when differentiated cells reverse to a progenitor cells), blocked differentiation (from progenitor

cells), trans- differentiation (differentiated cells can show a new phenotype of another lineage cell);

- non mutation epigenetic reprogramming: gene expression can be directly regulated by epigenetic modifications. This becomes relevant in the context of carcinogenesis because the tumor microenvironment can directly influence the epigenome;
- senescent cells: considered for a long time as a protective mechanism, it has been demonstrated that in some of these types of cells can stimulate cancer by producing a plethora of bioactive factors, contributing to proliferation instead of preventing it (Lee & Schmitt, 2019);
- polymorphic microbiomes: some variation of specific microbiomes (e.g., intestine), could raise species of bacteria that have been reported to enable the expression of hallmarks of proliferation, as for example in colon epithelium (Okumura et al., 2021).

Importantly, although the eight core hallmarks and this novel capability are conceptually distinguishable by definition, their regulation is at least partially interconnected in several, and possibly many, cancers. For instance, multiple hallmarks can be simultaneously modulated in certain tumor types by canonical oncogenic drivers such as *KRAS, MYC, NOTCH,* and *TP53*, (Hanahan, 2022).

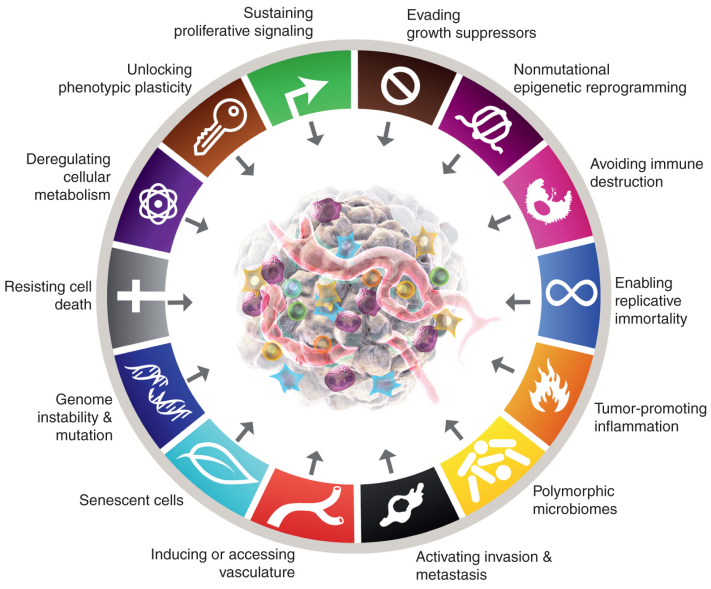

Figure I. All biological hallmarks acquired from cancer cells that define the transformation of a normal cell in a cancerous cell, updated in 2022 (Hanahan D., 2022).

1.2 Cancer therapies

The persistent rise in cancer-related deaths, coupled with the inherent risks and severe side effects of existing treatments, highlights the urgent need for more effective and personalized options. Despite the emergence of advanced therapies such as immunotherapy and gene therapy, traditional treatments remain the most commonly adopted due to their cost-effectiveness and widespread use. Therefore, ongoing efforts to improve and refine conventional cancer treatments—such as surgery, radiotherapy, chemotherapy, and hormonal therapy—remain essential, as illustrated in Figure II (Zafar et al., 2025).

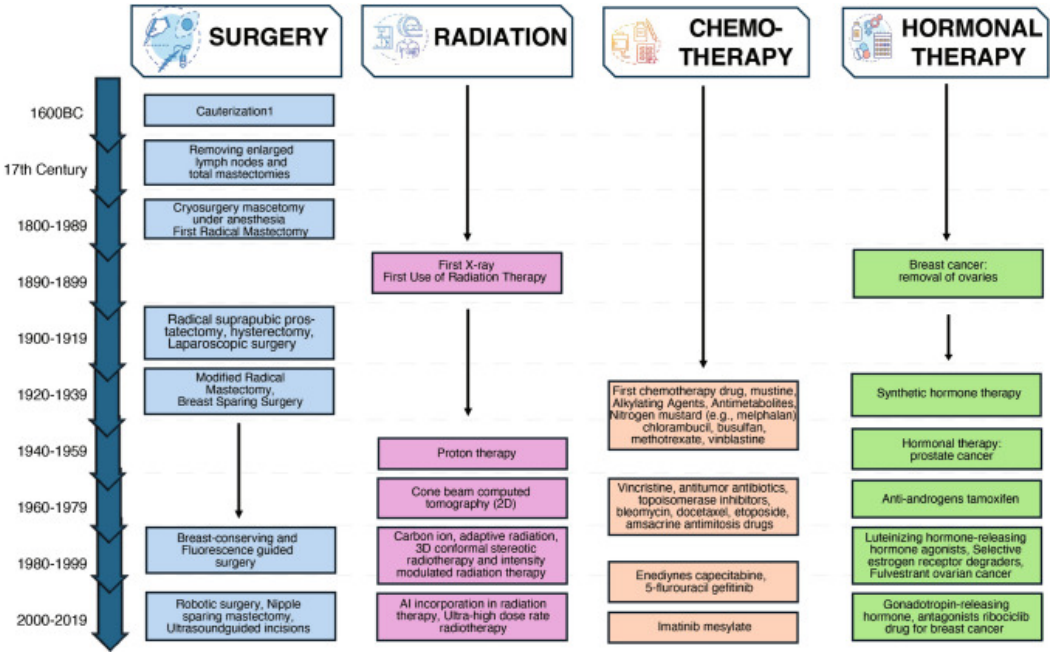

Figure II. Evolution and milestones of traditional anticancer therapies across centuries: A comprehensive overview of development and progress (Zafar et al., 2025).

Chemotherapy is one of the most widely used conventional approaches to cancer treatment. It targets key cell cycle phases to induce cell death. In particular, there are several classes of chemotherapeutics, which can be distinguished by their structures and mechanisms of action:

- alkylating agents (e.g., cisplatin, temozolomide, cyclophosphamide), first recognized for their clinical potential in 1942 with the introduction of nitrogen mustard gas, heralded a new era in chemotherapy. Like sulfur mustard, these agents form covalent bonds with nucleophilic sites on macromolecules (Hajdu, 2005). This interaction leads to the formation of DNA

adducts, which can cause either inter-strand or intra-strand crosslinking, disrupting replication and transcription and ultimately resulting in cell death (Karati et al., 2022).

- Antimetabolites (e.g., fluorouracil, hydroxyurea, aphidicolin) work by impairing DNA replication machinery either by depletion of deoxynucleotides or incorporation of chemically modified nucleotides, that transform into nucleotide analogs and prevent key enzymes from synthesizing DNA eventually prompting apoptosis (Parker, 2009).
- Antitumor antibiotics (e.g., bleomycin, calicheamicin, mitomycin) are one of the earliest forms of cancer treatment, particularly those obtained from Streptomyces species. These antibiotics target multiple cell cycle phases and induce cell growth arrest.
- Topoisomerase inhibitors: topoisomerase, due to its indispensable role in maintaining DNA integrity during cell proliferation and differentiation, may provide an important strategy to target tumor cells. Drugs such as amsacrine, etoposide, and doxorubicin target topoisomerase type II, while cytotoxic alkaloids and camptothecin (CPT) are recognized as inhibitors of type I (Khadka & Cho, 2013).
- Antimitotic drugs (e.g., paclitaxel, docetaxel) target the mitotic process by inhibiting microtubule assembly or stabilizing microtubules thereby halting cell division and inducing apoptosis or mitotic catastrophe.

The effectiveness of these chemotherapeutics is limited by chemoresistance, caused by dysregulation of molecular pathways involved in metabolism, cell proliferation, apoptosis, and autophagy. Furthermore, chemotherapy is unable to target specific cancer cells, and this could enhance toxicity to some treatments. New approaches in the last few years have revolutionized cancer treatment, and among those, targeted therapy has arised to grant a more specific and low toxicity treatment (Zhong et al., 2021).

The rapidly growing armamentarium of targeted therapeutics can be categorized according to their respective effects on one or more hallmark capabilities, as illustrated in Figure III.

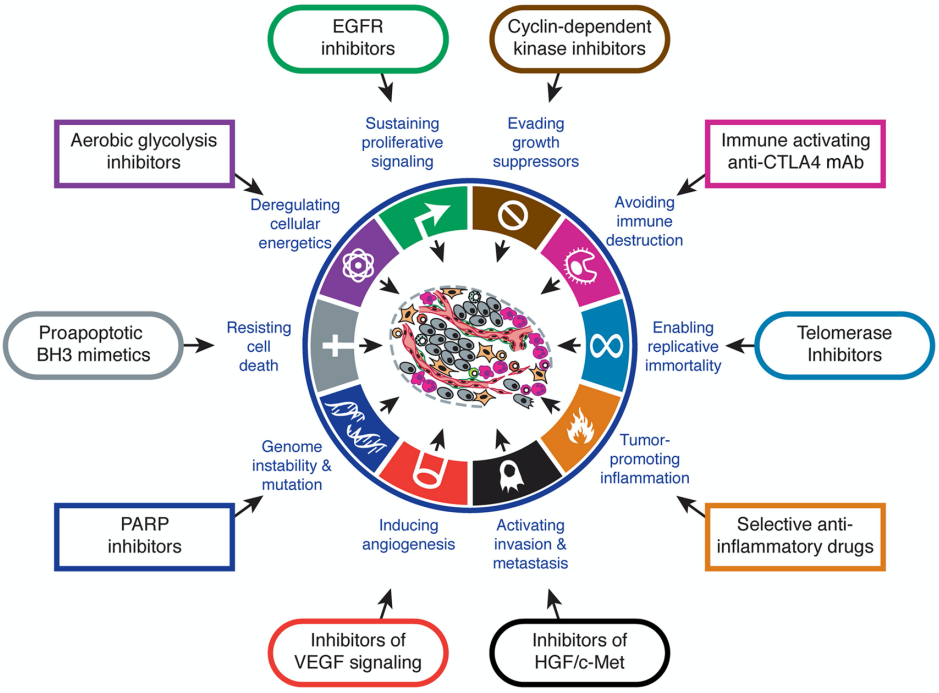

Figure III. Therapeutic targeting of the Hallmarks of Cancer. Illustrative examples of drugs that interfere with each of the acquired capabilities necessary for tumour growth and progression (Hanahan, 2022).

Targeted therapy has shown promising results in various cancer types, including breast, lung, colorectal, and melanoma. It has the potential to provide more effective and personalized treatment options, improving patient outcomes and minimizing side effects.

A groundbreaking milestone in oncology has been the recognition and targeted elimination of malignant cells through cancer immunotherapy, which harnesses the body's immune system to attack cancer. Over the past decade, the FDA has approved a wide range of immunotherapies, including monoclonal antibodies, immune checkpoint inhibitors, and cell-based therapies, many of which have significantly improved patient survival (Fig. IV). The research and development of mAbs for cancer treatment have advanced significantly, leading to improved patient outcomes and an expanding therapeutic landscape. Clinical trials continue to demonstrate the efficacy of targeted antibodies, highlighting their role in cancer immunotherapy (Bandara & Raveendran, 2025; Mc Neil & Lee, 2025).

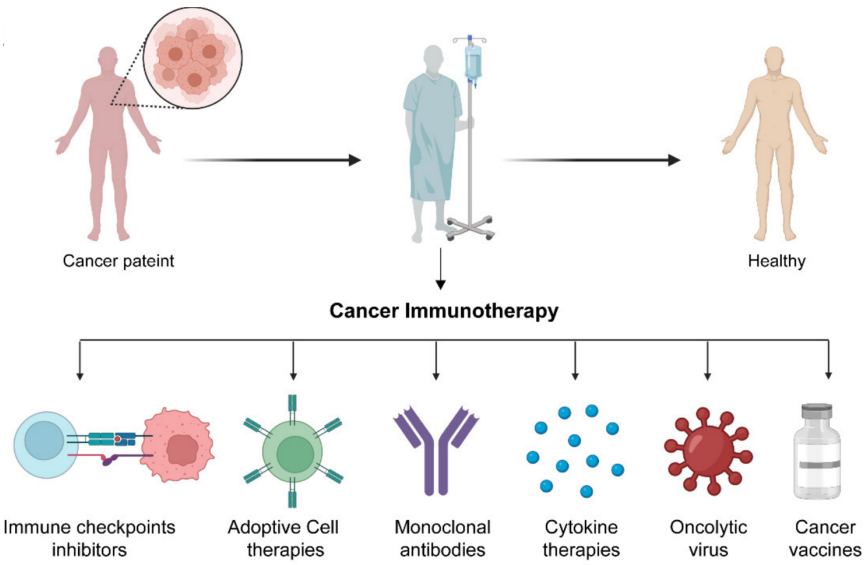

Figure IV. Illustration depicting various immunotherapy approaches for cancer treatment (Mishra et al., 2022).

1.3 Hematological malignancies

Among different types of cancers, one of the most aggressive is represented by blood cancers. The World Health Organization (WHO) classifies hematological malignancies based on lineage, morphology, phenotype, clinical features and it comprises leukemia, myeloma, chronic lymphoma, myeloproliferative disorders and myelodysplastic syndromes (Kansal, 2025; Xiao et al., 2024). These types of hematological cancers start in bone marrow, where normally hematopoietic cells are produced, or in immune system cells. In particular, leukemias are the most lethal hematological malignancy, that affects the blood and bone marrow, leading to an abnormal proliferation of immature leukocytes that disrupt the normal function of healthy blood cells, impairing the body's ability to fight infections and control bleeding (Oybek Kizi et al., 2025).

Although there are a multitude of specific diagnoses, leukemias are generally classified into subtypes defined by cell lineage (lymphocytic or myeloid) and stage of maturation arrest (acute or chronic). The most commonly seen and studied are:

- acute myeloid leukaemia (AML);
- acute lymphocytic leukaemia/lymphoma (ALL);
- chronic lymphocytic leukaemia/small lymphocytic lymphoma (CLL/SLL);

- chronic myeloid leukaemia (CML) (Bispo et al., 2020; Whiteley et al., 2021), as illustrated in Figure V:

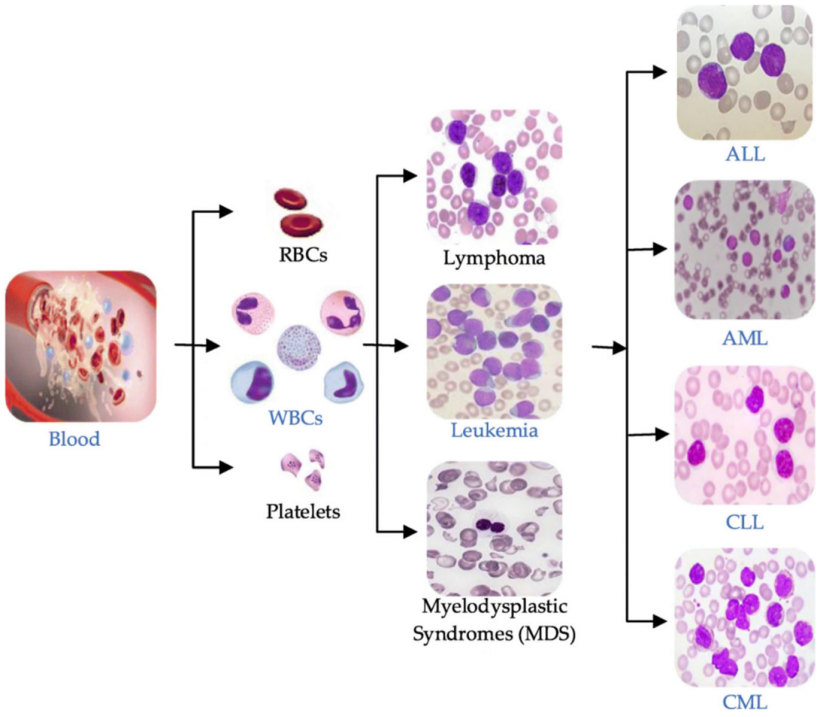

Figure V. Blood components and main types of leukemia (Oybek Kizi et al., 2025).

A leukemia diagnosis is usually made by analyzing a patient's blood sample through a complete blood count (CBC) or microscopic evaluation of the blood or flow cytometry (Oybek Kizi et al., 2025). According to GLOBOCAN database, in 2022 leukemia ranked as the second most common hematological malignancy after non-Hodgkin lymphoma worldwide and was among the top ten causes of cancer deaths in 71 countries (Sung et al., 2021). Globally, the leukemia disease burden is higher among males than females. The most commonly observed childhood leukemia was ALL, while among adults predominated AML and CLL (Dal Tveit et al., 2025; Miranda-Filho et al., 2018; Trallero et al., 2023).

A hallmark of AML is represented by a differentiation block of myeloid progenitors/precursors that accumulate in bone marrow and in the blood. One AML subtype, acute promyelocytic leukemia (APL), displays a unique sensitivity to retinoic acid, promoting the differentiation of leukemic promyelocytes to mature neutrophils (Breitman et al., 1981). This discovery has provided the rationale for initial clinical studies based on the use of all-trans retinoic acid (ATRA) in APL, which has supported the capacity of this drug to promote the *in vivo* differentiation of leukemic cells (Liang

et al., 2021; Rehman & Lübbert, 2025; Yanada, 2024). APL is characterized by a 15;17 chromosome translocation with breakpoints within the retinoic acid receptor α (RARA) gene on chromosome 17 and the PML gene, which encodes a transcription factor on chromosome 15; a PML-RARA fusion protein is formed because of the translocation. The specific targeting of this protein represents the molecular basis of the marked sensitivity of APL to ATRA (de Thé et al., 1990; Testa & Pelosi, 2024). The PML-RARA protein is responsible for all of the unique features of APL cells, such as the sensitivity to ATRA, block of cell differentiation at the promyelocyte stage, and increased proliferation due to diminished apoptotic cell death (Grignani et al., 1993; Minami et al., 2025). While significant therapeutic advances have been accomplished, a residual subset of APL patients persists for whom the development and evaluation of alternative treatment modalities remain necessary.

2. Macrocyclic compounds

Macrocycles are generally defined as organic molecules which contain a ring of at least 12 heavy atoms, with a cyclic skeleton, and they have unique spatial structures and physicochemical properties (Garcia Jimenez et al., 2023; Mallinson & Collins, 2012; Yudin, 2015).

The general interest in macrocycles across different fields of science started to grow some years before 1980 and then increased dramatically from 1990 and onward. In drug discovery, the rapid growth phase began at the turn of the millennium. Because of their challenging design and synthetic complexity, currently, most Food and Drug Administration (FDA)-approved macrocycles and clinical candidates are obtained as natural products (Garcia Jimenez et al., 2023; Mortensen et al., 2019), but de novo designed macrocycles have now begun to become approved as drugs. Erythromycin is a well-known example of a macrocyclic molecular drug (Washington & Wilson, 1985) (Figure VI).

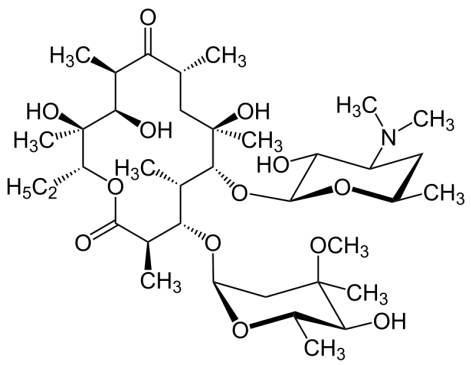

Figure VI. Erythromycin, a macrolide antibiotic, is one of many naturally occurring macrocycles (Hamilton-Miller, 1973).

There are many advantages of using macrocyclic molecules as drugs:

- their rigid conformations allow them with strong binding affinities and high selectivity to target proteins (Amrhein et al., 2022);
- reducing the degrees of freedom of molecules through macrocyclization can decrease their overall polarity, enhance their cell penetration capabilities, and increase their oral bioavailabilities (Dougherty et al., 2019; Marsault & Peterson, 2011), as well as improve metabolic stabilities, pharmacokinetics, and pharmacodynamic parameters (Driggers et al., 2008; Mallinson & Collins, 2012; Marsault & Peterson, 2011);
- the lower molecular weights allow better pharmacological characteristics, such as permeabilities, and are less susceptible to proteolytic degradation, which increases their longevity in vivo (Fairlie DP et al., 1994).

Infectious disease is the major therapeutic indication treated by macrocyclic drugs (44.4% of all macrocyclic drugs). Within this class, most are used as antibacterial agents, but antivirals (6.9%) and antifungals (8.3%) are also important. Oncology (20.8%), autoimmune disorders (5.6%), and immunosuppressants (5.6%) are the three other major therapeutic indications.

2.1 Macrocycles in cancer therapy

The remarkable advantages of macrocyclic molecule drugs have made them one of the hot spots for medicinal chemistry in the past 20 years (Song et al., 2023). Many proteins critical for cancer processes have serve as successful targets of macrocyclic molecules, including mammalian target of rapamycin (mTOR), Janus kinase (JAK2), cyclin-dependent kinases (CDKs), and histone deacetylase (HDAC) (Figure VII).

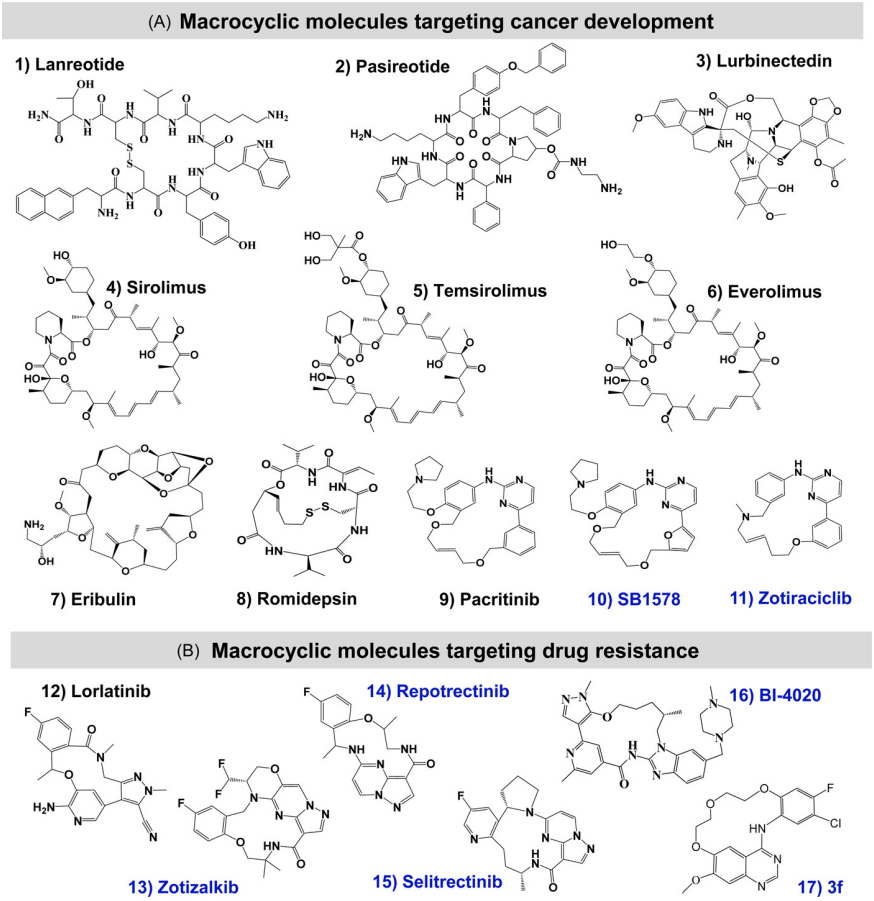

Figure VII. The structures of approved macrocyclic drugs and investigating macrocyclic compounds for cancer therapy (Song et al., 2023).

Among them, three approved macrolide molecules, sirolimus (rapamycin), temsirolimus, and everolimus target the mTORC1 protein complex to inhibit tumor growth (Gupta et al., 2024; Wagner et al., 2021; Westin et al., 2013). Pacritinib, an orally available small macrocyclic molecule, and its analog SB1578 are the second generation of JAK2 kinase inhibitor (Hart et al., 2011; Lamb, 2022; Mascarenhas, 2022). The most studied CDK9 inhibitor in cancer cells is zotiraciclib, a pacritinib analog; this compound has shown potent anticancer activities in vitro and in vivo in patients (R. Chen et al., 2021; Lucke-Wold et al., 2024). Moreover, approved drug romidepsin target HDAC activities, for treatment of PTCL patients (Falchi et al., 2021; Pojani & Barlocco, 2021; Shi et al., 2021). Among HDACi drugs, romidepsin showed the most selectivity and potency against disease-related HDACs (Bondarev et al., 2021).

3. Oxadiazoles derivatives

Oxadiazoles are an interesting class of five-membered heterocyclic compounds containing two atoms of nitrogen and one atom of oxygen, with the molecular formula $C_2H_2N_2O$. They exist in four different regioisomeric form:

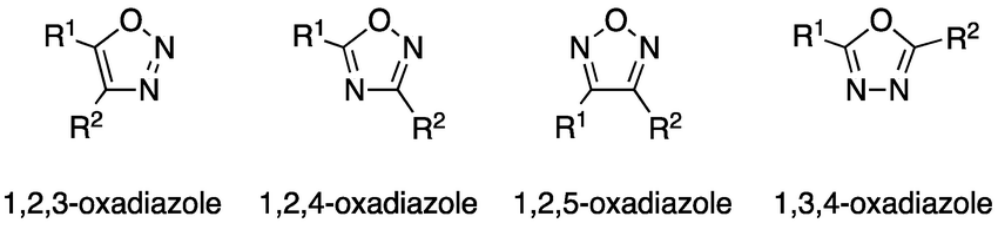

Figure VIII. Structures of the different oxadiazole isomers (Salassa & Terenzi, 2019).

1,2,4- and 1,3,4-isomers are by far more represented in literature. Oxadiazoles exhibit a broad range of uses in medicinal chemistry they were employed as drug candidates for several diseases, in organic synthesis as useful intermediates, and in material science as building blocks for new polymers (Dhameliya et al., 2022; G. Kumar et al., 2024; Sharma et al., 2021).

3.1 Oxadiazoles in cancer therapy

Heterocyclic scaffolds particularly oxadiazoles have emerged as promising bio-isosteres in medicinal chemistry due to their favorable physicochemical properties such as electronic stability, metabolic resilience, hydrogen-bonding capability, and synthetic flexibility (Sethi G et al., 2024). Many oxadiazole-based molecules have been developed against cancer, inflammation, infection, diabetes, and other diseases (Boström et al., 2012; Khan et al., 2014; Salahuddin et al., 2017; Vaidya et al., 2016). The anticancer activity of oxadiazoles is in large measure a result of their ability to engage molecular targets of great significance in the regulation of tumor growth, cell proliferation, apoptosis, and metastasis. These targets include:

- Inhibition of Epidermal Growth Factor Receptor (EGFR) Signaling (González et al., 2021; London & Gallo, 2020)
- Modulation of the PI3K/Akt/mTOR Axis (Chamcheu et al., 2019; Karami Fath et al., 2023; Palombo et al., 2023)
- p53 Upregulation and Induction of Apoptosis (Diepstraten et al., 2024; W. Wu et al., 2024)

- Reactive Oxygen Species (ROS) Generation and DNA Damage (Das, 2023; Juan et al., 2021).

3.2 POXAPy-macrocycle, a novel oxadiazole compound

In light of the above considerations, the POXAPy-macrocycle molecule was synthesized at the Supramolecular Chemistry Laboratory of the University of Urbino Carlo Bo, under the supervision of Prof. Vieri Fusi, with the aim of investigating and assessing its potential antiproliferative activity on tumor cell lines. POXAPy-macrocycle (13,16,19-trimethyl-36,37-dioxa-3,4,13,16,19,28,29,35-octaaza-hexacyclo[29.3.1.1(2,5).1(27,30).0(6,11).0(21,26)]eptatriaconta 2,4,6,8,10,21,23,25,27,29,31,33,1(35)-tridecene) results from the cyclization of the POXAPy component [2,6-bis(5-(2-methylphenyl)-1,3,4-oxadiazol-2-yl)pyridine], comprising five aromatic moieties, with a polyamine [1,4,7-trimethyl-1,4,7-triazaheptane] (Figure IX) (Ambrosi et al., 2020).

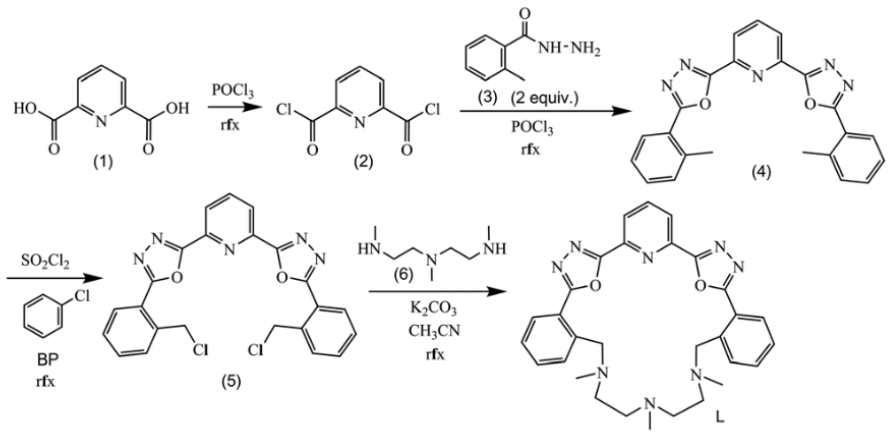

Figure IX. The synthesis of POXAPy-macrocycle molecule, that integrates the 1,3,4-oxadiazole groups within a macrocyclic framework (Ambrosi et al., 2020).

The biological activity of POXAPy was evaluated at the cellular level using the promonocytic leukemia U937 cell line as a model system. As shown in Figure X (panel A), the compound reduced U937 cell survival in both a time- and dose-dependent manner. Notably, the biological effect became detectable at concentrations as low as 1 μM, while at higher doses cell survival progressively declined, reaching values close to zero depending on the incubation time.

The cellular response was further investigated by analyzing the perturbations in cell-cycle distribution following exposure to POXAPy. As shown in Figure X (panel B), treatment with 5 μM

POXAPy resulted in a modest increase in the proportion of cells in the G1 phase, whereas exposure to 10 μM led to an accumulation of cells in the G2/M phase. The effects observed after 24 h treatments at 5 μM and 10 μM are consistent with a cellular response typically associated with intercalating agents. When cells were exposed to a lethal concentration of L (50 μM for 24 h), the cell-cycle profile became uninterpretable, and an increase in hypodiploidy was observed, suggesting the possible induction of apoptotic processes (Ambrosi et al., 2020).

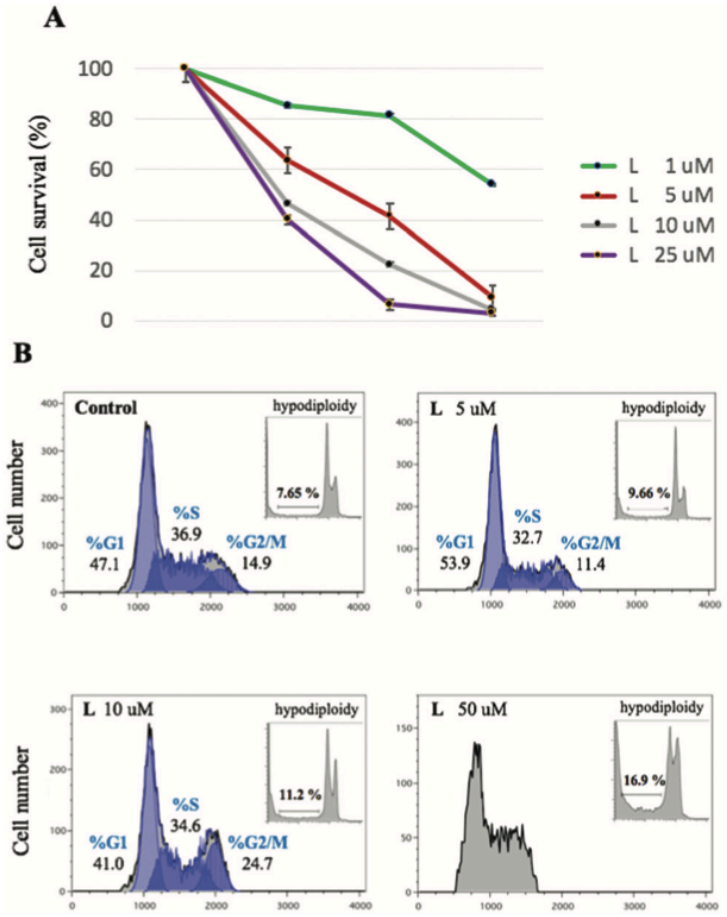

Figure X. Biological activity of POXAPy against a neoplastic human cellular model. (A) Evaluation of cell survival. Values are reported as the mean ± SD of three independent experiments. (B) Cell-cycle profile analysis. L: POXAPy-macrocycle molecule (Ambrosi et al., 2020).

4. Autophagy and Mitophagy

Autophagy is a fundamental, evolutionarily conserved process through which eukaryotic cells degrade and recycle intracellular components, such as damaged organelles, misfolded proteins, and invading pathogens, via the lysosomal pathway. It plays a crucial role in maintaining cellular homeostasis, especially under stress conditions including nutrient deprivation, oxidative stress, loss of growth factors, or treatment with cytotoxic agents. Autophagy involves several stages: initiation, nucleation of the phagophore, expansion and closure to form the autophagosome, fusion with lysosomes, and degradation/recycling of cargo (Figure XI). Selective forms of autophagy (such as mitophagy) specifically target damaged mitochondria or other cellular organelles (Lee et al., 2023; L. Liu et al., 2023; Onishi et al., 2021).

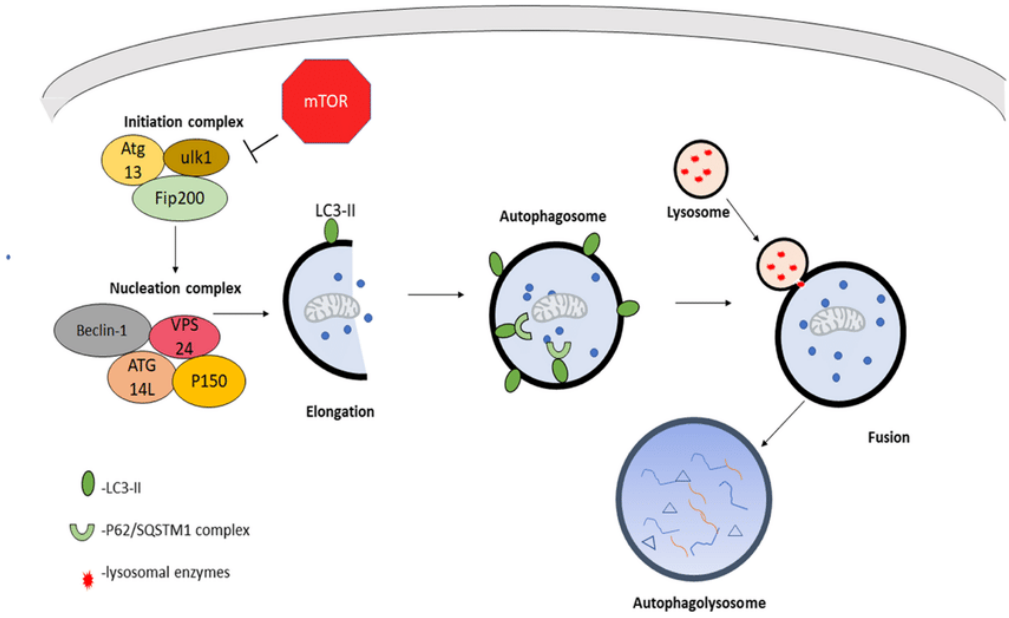

Figure XI. Autophagy mechanism. Autophagy is a cellular mechanism by which metabolites, organelles, proteins, and protein aggregates are enveloped by a vesicular membrane to form an autophagosome. The autophagosome is trafficked to a lysosome where fusion occurs, and lysosomal degradative enzymes break down the cargo (Soto-Avellaneda & Morrison, 2020)

Mitophagy is the selective elimination of dysfunctional or superfluous mitochondria, crucial for mitochondrial quality control. It can be triggered by stimuli like mitochondrial depolarization, oxidative stress, or hypoxia. Through mitophagy, cells remove damaged mitochondria that might

otherwise produce excessive reactive oxygen species (ROS) or release apoptotic signals (L. Liu et al., 2023; Onishi et al., 2021).

A commonly used pair of markers to monitor autophagy are LC3B (microtubule-associated protein 1 light chain 3 beta) and p62 (also known as SQSTM1). LC3B exists in a cytosolic form (LC3B-I) which, upon induction of autophagy, is lipidated to LC3B-II and associates with the membranes of forming autophagosomes. The increased conversion to LC3B-II and appearance of LC3B puncta (spots) in microscopy are indicative of autophagosome formation and expansion (SchlÃ¤fli et al., 2015; Zhao et al., 2024).

p62 is a selective autophagy receptor that binds ubiquitinated protein aggregates and interacts with LC3B to deliver these aggregates into autophagosomes. Importantly, p62 itself is degraded during normal autophagic flux. Thus, accumulation of p62 indicates a blockage or impairment in the autophagic degradation step, whereas decreased levels can suggest active flux. However, interpretation of p62 levels requires caution, because its expression is also regulated transcriptionally and can be affected by other stress pathways (Langer et al., 2018; Zhao et al., 2024).

In the context of cancer biology, autophagy and mitophagy have dual and context-dependent roles. On one hand, basal autophagy supports cell survival under metabolic or oxidative stress by providing essential building blocks and energy. On the other, if excessively activated or dysregulated, these pathways can promote cell death or interfere with tumor-promoting signaling. Moreover, autophagy frequently interacts with major oncogenic pathways, particularly PI3K/AKT/mTOR, which negatively regulates autophagy, and with MAPK/ERK signaling. Crosstalk among these pathways can influence tumor progression, response to therapy, and drug resistance (L. Liu et al., 2023; Rajendran et al., 2024; J. Zhang et al., 2023; M. Zhang et al., 2023).

Recent reviews have underlined the importance of understanding how selective autophagy contributes to cancer cell plasticity, metastasis, and treatment response. For example, “Unraveling the Intricacies of Autophagy and Mitophagy: Implications in Cancer Biology” (Sunmi Lee et al., 2023) discusses how these processes are regulated in different tumor contexts, and how they may be targeted therapeutically (Lee et al., 2023).

MDPI Another recent work, “Crosstalk between mitochondrial biogenesis and mitophagy to maintain mitochondrial homeostasis” (2023), emphasises that sustaining mitochondrial integrity

via mitophagy is essential to avoid mitochondrial dysfunction and excessive ROS production, which can otherwise contribute to oncogenic transformation (L. Liu et al., 2023).

Understanding these mechanisms is especially relevant for leukemia models like NB4 cells, where both survivals signaling (via mTOR, ERK, etc.) and stress responses (including autophagy/mitophagy) may determine the cellular outcome upon treatment with novel compounds such as POXAPy-macrocycle.

AIM OF THE STUDY

The focus of my PhD work was centered on the characterization of the biological activity of a novel oxadiazole-based macrocyclic compound, named POXAPy, designed and synthesized within our research group. Previous studies on structurally related macrocyclic molecules suggested a potential anticancer activity, prompting us to investigate whether POXAPy could exert cytotoxic or cytostatic effects in acute promyelocytic leukemia NB4 cells and to elucidate the underlying molecular mechanisms.

To this aim, an initial assessment of cell viability and proliferation was performed, revealing that POXAPy exerts a dose-dependent inhibition of cell growth, with the concentration of 10 μM identified as sub-lethal through wash-out experiments. Subsequent transcriptomic and proteomic analyses demonstrated that POXAPy profoundly remodels gene and protein expression profiles, significantly affecting pathways involved in cell cycle regulation, DNA repair, and mTOR signaling.

Given the crucial role of the PI3K/AKT/mTOR and RAF/MEK/ERK pathways in tumor progression, further investigations confirmed that POXAPy treatment leads to a marked downregulation of mTOR and ERK proteins, as well as a reduction of their phosphorylated forms, indicating a coordinated inhibition of these survival signaling cascades.

In addition, POXAPy exposure was found to trigger a strong autophagic and mitophagic response, as demonstrated by the accumulation of LC3B, the decrease of p62, and the appearance of double-membrane autophagosomes observed through transmission electron microscopy (TEM). These findings suggest that autophagy might represent a cellular adaptive mechanism to POXAPy-induced stress.

Considering the involvement of mitochondria in oxidative stress responses, we further explored the production of reactive oxygen species (ROS), observing a mild ROS increase only at the highest drug concentrations, supporting the hypothesis that mitochondrial stress contributes to, but does not dominate, the cellular response to POXAPy.

Finally, to investigate potential direct interactions with genomic structures, a cell-free assay was performed to evaluate the binding of POXAPy to G-quadruplex (G4) DNA motifs. Thermal denaturation studies revealed a specific stabilization of G4 structures within the c-Myc and c-Kit promoters, but not in telomeric or double-stranded DNA sequences, suggesting a possible selectivity

of POXAPy for oncogenic G4 motifs. Consistently, both Myc transcript and protein levels were found to be significantly downregulated upon treatment, supporting a possible G4-mediated modulation of gene expression.

Overall, this work aimed to comprehensively characterize the biological effects of POXAPy and to elucidate its molecular targets and mechanisms of action, integrating cellular, biochemical, and biophysical data to shed light on its anticancer potential and multimodal activity.

MATERIALS AND METHODS

Cell culture and molecule preparation

Acute promyelocytic leukemia (NB4) tumor cell line was obtained from American Type Culture Collection (ATCC) repository. Cells were grown in RPMI 1640 medium (Lonza, Belgium) supplemented with 10% FBS (Gibco, UK), 1% penicillin/streptomycin (Euroclone, Italy) and 1% L-glutamine (Lonza, Belgium). All cell lines were maintained with 5% CO_2 and a temperature of 37°C (Fanelli et al., 2008).

POXAPy-macrocycle was synthesized as already described (Ambrosi et al., 2020). Stock solution was prepared starting from powder of POXAPy-macrocycle, resuspended to a final concentration of 10 mM in 100% ethanol and stored at -80°C prior to use.

Treatments and cell viability evaluation

Treatments were carried out at different concentrations and time points as reported in the result section. For POXAPy-macrocycle, dose response experiments were performed at the doses of 3, 5, 10, 17.5, and 25 μM for 24, 48 or 7h hours of treatment. Cellular viability was evaluated by Trypan blue dye exclusion assay using DeNovix automatic cell counter (DeNovix, USA). The percentage of cell survival was determined as the percentage of viable cells in treated samples relative to control cultures, according to the formula: (treated/control) × 100.

Data are reported as bar plots the mean ± standard deviation (SD) of triplicate counts.

Cell cycle analysis, hypodiploid cells estimation and DNA laddering assay

NB4 cells were cultured at 1.5 x 10^5 cells/mL and treated at reported concentrations of POXAPy-macrocycle. After 24h, cells were harvested and centrifuged at 189 RCF for 3 minutes at 4°C. Then, cells were washed with 10 mL cold 1x PBS and centrifuged as before. Pellets were immediately fixed by adding 10 mL of ice-cold 70 % EtOH and samples were stored O/N at 4°C. The day after, samples were centrifuged at 426 RCF for 3 minutes at 4°C and pellets were resuspended with 1 mL of propidium iodide (PI) staining solution (1x PBS, 0.1% Triton X-100, PI 50 μg/mL, RNAse A 250

μg/mL) every 2.5 x 10^5 cells. Samples were incubated for at least 2 hours at 4°C. Cytofluorimetric acquisition was carried out using the BDAccuri C6 Plus flow cytometer (BD Life Sciences, USA). Cell cycle analyses were obtained through FlowJo software v10.8 (BD Life Sciences, USA) by using Watson-Pragmatic algorithm and results are displayed in a stacked bar plot of the mean ± standard deviation (SD) of triplicate acquisitions.

DNA fragmentation was assessed by DNA laddering assay. Cells were treated with the POXAPy-macrocycle at concentrations of 25 and 50 μM for 24 h. After treatment, genomic DNA was isolated and subjected to electrophoresis on agarose gel. DNA fragmentation patterns were visualized under UV illumination and documented with a gel imaging system.

Western blotting

NB4 cells were treated with 10 μM POXAPy-macrocycle for 24 h. Then, cells were resuspended in 100 μL of 1x Sample Buffer (62.5 mM Tris-HCl pH 6.8, 2% SDS, 0.003% bromophenol blue, 10% glycerol, 5% β-mercaptoethanol) every 10^6 cells. A volume of 25 μL of total lysates were loaded on 10% SDS polyacrylamide gel electrophoresis and immunoblotted against the following antibodies: anti-mTOR (#2972, Cell Signaling Technology, Danvers, Massachusetts, USA 1:1000 diluition), anti-phospho mTOR (#2971, Cell Signaling Technology, Danvers, Massachusetts, USA, 1:1000 diluition), anti-α-tubulin (#T9026, Sigma-Aldrich, Merck KGaA, Darmstadt, Germany, 1:2000 dilution), anti-ERK1/2 (#9102, Cell Signaling Technology, Danvers, Massachusetts, USA, 1:1000 diluition), anti-phospho ERK1/2 (#9101, Cell Signaling Technology, Danvers, Massachusetts, USA, 1:1000 diluition), anti-c-MYC (Y69, Abcam, Cambridge, MA, USA, 1:1000 dilution), anti-LC3B (#2775, Cell Signaling Technology, Danvers, Massachusetts, USA, 1:1000 diluition). Images were acquired using the Vü-C Imaging system (PopBio, UK). Densitometric analysis was carried out using the FiJi software package.

RNA extraction and sequencing

RNA was isolated starting from 2 x 10^6 NB4 cells, not treated (n.t.) and treated with 10 μM POXAPy-macrocycle, using the RNeasy Mini Kit (QIAGEN, Germany) following the manufacturer's instructions. Purified RNA was fluorometrically quantified by Qubit RNA HS assay (Invitrogen, USA).

RNA sequencing libraries were prepared at the European Institute of Oncology (EIO, Italy) according to Bonora B.M., *et al.*, 2022. Reads pre-processing and alignment was also performed as previously reported (Amatori et al., 2023; Bonora et al., 2022). Differential gene expression analysis was performed using the edgeR package. Low expressed genes (≤2 counts per million (CPM) in at least two samples per group) were filtered out prior to normalization. The remaining genes were normalized using the Trimmed Mean of M-values (TMM) method. A multidimensional scaling (MDS) plot was generated using the plotMDS function from edgeR with default parameters.

Genes were identified as differentially expressed (DEGs) when the following criteria were met: false discovery rate (FDR) ≤ 0.05 and fold change (FC) ≥ 2 or ≤ -2. Where not specified, all plots were generated using ggplot2 R package.

Proteomic analysis

Upon achieving confluence, samples were processed by EasyPep MS Sample Kit (Thermo Scientific Pierce) for label free quantification (LFQ) bottom-up analysis. After elution, samples were dried with a Speed vacuum centrifuge (Savant-SPD121P). Prior MS analysis they were solubilized in 0.1% formic acid, and the peptide content was quantified through the quantitative colorimetric peptide assay (Thermo Fisher Scientific).

1.5 micrograms of each sample was injected into an UltiMate 3000 RSLC nano system coupled to the Exploris 240 mass spectrometer (Thermo Fisher Scientific) and resolved by Easy-Spray Pepmap RSLC 18 (2 µm, 50 cm × 75 µm) at a flow rate of 300 nL/min with a gradient of phase B from 2% to 50% in 200 min. Then (B) was changed to 99% in 20 min, kept for 14 min, and then the column was re-equilibrated for 15 min. Data was acquired in a positive mode and data dependent manner. For MS1 m/z range was set to 350– 1500 at 120,000 resolution (at m/z 200), AGC target 3e6, and auto maximum injection time. MS2 switch when ions intensity was above 5e3, with m/z range in auto mode, normalized HCD energy 30%, AGC target 7.5e4, and maximum injection time 40ms. The resolution was set to 15,000 at m/z 200 and the internal calibrant for employed in run start mode. LFQ analysis was performed in quadruplicate.

Raw data generated by Xcalibur 4.2 software (Thermo Fisher Scientific) were analyzed using Proteome Discoverer 2.5 (Thermo Fisher Scientific), by using SEQUEST and MSPep Search algorithms. In the analysis was considered the fixed modification Cysteine carbamidomethylation

and the variable serine, threonine or tyrosine phosphorylation. Also, variables oxidation (M) and deamidation (N, Q) were considered. The false discovery rate was evaluated by a target-decoy strategy in concatenated q-value manner. FDR (strict) was set as 0.01, while FDR (relaxed) was set as 0.05.

Pathway analysis

Pathway analysis was conducted using iPathwayGuide software (Advaita Bioinformatics, United States) to identify the biological pathways associated with the differentially expressed genes observed in the three experimental conditions. The Molecular Signatures Database (MSigDB) Hallmark signatures gene set was used, and the pathways were considered significantly enriched when the FDR was lower than 0.01. All the filtered lists of DEGs described in the previous paragraph were used to perform the analysis.

Transmission Electron Microscopy (TEM) analysis

After POXAPy-treatments, cells were collected, washed in PBS and fixed in 2.5% glutaraldehyde in 0.1 M sodium cacodylate buffer (pH 7.2) overnight at 4 °C. Samples were washed and post-fixed in 1% osmium tetroxide for 1h at 4 °C. Following rinses, specimens were dehydrated through a graded ethanol series and embedded in epoxy resin (Epon/Araldite). Ultrathin sections (~60–80 nm) were cut with an ultramicrotome, mounted on copper grids and stained with 2% uranyl acetate and lead citrate. Sections were examined under standard operating conditions, using a Philips CM10 transmission electron microscope.

Immunofluorescence assay using anti-G-quadruplex antibody (BG4)

HeLa cells were seeded on glass coverslips and cultured until reaching approximately 70–80% confluence. Cells were fixed at room temperature (RT) for 5 min with 3.7% formaldehyde in 1× PBS, followed by a quick wash in 1× PBS. Permeabilization was performed for 10 min at RT using 0.1% Triton X-100 and 1% FBS in 1× PBS, after which cells were washed again and incubated for 30 min in a humid chamber for blocking.

After a brief rinse in PBS, cells were incubated for 2 h in a humidified chamber, in the dark, with the primary antibody anti-G-quadruplex structures (clone BG4, Sigma-Aldrich, MABE917-25UL) diluted 1:50 in PBS. As a positive control, an anti-H3K9me3 antibody (Active Motif) was used at a 1:500 dilution. Following primary antibody incubation, cells were washed three times with PBS and then incubated for 1 h with His-Tag Antibody (#2365, Cell Signaling Technology) at a 1:800 dilution, which specifically recognizes the BG4 clone.

After washing, cells were incubated for 30 min with Alexa Fluor 488-conjugated secondary antibody (1:400 dilution). Nuclei were counterstained with DAPI (1:3000 dilution), and coverslips were mounted using Mowiol mounting medium. Fluorescence images were acquired using an Olympus BX51 Fluorescence Microscope equipped with appropriate filter sets for DAPI and Alexa Fluor 488, and processed using the CellSens software (Olympus).

RESULTS

1. Antiproliferative activity of POXAPy-macrocycle

The antiproliferative activity of POXAPy-macrocycle (Fig.1) was initially assessed using the NCI-60 human tumor cell line panel, which includes 60 cancer cell lines derived from leukemia, melanoma, and cancers of the lung, colon, central nervous system (CNS), ovary, kidney, prostate, and breast. Cells were exposed to the compound at a single concentration (10 μM), and the mean growth percent (MGP) was calculated for each cell line following 48 hours of treatment.

The POXAPy-macrocycle exhibited a broad spectrum of activity, with variable growth inhibition across the different tumor types. The most pronounced antiproliferative effects were observed in leukemia (notably NB4, 23.85% growth), colon cancer (HCT-116, 26.45%; KM12, 18.47%), and melanoma (MALME-3M, 73.07%; M14, 60.16%). In contrast, limited or negligible activity was detected in certain non-small cell lung cancer (HOP-62, 105.20%), CNS (SNB-75, 103.31%), and renal cancer (A498, 120.74%) cell lines.

These preliminary findings justified further in-depth investigations on leukemia models, particularly the NB4 cell line, which was found to be one of the more sensitive to the compound. The data are summarized in Figure 2.

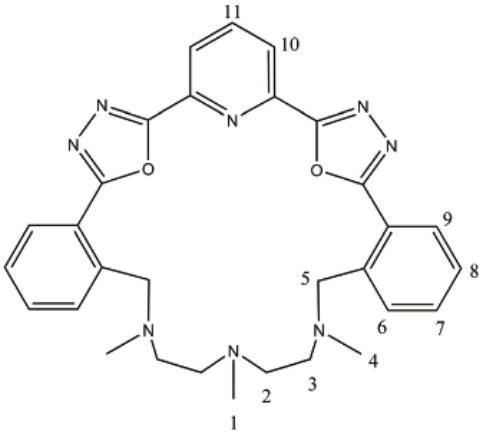

Figure 1. Chemical structure of POXAPy-macrocycle

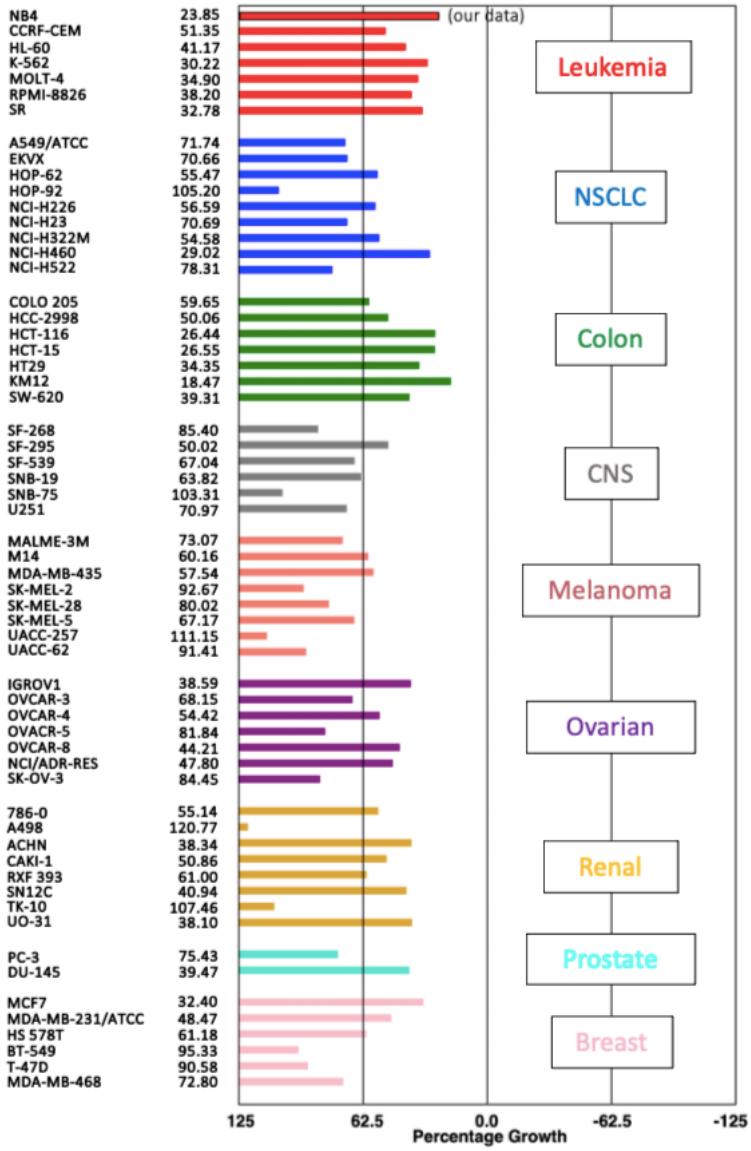

Figure 2. Effect of POXAPy on the growth of different cancer cell lines. Monster molecule was enrolled and tested in the Developmental Therapeutics Program (DTP) of the National Cancer Institute (NCI/NIH). NCI-60 human tumor cell line anti-cancer drug screening is based on the treatment of 60 different cancer cell lines at the concentration of 10 μM for 48 hours. Data are reported as mean growth percentage. Analyses were done as described at http://dtp.cancer.gov/discovery_development/nci-60. NB4 cells (APL model) were cultured and treated at the same conditions (our data) used in the NCI-60 protocol and added to the graph.

1.1 POXAPy antiproliferative effects against NB4 cell line

The antiproliferative activity of the newly synthesized oxadiazole-derived macromolecule was evaluated on the NB4 human leukemia cell line. Cells were treated with increasing concentrations of the compound (3, 5, 10, 17.5, and 25 μM) for 24, 48, and 72 hours.

The results demonstrated a clear dose- and time-dependent reduction in cell viability. After 24 hours of treatment, cell survival decreased from approximately 93% at 3 μM to 38% at 25 μM. Prolonged exposure further enhanced the cytotoxic effect: at 48 hours, cell viability ranged from ~75% at 3 μM to ~12% at 25 μM, while after 72 hours, viability declined dramatically to ~60% at 3 μM and ~5% at 25 μM.

Notably, a marked reduction in cell survival was already evident at 10 μM, where viability decreased to ~75% (24h), ~35% (48h), and ~20% (72h). These findings indicate a potent and sustained antiproliferative effect of the compound on NB4 cells, which becomes particularly pronounced at higher concentrations and longer treatment durations. The data are summarized in Figure 3.

A clear dose–response relationship was observed, with increasing concentrations of the compound leading to progressively lower cell viability across all time points. These results suggest that the antiproliferative effect of the macromolecule is both concentration- and time-dependent, and that prolonged exposure amplifies its cytotoxic potency against NB4 cells.

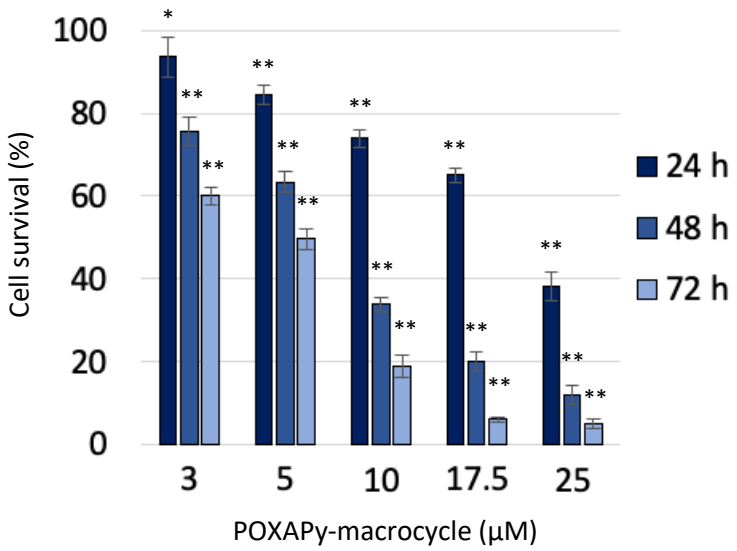

Figure 3. Dose-response and time-course experiments of POXAPy-induced cell survival reduction of NB4 cells. NB4 cells were treated with the reported concentrations of monster for 24, 48 and 72 hours and cell survival were evaluated by trypan blue exclusion-based assay using an automatic cell counter. Data are reported as mean ± standard deviation of three independent experiments. Statistical significance versus non-treated (not sown in the graph) cells was assessed by Student's *t*-test (*$p < 0.05$, **$p < 0.01$)

1.2 Analysis of POXAPy-mediated cell cycle perturbations and induction of programmed cell death

To investigate the effects of POXAPy-macrocycle on cell cycle distribution, cells were treated with increasing concentrations of the compound (1–25 μM) for 24 hours, stained with propidium iodide and subsequently analyzed by flow cytometry. The results demonstrated that POXAPy-macrocycle induced concentration-dependent alterations in the distribution of cell cycle phases (Fig. 4 and Fig. 5).

At lower concentrations (1–10 μM), a modest increase in the proportion of cells in the G1 phase was observed, rising from 31.5% in untreated cells to a peak of 43.1% at 5 μM, accompanied by a corresponding decrease in S phase cells (from 57.2% to 50.1%). Notably, treatment with the highest concentration (25 μM) markedly reduced the G1 population to 26.9%, while the percentage of cells in G2/M phase nearly doubled, increasing from 10.1% in controls to 19%. These data indicate that POXAPy-macrocycle induces a G2/M phase accumulation at higher doses, suggesting the onset of cell cycle arrest at this checkpoint.

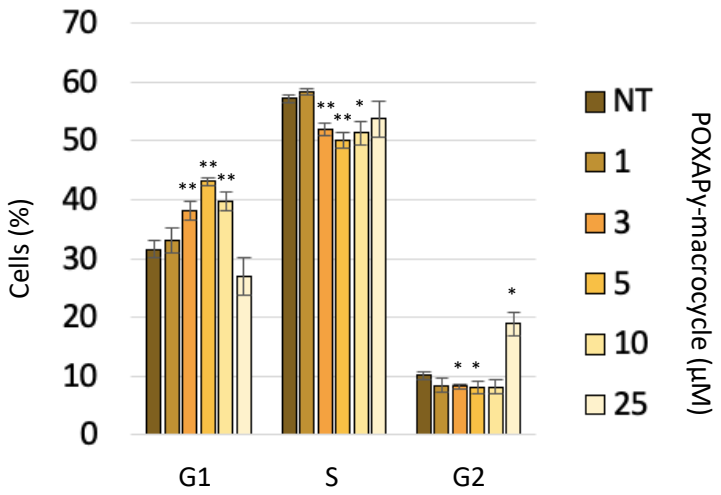

Figure 4. NB4 cells cell cycle analysis after 24 h treatment with POXAPy. NB4 cells cycle analysis of 24 hours dose response with molecule at reported concentrations. Data are presented as mean ± standard deviation (s.d.) of three independent experiments. Statistical significance versus non-treated (NT) cells was assessed by Student's *t*-test (*p < 0.05, **p < 0.01).

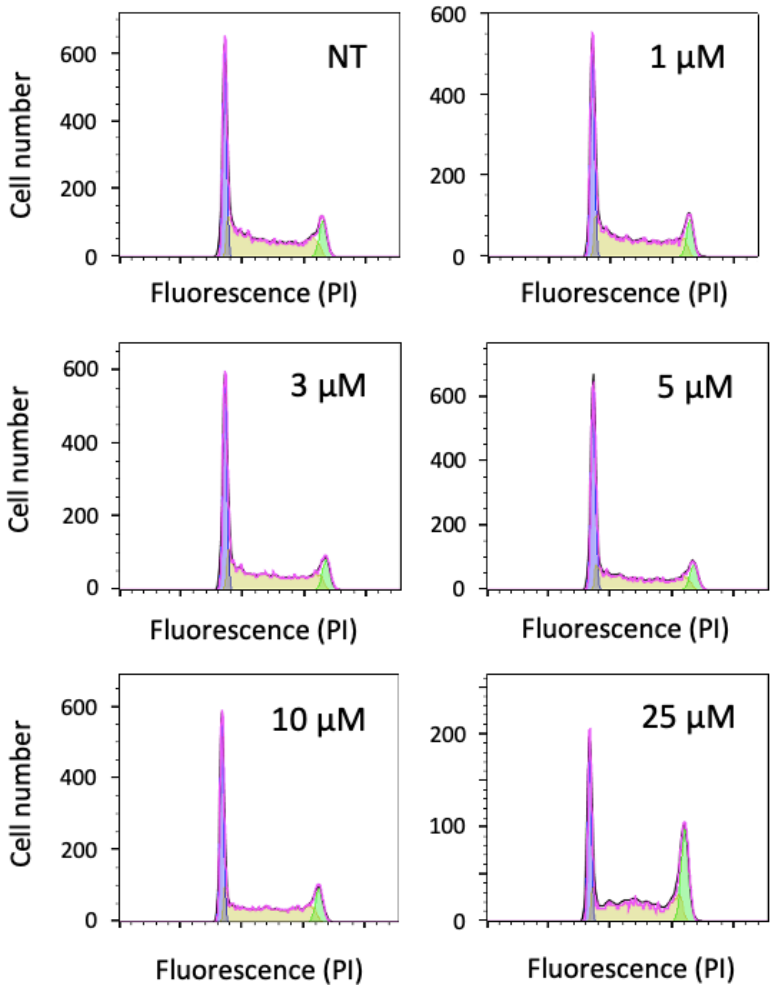

Figure 5. Cell-cycle analysis of NB4 cells treated with increasing concentrations of the POXAPy-macrocycle. Representative histograms obtained by flow cytometric analysis after propidium iodide staining. NT indicates untreated cells, while the other panels correspond to cells exposed to 1, 3, 5, 10, and 25 µM POXAPy-macrocycle for 24 h. The colored peaks represent the G_1 (purple), S (green), and G_2/M (blue) phases of the cell cycle. A concentration-dependent alteration in the cell-cycle distribution can be observed following treatment.

Analysis of the hypodiploid cell fraction revealed a dose-dependent increase in the percentage of hypodiploid cells following 24-hour treatment with POXAPy. As shown in Figure 6A-B, concentrations ranging from 1 to 10 µM induced only a modest increase in the hypodiploid population compared to the untreated control, with values remaining below 8%. However, exposure to 25 µM POXAPy resulted in a marked rise in the percentage of hypodiploid cells, reaching 35.1 ± 1%. These findings suggest that higher concentrations of the compound may promote apoptotic cell death, as indicated by the accumulation of cells with a sub-G1 DNA content.

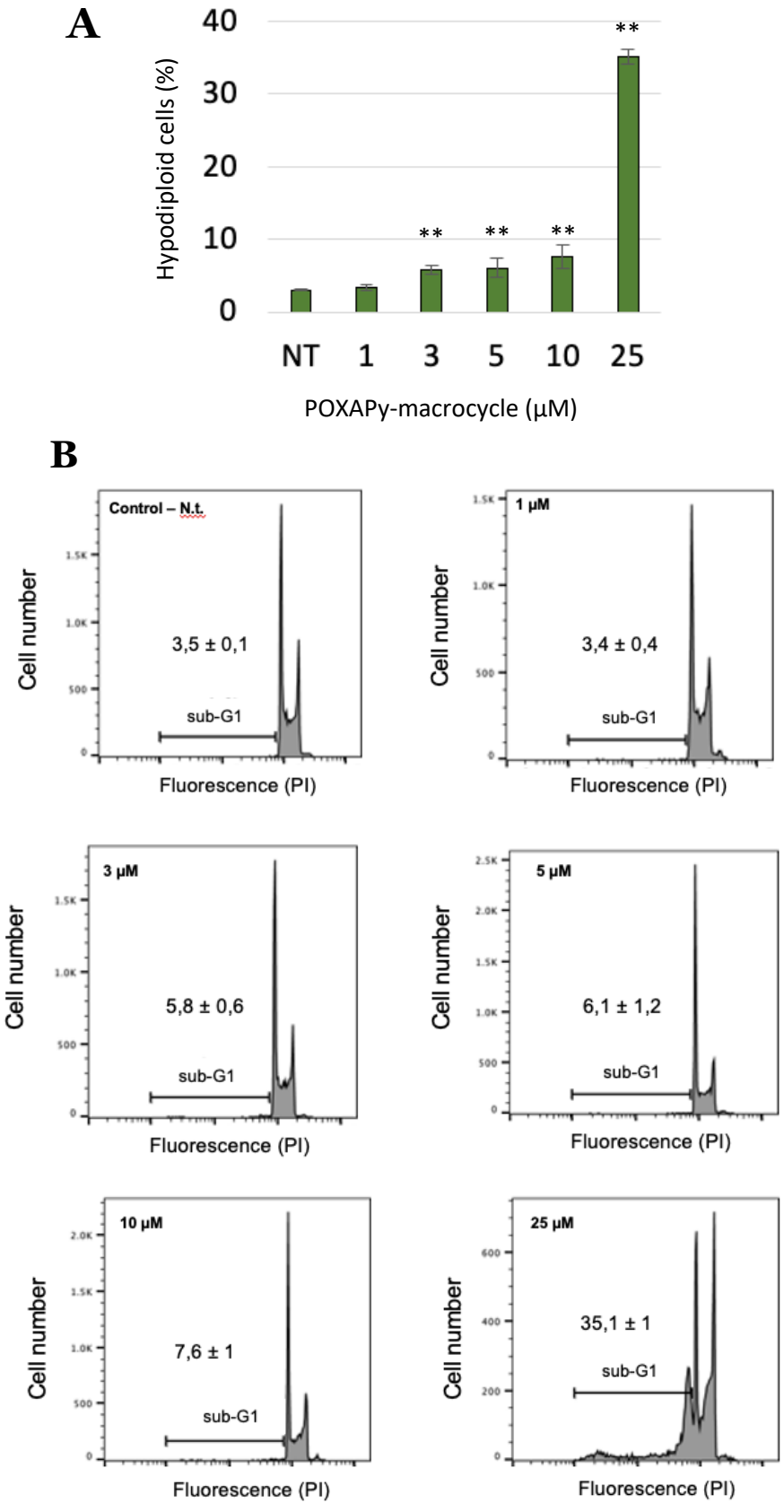

Figure 6. Quantitative analysis of hypodiploid cells in NB4 cultures treated with increasing concentrations of the POXAPy-macrocycle. (A) A dose-dependent increase in the hypodiploid population was observed following treatment. Data are presented as mean ± standard deviation (s.d.) of three independent experiments. Statistical significance

versus non-treated (NT) cells was assessed by Student's *t*-test (**p < 0.01) **(B)** Cell cycle data in logarithmic scale highlighting hypodiploid cells.

The activation of the apoptotic program was confirmed by evaluating the DNA fragmentation by agarose gel electrophoresis following POXAPy treatment. As shown in Fig. 7, exposure of NB4 cells to POXAPy at 25 and 50 μM for 24 hours induced the typical DNA fragmentation (laddering) associated with the apoptosis-related internucleosomal cleavage, which was absent in untreated cells.

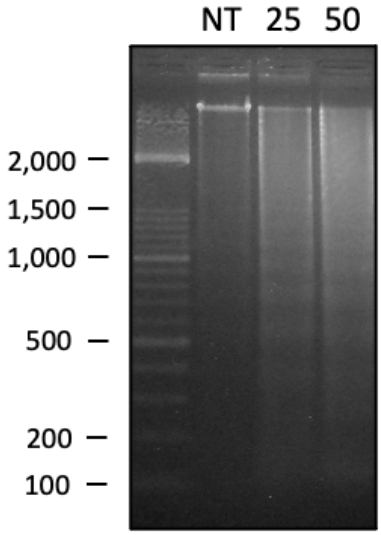

Figure 7. Apoptosis-related DNA fragmentation induced by 24 h POXAPy exposure at the final concentrations of 25 and 50 μM (N.t. = not treated cells)

1.3 Evaluation of the reversibility of POXAPy effect on NB4 cell growth

To investigate whether the growth inhibition induced by POXAPy was reversible, NB4 cells were treated with increasing concentrations of the compound (10, 17.5, and 25 μM) for 24 hours. After this period, the medium containing POXAPy was removed, and cells were washed and cultured in fresh drug-free medium for an additional 48 hours. Cell viability was monitored throughout the experiment to assess post-treatment recovery.

As shown in Figure 8, untreated (NT) cells exhibited continuous exponential growth over the entire experimental period, reaching approximately a tenfold increase in viable cell number after 72 hours. In contrast, exposure to POXAPy resulted in a clear, dose-dependent inhibition of proliferation.

Cells treated with 10 µM POXAPy showed a transient growth arrest during the initial 24-hour treatment phase but were able to resume proliferation after compound removal, as indicated by the gradual increase in viable cell number at 24h and 48h post-wash-out. This behavior suggests that 10 µM POXAPy exerts a reversible and sub-lethal cytostatic effect.

Conversely, at 17.5 µM and 25 µM, POXAPy treatment led to a persistent loss of viability, even after the compound was removed. In these conditions, the viable cell count continued to decline, indicating that cell death was already irreversibly triggered during the 24-hour exposure phase.

Overall, these results demonstrate that POXAPy induces dose-dependent cytostatic and cytotoxic effects in NB4 cells, with 10 µM representing a threshold concentration below which the growth inhibition remains reversible. Based on these observations, the 10 µM concentration was selected for all subsequent experiments.

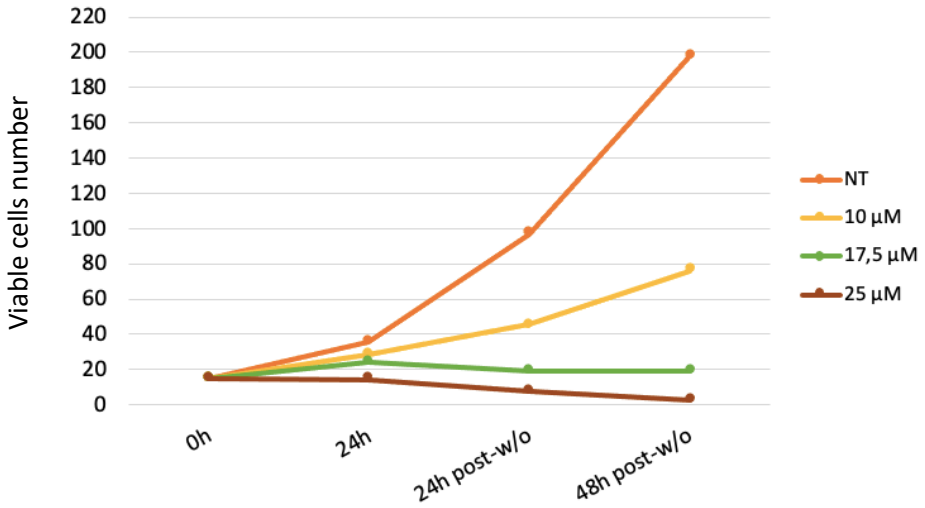

Figure 8. Cell growth curves of NB4 cells after POXAPy wash-out. Cells were treated with increasing concentrations of POXAPy (10, 17.5, and 25 µM) for 24 h, then washed and cultured in drug-free medium for up to 48 h. Cell proliferation resumed only at 10 µM, indicating a reversible, sub-lethal effect.

2. Gene expression modulation in NB4 cells

The gene expression profile of the NB4 cells was analyzed to define the biological response of POXAPy-macrocycle. The experiment was performed in three biological replicates of not treated and treated cells with 10, 17.5 and 25 μM of POXAPy-macrocycle for 24 hours where, after RNAs extraction, they were sequenced and analyzed.

Multidimensional scaling (MDS) analysis was performed on the transcriptomic profiles of NB4 cells treated with the POXAPy-macrocycle to assess global similarities and differences among samples. As shown in Figure 9, the MDS plot clearly separates untreated (NT) samples from treated ones along the first dimension, which accounts for most of the variance. Samples treated with 10 μM and 17.5 μM POXAPy-macrocycle form distinct clusters, indicating a dose-dependent transcriptional response. The strong separation between treated and untreated groups demonstrates that POXAPy-macrocycle exposure significantly affects global gene expression patterns in NB4 cells.

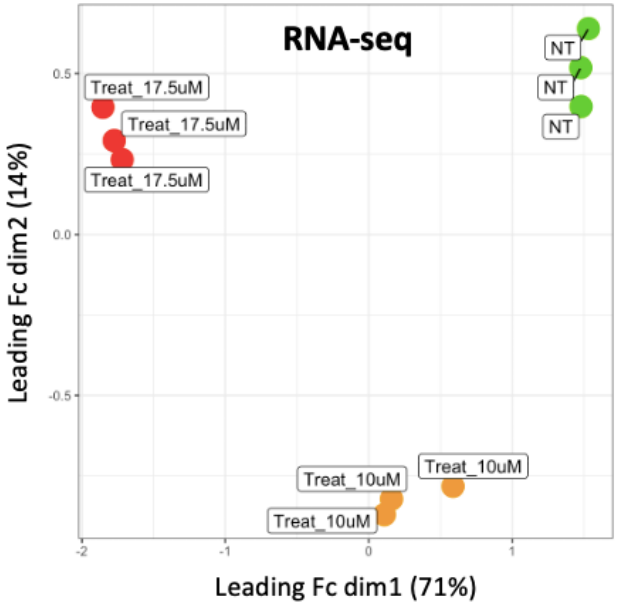

Figure 9. Multidimensional scaling (MDS) analysis. MDS analysis comparing NB4 cells untreated (NT) or treated with the reported concentrations of POXAPy-macrocycle.

The heatmap in Figure 10 illustrates the expression profile of selected genes (or the most variable/differentially expressed genes) across untreated (NT) and POXAPy-treated (10 μM) NB4 samples. The color scale (Z-score) indicates relative gene expression: red tones for up-regulation (higher expression) and blue tones for down-regulation (lower expression) compared to the mean.

In this case, untreated and treated samples clearly segregate, indicating that POXAPy treatment induces a consistent shift in gene expression. Several clusters of genes show up-regulation upon treatment, while others are down-regulated, suggesting distinct transcriptional responses to the compound.

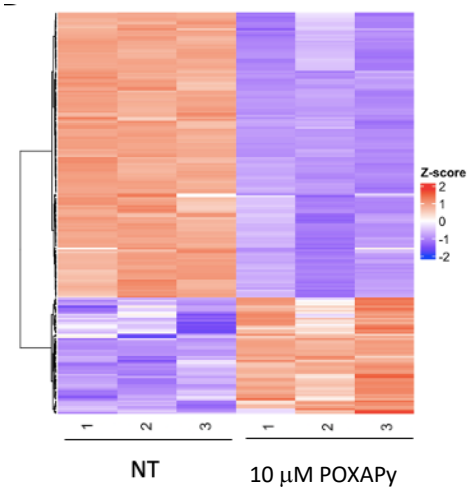

Figure 10. Hierarchical clustering heatmap of all DEGs (FDR ≤ 0.05) of untreated and 10 μM POXAPy-treated cells. As reported in the color key, positive Z-scores (red) are associated with higher expression values while negative Z-scores (blue) indicate a lower expression value.

Differential enrichment analysis allowed the identification of 200 differentially expressed genes (DEGs) as significantly affected, among which 142 genes were down- and 58 up-regulated genes, as reported in the volcano plot shown in Figure 11A. The DEGs were analyzed for pathway enrichment using the iPathwayGuide software. According to results, we found two pathways as significantly enriched (Figure 11B): mTORC1 signaling ($p < 0.01$) and unfolded protein response ($p < 0.01$). These pathways are inhibited by POXAPy-macrocycle exposure, as suggested by the downregulation of their related genes.

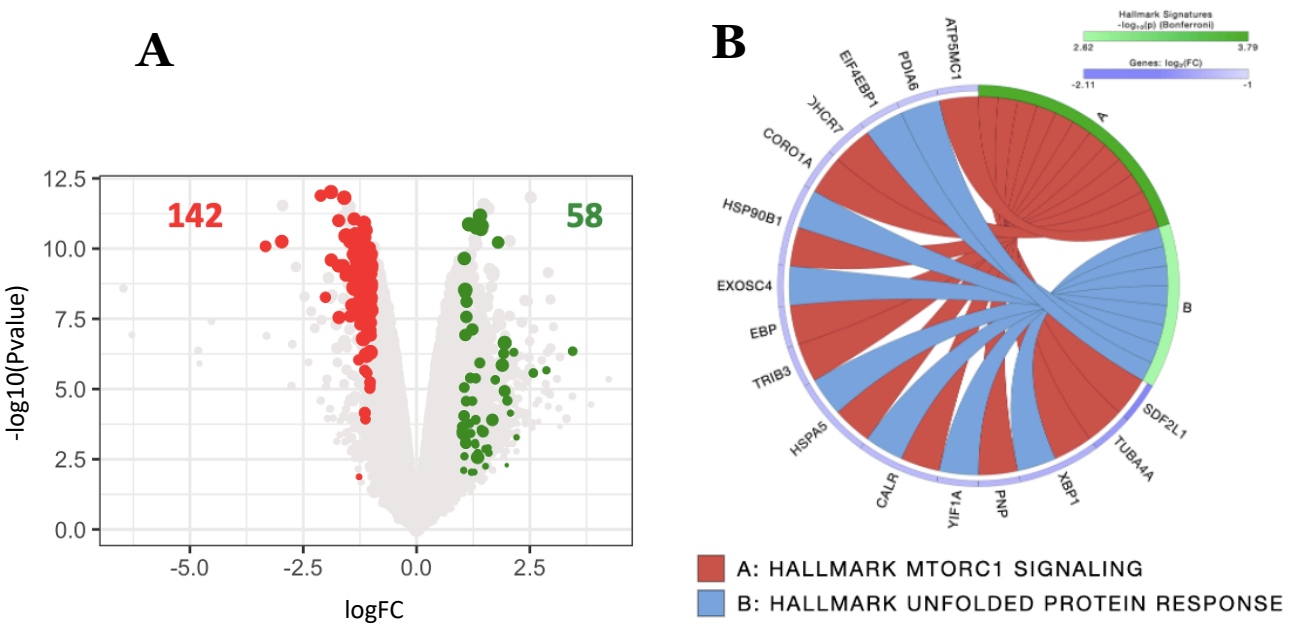

Figure 11. Volcano plot and iPathwayGuide analysis of 10 µM POXAPy-treated cells. (A) Volcano plot of DEGs obtained comparing untreated and 10 µM monster-treated cells. Significantly downregulated genes are shown in red, while up-regulated genes are shwon in green. **(B)** Circos plot showing the pathways found modulated using the Molecular Signatures Database (MSigDB) Hallmark signatures and relative DEGs obtained comparing untreated and monster-treated NB4 cells. Pathways were considered significantly enriched when p<0.01 and are reported in figure.

Exposure of NB4 cells to the dose of 17.5 µM POXAPy-macrocycle for 24 h induced, even in this case, a strong remodulation of the gene expression profile, as indicated by the hierarchical clustering (Euclidian distance) analysis (Figure 12A). Differential enrichment analysis allowed the identification of 725 down- and 207 up-regulated genes, as reported in the volcano plot shown in Figure 12B. iPathwayGuide analysis of DEGs showed that four pathways were significantly enriched by POXAPy-macrocycle treatments: Myc targets V1 ($p < 0.01$), mTORC1 signaling ($p < 0.01$), oxidative phosphorylation ($p < 0.01$) and Myc targets V2 (Figure 12C).

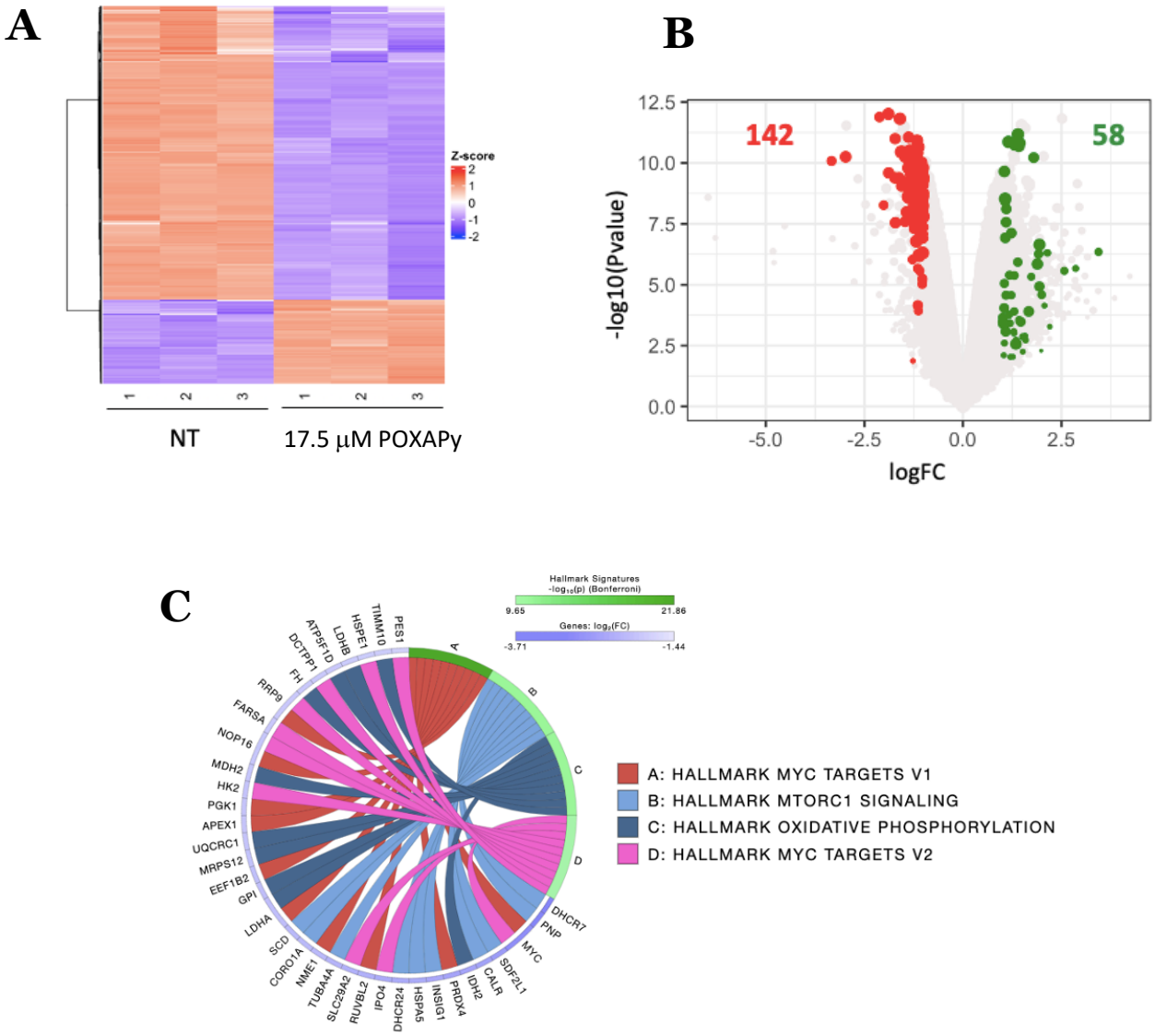

Figure 12. Genome-wide analysis of the transcripts modulations induced by lethal doses of POXAPy (17.5 µM) in NB4 cells. NB4 cells were treated or left untreated for 24 h and analyzed by RNA-seq. All experiments have been conducted in triplicate. **(A)** Hierarchical clustering heatmap of all DEGs (FDR ≤ 0.05) of untreated and treated cells. As reported in the color key, positive Z-scores (red) are associated with higher expression values while negative Z-scores (blue) indicate a lower expression value. **(B)** Volcano plot of DEGs obtained comparing untreated and 17.5 µM POXAPy-treated cells. Significantly downregulated genes are shown in red, while up-regulated genes are shown in green. **(C)** Circos plot showing the pathways found modulated using the Molecular Signatures Database (MSigDB) Hallmark signatures and relative DEGs obtained comparing untreated and treated NB4 cells. Pathways were considered significantly enriched when $p<0.01$ and are reported in figure.

2.1 Proteomic analysis of POXAPy-treated NB4 cells

Following the transcriptomic analysis, a mass spectrometry-based proteomic approach was employed to further explore the global protein alterations induced by POXAPy-macrocycle treatment.

Proteomic alterations induced by 10 µM POXAPy-macrocycle were investigated by combining heatmap and volcano plot analyses with pathway enrichment analysis performed using iPathwayGuide, in order to identify the most significantly modulated biological processes.

As shown in Fig. 13, principal component analysis (PCA) grouped the quadruplicates into distinct clusters according to the treatments (NT, 10 µM and 17.5 µM). PCA shows that principal component 1 (PC1), which explains 31.97% of total variability of our dataset, is driven by the treatment, while PC2 (17.14%) variation seems to be related to intragroup variability. These results confirm the strong impact of POXAPy-macrocycle on protein expression, in line with transcriptomic findings.

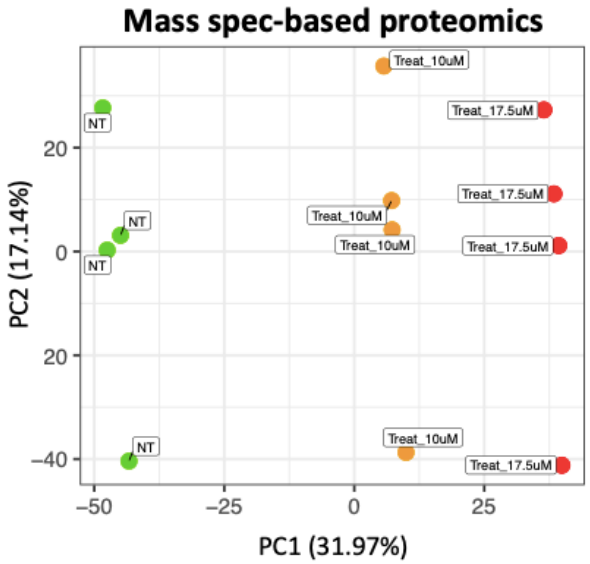

Figure 13. Multidimensional scaling (MDS) analysis. MDS analysis comparing NB4 cells untreated (NT) or treated with the reported concentrations of POXAPy-macrocycle.

Regarding the modulations induced by the 10 µM condition, hierarchical clustering (Euclidean distance) revealed a clear segregation of triplicates between untreated and POXAPy-macrocycle–treated NB4 cells, confirming a marked treatment-induced effect (Figure 14).

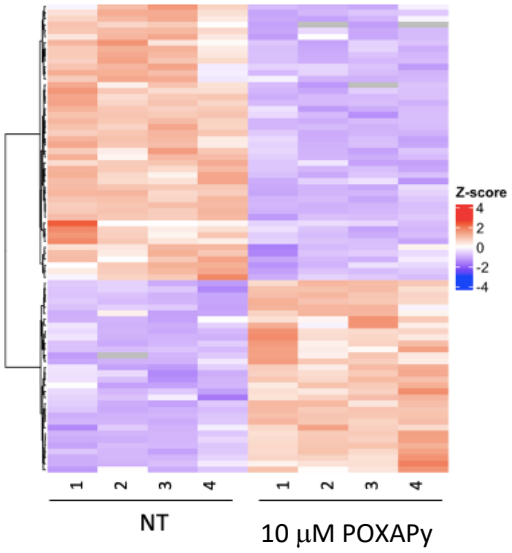

Figure 14. Hierarchical clustering heatmap of all DEPs (FDR ≤ 0.05) of untreated and 10 µM POXAPy-treated cells. As reported in the color key, positive Z-scores (red) are associated with higher expression values while negative Z-scores (blue) indicate a lower expression value.

Volcano plot in Figure 15A shows a total of 78 proteins as significantly regulated by POXAPy exposure, among which 46 were down- and 32 up-regulated. Analysis of DEPs with iPathwayGuide revealed a significant modulation of two key pathways (Figure 15B), PI3K/AKT/mTOR signaling and the G2/M checkpoint ($p < 0.01$), in which the majority of proteins were found to be downregulated.

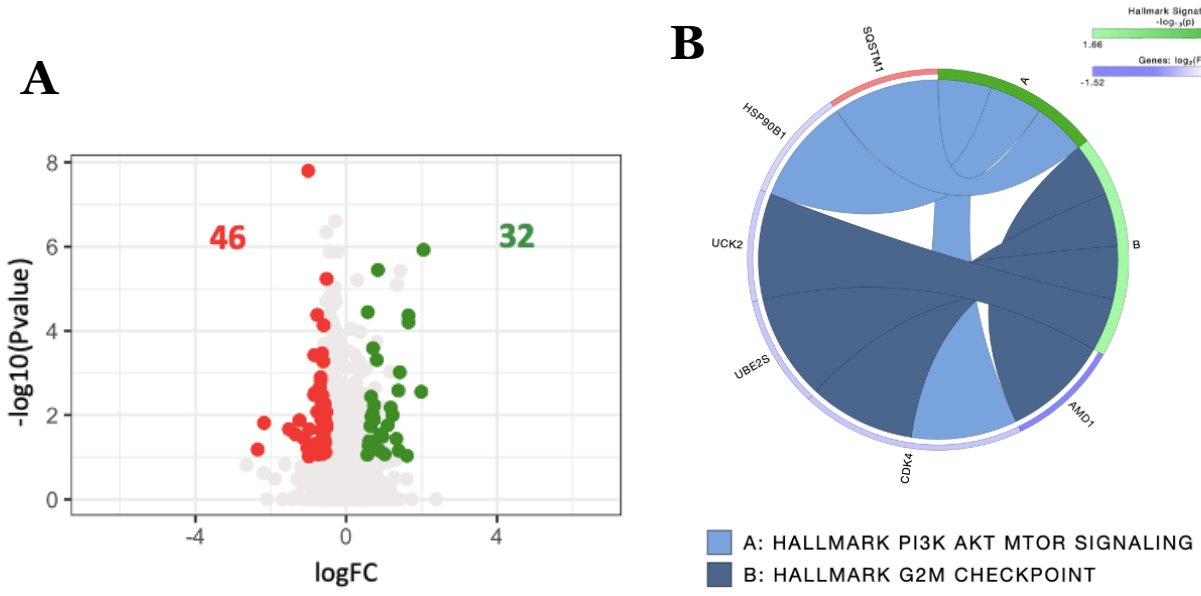

Figure 15. Genome-wide analysis of the protein modulations induced by POXAPy (10 µM) in NB4 cells. (A) Volcano plot of DEPs obtained comparing untreated and 10 µM POXAPy-treated cells. Significantly downregulated genes are shown in red, while up-regulated genes are shown in green. **(B)** Circos plot showing the pathways found modulated

using the Molecular Signatures Database (MSigDB) Hallmark signatures and relative DEGs obtained comparing untreated and treated NB4 cells. Pathways were considered significantly enriched when p<0.01 and are reported in figure.

We extended our analysis to evaluate the global protein-level effects induced by the 17.5 µM POXAPy treatment, which revealed a strong remodeling of the expression profile, as shown by the hierarchical clustering (Euclidean distance) analysis in Figure 16.

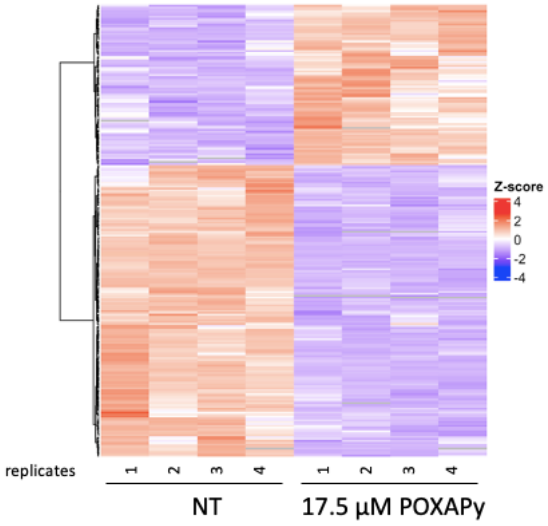

Figure 16. Hierarchical clustering heatmap of all DEPs (FDR ≤ 0.05) of untreated and 17.5 µM POXAPy-treated cells. As reported in the color key, positive Z-scores (red) are associated with higher expression values while negative Z-scores (blue) indicate a lower expression value.

As shown in the volcano plot (Figure 17A), differential enrichment analysis identified 155 downregulated and 85 upregulated genes. iPathwayGuide analysis of DEPs confirmed the enrichment of the same pathways observed at 10 µM, including G2M checkpoint and PI3K-AKT-mTOR signaling (Figure 17B).

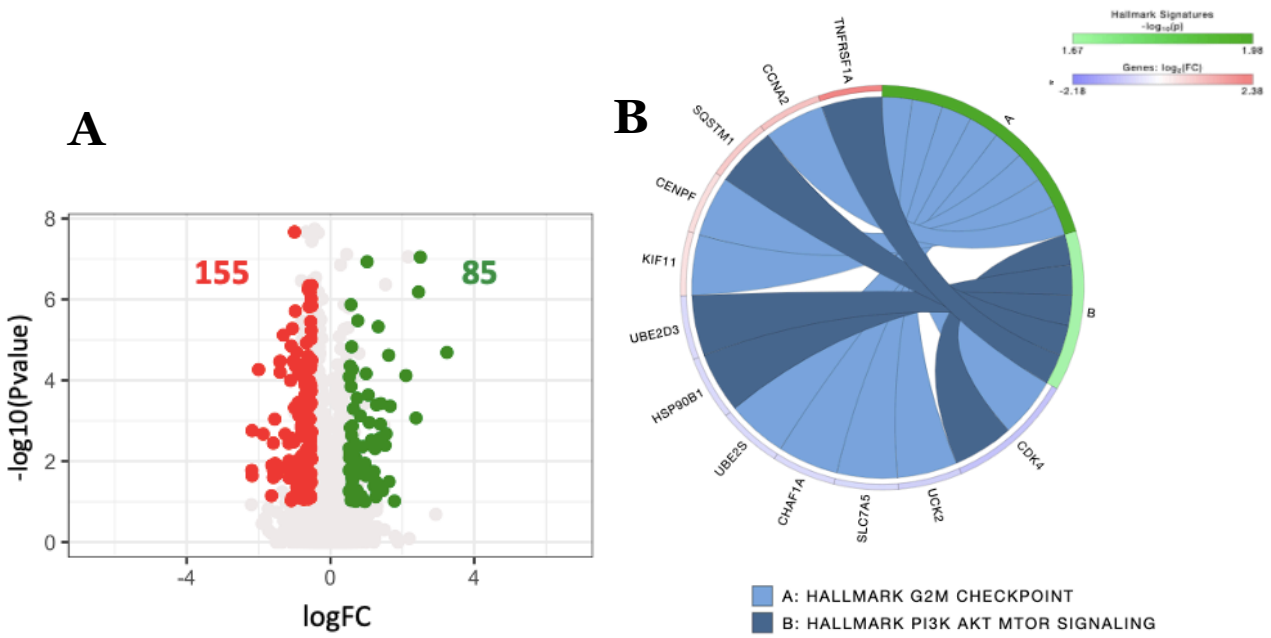

Figure 17. Genome-wide analysis of the protein modulations induced by POXAPy (17.5 µM) in NB4 cells. (A) Volcano plot of DEPs obtained comparing untreated and 17.5 µM POXAPy-treated cells. Significantly downregulated genes are shown in red, while up-regulated genes are shown in green. **(B)** Circos plot showing the pathways found modulated using the Molecular Signatures Database (MSigDB) Hallmark signatures and relative DEGs obtained comparing untreated and treated NB4 cells. Pathways were considered significantly enriched when p<0.01 and are reported in figure.

Mass spectrometry analysis was also performed to evaluate the effects induced by the 25 µM POXAPy treatment, which revealed a marked remodeling of the protein expression profile (Figure 18A). A total of 324 downregulated and 133 upregulated proteins were identified (Figure 18B). In this condition, the pathways significantly enriched by monster exposure ($p < 0.01$) included Myc targets V2, G2M checkpoint, PI3K-AKT-mTOR signaling, DNA repair, and E2F targets (Figure 18C).

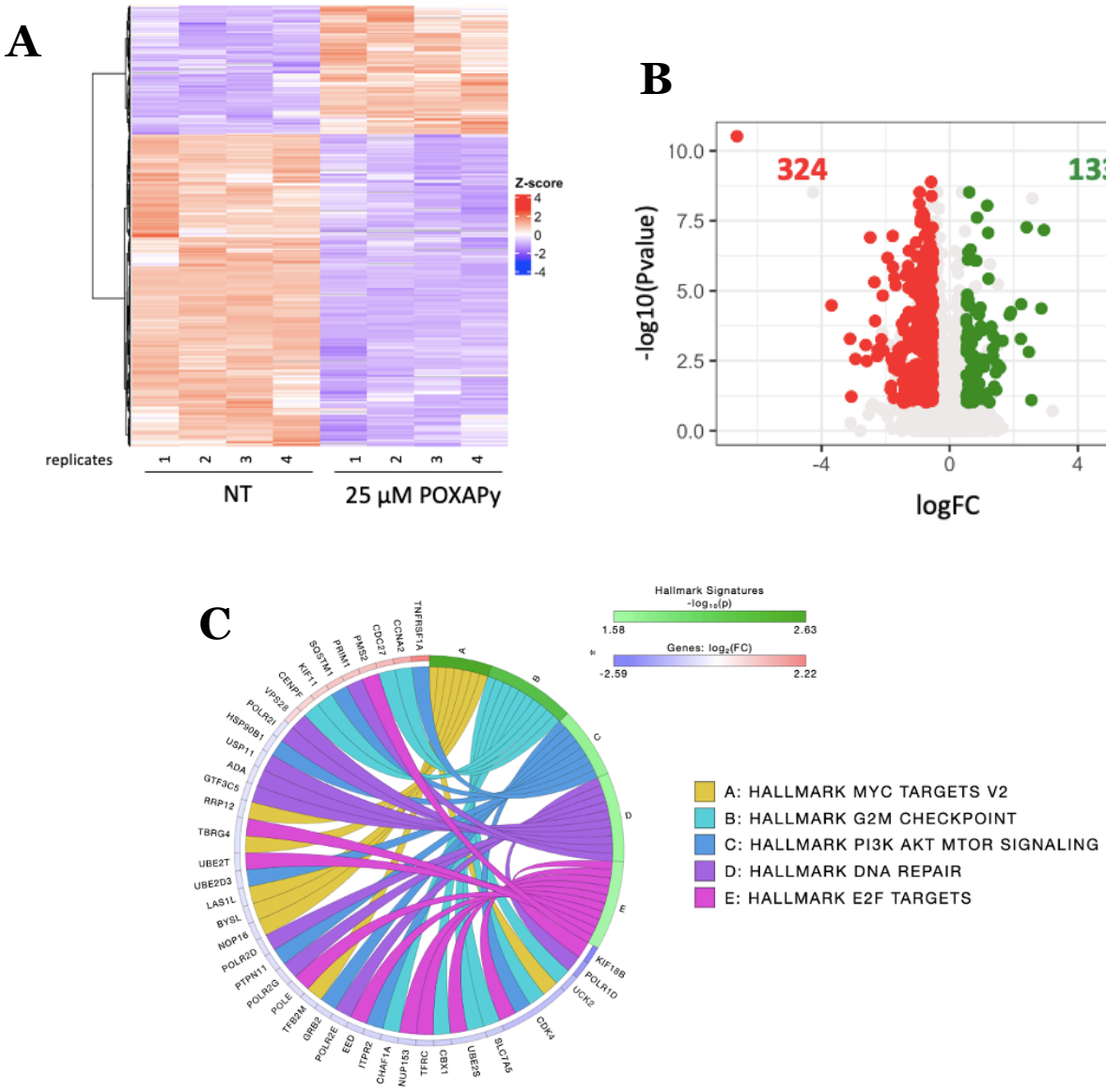

Figure 18. Genome-wide analysis of the protein modulations induced by lethal doses of POXAPy 25 µM in NB4 cells. NB4 cells were treated with monster or left untreated for 24 h and analyzed by mass spectrometry-based proteomics. All experiments have been conducted in triplicate. **(A)** Hierarchical clustering heatmap of all DEPs (FDR ≤ 0.05) of untreated and treated cells. As reported in the color key, positive Z-scores (red) are associated with higher expression values while negative Z-scores (blue) indicate a lower expression value. **(B)** Volcano plot of DEPs obtained comparing untreated and treated cells. Significantly downregulated genes are shown in red, while up-regulated genes are shwon in green. **(C)** Circos plot showing the pathways found modulated using the Molecular Signatures Database (MSigDB) Hallmark signatures and relative DEPs obtained comparing untreated and treated NB4 cells. Pathways were considered significantly enriched when $p<0.01$ and are reported in figure.

2.2 Modulation of the mTOR Signaling Pathway following POXAPy-macrocycle exposure

Consistent with transcriptomic and proteomic data indicating a downregulation of the mTOR pathway, we further investigated the effects of POXAPy-macrocycle on total and phosphorylated mTOR protein levels by Western blot analysis. NB4 cells were treated with a sublethal concentration of 10 μM POXAPy-macrocycle for 24 hours, and changes were also monitored at intermediate time points (2, 4, and 8 hours). A reduction in total mTOR protein became evident after 8 hours of treatment (0.60-fold), while a marked decrease in mTOR phosphorylation was detected only after 24 hours (0.43-fold) (Figure 19A-C).

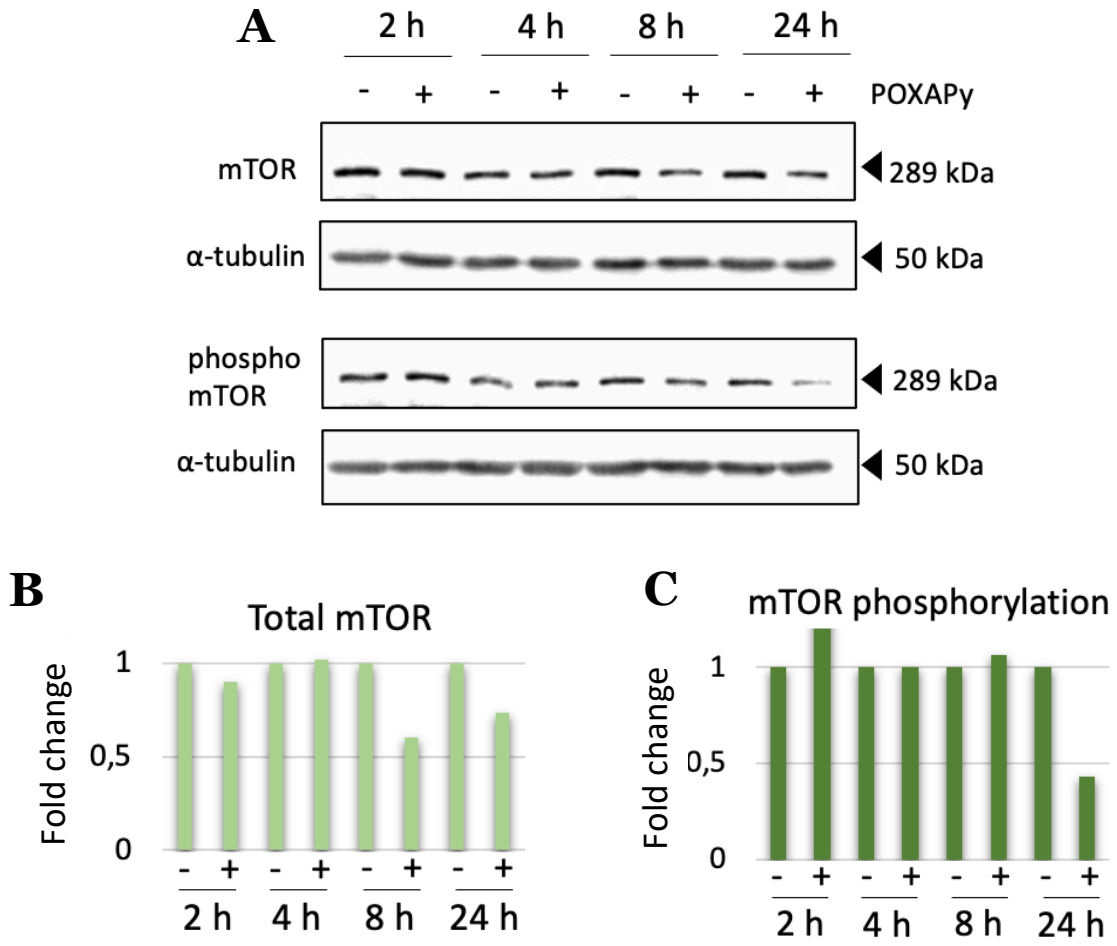

Figure 19. POXAPy-induced inhibition of mTOR signaling pathway. NB4 cells were treated with 10 μM POXAPy-macrocycle or left untreated, collected at the reported timings and analyzed by Western blotting. **(A)** Changes induced by POXAPy-macrocycle to total mTOR abundance and mTOR phosphorylation in NB4 cells. **(B,C)** Densitometric analysis was conducted, and fold change was calculated normalizing using tubulin or total mTOR for, respectively, total mTOR and mTOR phosphorylation.

2.2 Regulation of ERK/MAPK signaling pathway following POXAPy-macrocycle treatment

Following the analysis of mTOR signaling, we next investigated the regulation of the ERK pathway. Given the well-established crosstalk between the RAF/MEK/ERK and PI3K/AKT/mTOR cascades, both known to drive tumor growth and survival, their coordinated modulation represents a key element in anticancer response mechanisms (Li et al., 2022; McCubrey et al., 2006).

In line with proteomic data showing a 0.49-fold decrease in ERK abundance upon 10 µM POXAPy-macrocycle treatment, Western blot analysis demonstrated a clear downregulation of total ERK levels starting from 4 hours (Figure 20A–C). Notably, a pronounced reduction in ERK phosphorylation was observed as early as 2 hours after exposure, confirming the rapid impact of the molecule on this signaling pathway.

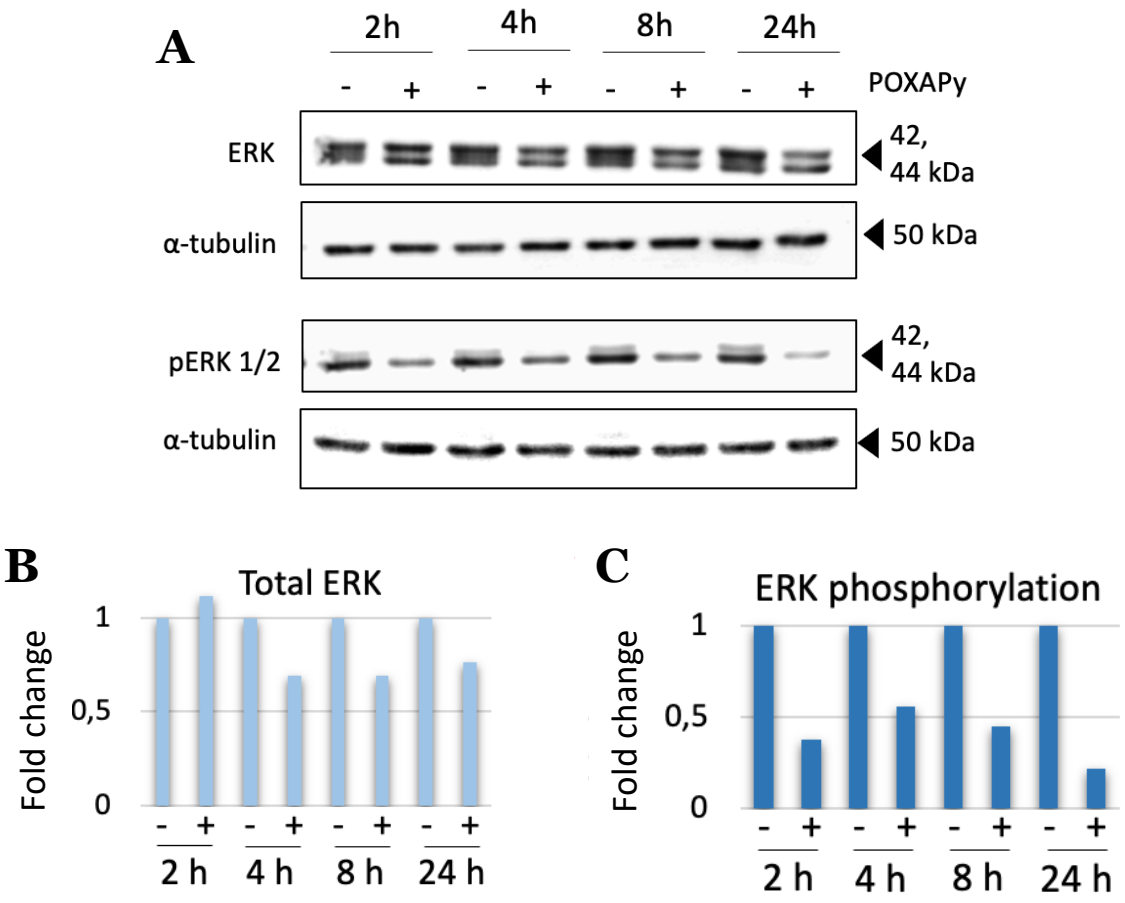

Figure 20. POXAPy-induced inhibition of ERK/MAPK signaling pathways. NB4 cells were treated with 10 µM POXAPy-macrocycle or left untreated, collected at the reported timings and analyzed by Western blotting. **(A)** Evaluation of changes induced by monster to total ERK and ERK phosphorylation in NB4 cells. **(B,C)** Densitometric analysis and fold change calculation normalizing using tubulin or total ERK for, respectively, total ERK and ERK phosphorylation.

2.3 POXAPy-macrocycle triggers autophagy in NB4 cells

Given the observed inhibition of the mTOR pathway — a well-known regulator of autophagy — we next sought to determine whether POXAPy-macrocycle treatment could trigger an autophagic response in NB4 cells. These catabolic pathways play a crucial role in maintaining cellular homeostasis and have been extensively associated with the response of cancer cells to stress and anticancer treatments.

Cells were treated with 10 µM POXAPy for 24 hours and, in parallel, analyzed also at intermediate time points (2, 4, and 8 hours). The first focus was placed on the accumulation of LC3B, a ubiquitin-like protein that is part of the core autophagic machinery and is widely recognized as a key marker of autophagy. As expected, LC3B levels started to increase as early as 2 hours after treatment, showing a progressive accumulation that reached a 531-fold induction at 24 hours. As a positive control for autophagy, cells were treated with chloroquine (C), a well-known inhibitor of autophagosome degradation, which induces LC3B accumulation by blocking the late stages of the autophagic flux (Figure 21A-B).

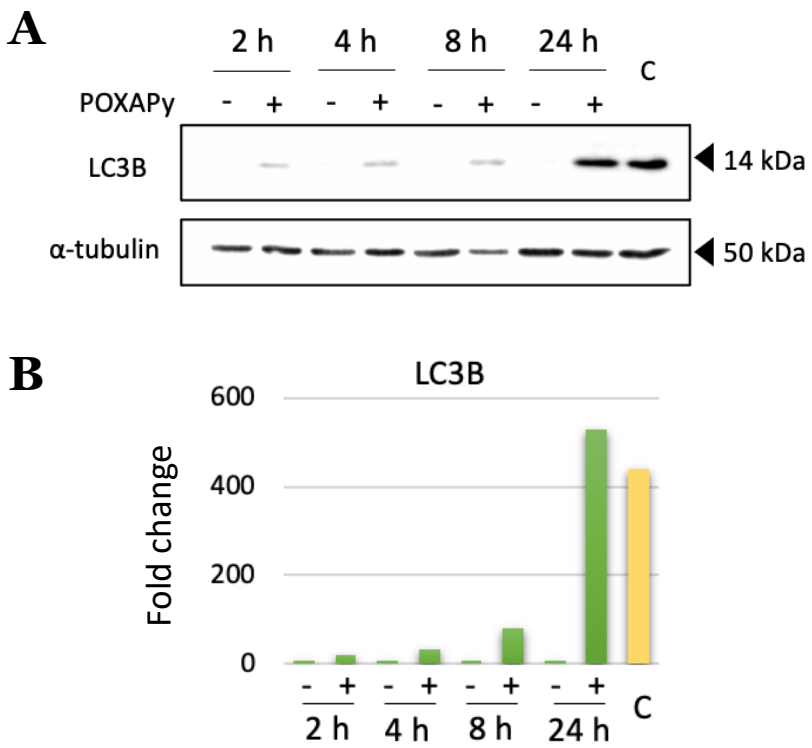

Figure 21. Evaluation of POXAPy-macrocycle ability to activate autophagic marker in NB4 cells. (A) NB4 cells were treated for 24 h at the final concentration of 10 µM, and total cell lysates were analysed for LC3B abundance by Western blotting. NB4 cells treated with chloroquine were used as a positive control of LC3B accumulation. **(B)** LC3B fold

change induction was estimated by a densitometric analysis and normalized using α-tubulin expression.

Following the biochemical evidence of LC3B accumulation, ultrastructural analysis of NB4 cells treated with 10 μM POXAPy was performed by transmission electron microscopy (TEM), considered the gold standard for the investigation of the autophagic response (X. Chen et al., 2024). The observations revealed the formation of numerous double-membraned vesicular structures, morphologically consistent with autophagosomes.

In untreated NB4 cells, mitochondria appeared well preserved, displaying an elongated morphology with clearly defined cristae, consistent with a healthy cellular phenotype (Figure 22A). In POXAPy-treated cells, the formation of double- and multi-membrane vesicular structures was clearly observed, consistent with the presence of autophagosomes (Figure 22B). In Figure 22C, transmission electron microscopy revealed the presence of vesicular structures with a characteristic double membrane, often enclosing cytoplasmic components and organelles. In several cases, mitochondria appeared partially or completely surrounded by these electron-dense double-membrane structures, suggesting the occurrence of mitophagy events triggered by POXAPy exposure. In Figure 22D, TEM analysis of POXAPy-treated NB4 cells shows swollen mitochondria that lost the cristae ultrastructure, and engulfment of mitochondria by autophagic membranes. Autolysosomes can be recognized by the presence of a limiting membrane, which separates the contents of the autolysosome from the cytoplasm. Within these vesicles, partially degraded organelles, including mitochondria, can be observed, indicating that POXAPy treatment promotes the sequestration of damaged mitochondria within autophagic compartments, thus suggesting the activation of a mitophagic process.

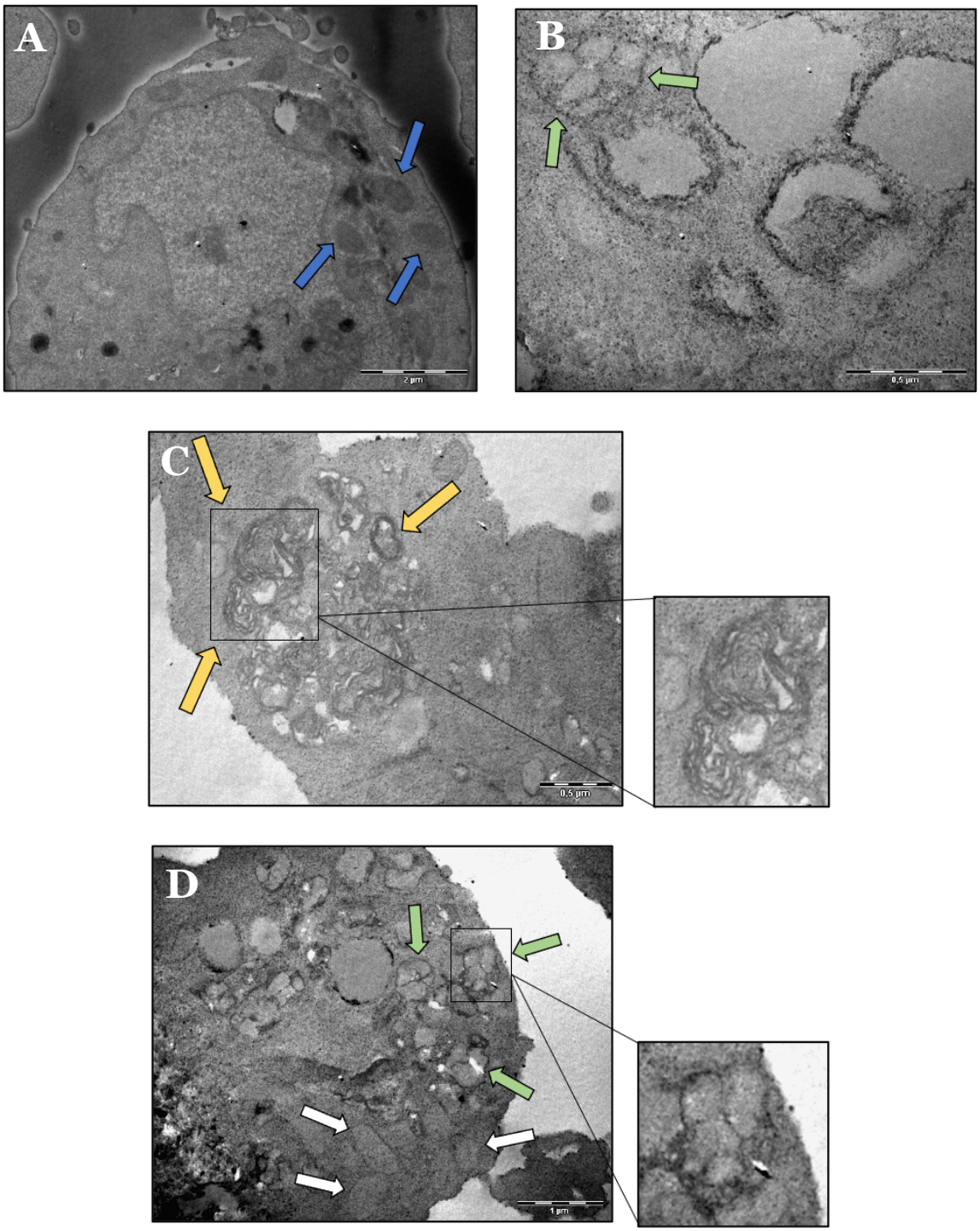

Figure 22. Ultrastructural analysis of NB4 cells by transmission electron microscopy (TEM) following 24 hours of 10 µM POXAPy exposure (A) Not treated NB4 cells. **(B)** POXAPy-treated NB4 cells in which autophagosomes appear as double- or multi-membrane structures (yellow arrows). **(C)** Engulfment of mitochondria by autophagic membranes (green arrows). **(D)** Swollen mitochondria that lost the cristae ultrastructure (white arrows) and engulfment of mitochondria by autophagic membranes (green arrows). Autolysosomes can be recognized by the presence of a limiting membrane, which separates the contents of the autolysosome from the cytoplasm.

2.4 Assessment of ROS production following POXAPy exposure

At the light of the mitochondrial stress and mitophagic response observed by TEM analysis, we next aimed to evaluate whether POXAPy treatment was associated with reactive oxygen species (ROS) accumulation in NB4 cells. To this purpose, intracellular ROS levels were quantified using the fluorescent dye 2',7'-dichlorodihydrofluorescein diacetate (DCFDA) and analyzed by flow cytometry (BD Accuri C6+). As expected, hydrogen peroxide (H_2O_2) was used as a positive control, leading to a strong increase in fluorescence intensity, indicative of robust ROS production.

As shown in Figure 23, POXAPy treatment led to a dose-dependent increase in DCFDA fluorescence, indicating elevated ROS levels at higher concentrations of the compound. Notably, significant ROS accumulation was observed only at 50 and 100 µM, while the increase detected at 10, 17.5, and 25 µM remained modest compared to the control. These results suggest that POXAPy induces oxidative stress only at high concentrations, whereas lower, sub-lethal doses do not cause substantial ROS production.

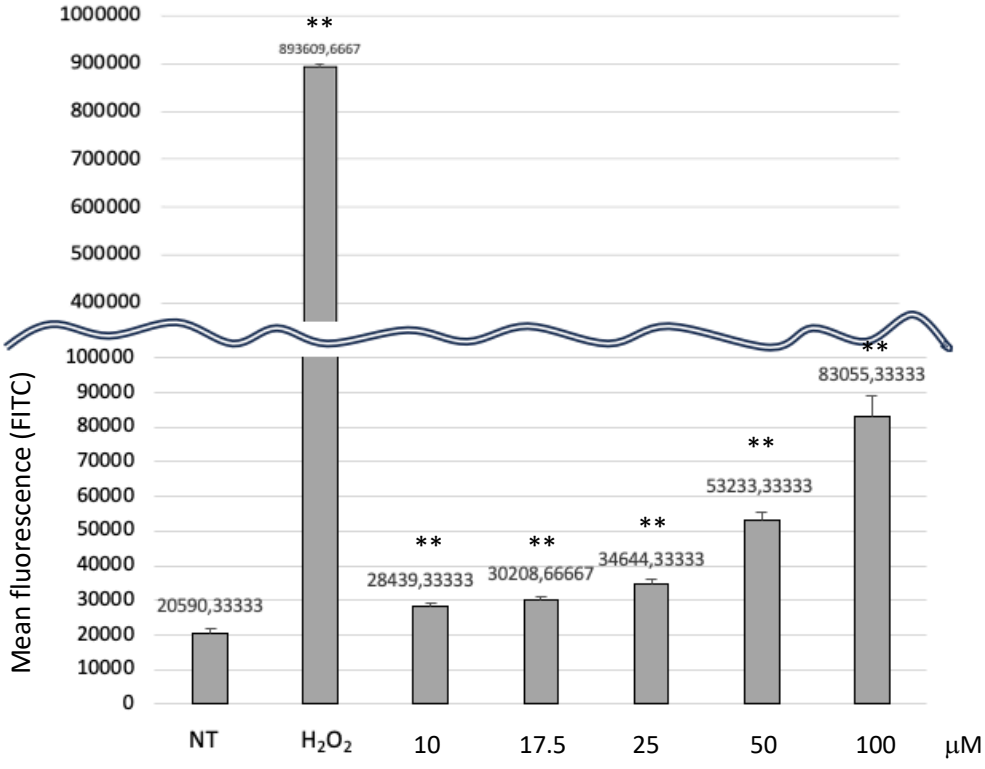

Figure 22. Measurement of ROS levels in NB4 cells after POXAPy treatment. NB4 cells were exposed to increasing concentrations of POXAPy (10–100 µM) for 24 h, and intracellular ROS production was assessed by DCFDA staining followed by flow cytometric analysis (BD Accuri C6+). Hydrogen peroxide (H_2O_2) was used as a positive control, inducing a strong fluorescence signal indicative of oxidative stress. Data are expressed as mean fluorescence intensity (FITC channel), showing a dose-dependent increase in ROS levels upon POXAPy treatment.

3. Evaluation of POXAPy-macrocycle interaction with DNA sequences forming G-quadruplex structures

Several studies from the literature indicate that macrocyclic compounds can interact with and stabilize G-quadruplex DNA structures (Andréasson et al., 2022). Thus, we performed a cell-free melting assay to test whether POXAPy can bind to G-quadruplexes of the c-Kit2 and c-Myc promoter regions. In these experiments, we monitored melting temperature shifts (ΔT_m) upon addition of increasing concentrations of POXAPy, as an indicator of ligand-induced stabilization (Figure 24A–C).

Results revealed that POXAPy can increase the melting temperature of both G4 structures in a concentration-dependent manner, indicating a direct interaction and stabilization of the quadruplex conformation. For the c-Kit2 G4, the ΔT_m ranged from 2.92°C at a 1:5 DNA:POXAPy ratio up to 10.98°C at 1:20. Similarly, for the c-Myc G4, the stabilization effect was even more pronounced, with a ΔT_m of 9.77°C at 1:5 and reaching 17.5°C at 1:15 (Figure 24C).

These results demonstrate that POXAPy strongly interacts with G-quadruplex DNA, especially within the c-Myc promoter sequence, suggesting a potential mechanism through which the compound may exert transcriptional regulation and antiproliferative effects.

A

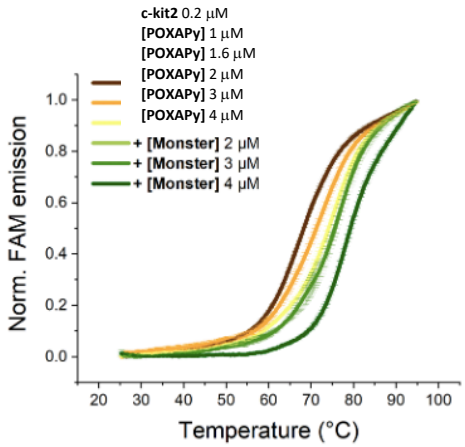

B

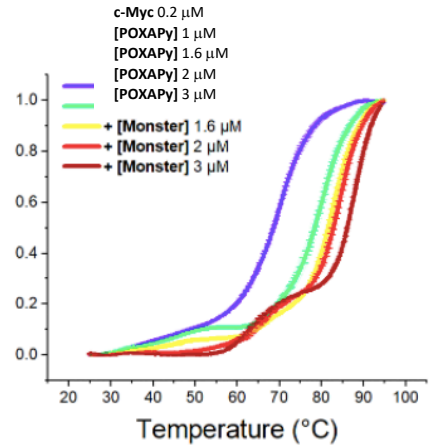

C

dT (°C)	c-Kit2	C-Myc
1:5	2.92	9.77
1:8	5.85	12.99
1:10	7.34	14.21
1:15	7.34	17.5
1:20	10.98	//

(B) structures in the presence of increasing concentrations of POXAPy-macrocycle. The compound induces a dose-dependent stabilization of both G4 sequences, **(C)** as indicated by the progressive increase in melting temperature (ΔT).

To verify the specificity of POXAPy binding toward G-quadruplex structures, two negative controls were included in the thermal denaturation assay. In the first experiment (Figure 25A), the compound was incubated with the human telomeric sequence (h-Telo), which is known to readily form G4 structures. However, unlike what was observed for the c-Myc and c-Kit sequences, the addition of POXAPy did not induce any detectable shift in the melting temperature (T_m), indicating lack of interaction with this specific G-quadruplex conformation. The control compound Maltonis, used as an additional negative control, also did not affect the thermal stability of the sequence.

In the second experiment (Figure 25B), the same analysis was performed using a double-stranded DNA (ds-DNA) sequence, which does not form G4 structures. As expected, neither POXAPy nor Maltonis produced any significant variation in the denaturation curve, confirming that POXAPy selectively interacts with oncogenic G-quadruplex structures and not through unspecific binding to DNA.

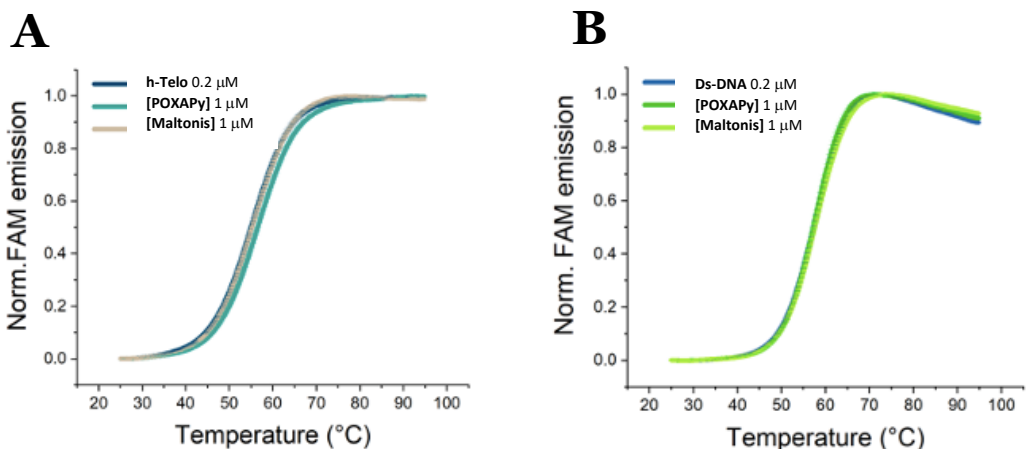

Figure 25. Thermal denaturation profiles of h-Telo (A) and ds-DNA (B) in the presence of POXAPy or Maltonis. No variation in melting temperature (T_m) was observed, confirming the selectivity of POXAPy for oncogenic G-quadruplex structures.

To further explore the binding selectivity of POXAPy toward different G-quadruplex (G4) structures, additional sequences derived from relevant oncogenes were tested in the thermal denaturation assay. As shown in Figures 26A-B, POXAPy was incubated with the Bcl-2 and c-Kit1 sequences both known to form G4 structures. In both cases, the melting profiles did not show any significant temperature shift upon POXAPy addition, indicating lack of interaction between the compound and these G4 topologies.

In contrast, a clear stabilization effect was observed with the c-Kit2 sequence (Figure 26C), where POXAPy induced an evident increase in the melting temperature (ΔT_m), confirming its ability to interact with this G4 motif.

Similarly, in the case of the c-Myc sequence (Figure 26D), POXAPy caused a pronounced temperature shift, while the reference compound Maltonis did not. This demonstrates that POXAPy selectively binds and stabilizes the c-Myc and c-Kit2 G-quadruplexes, whereas it does not interact with Bcl-2 or c-Kit1 G4 structures.

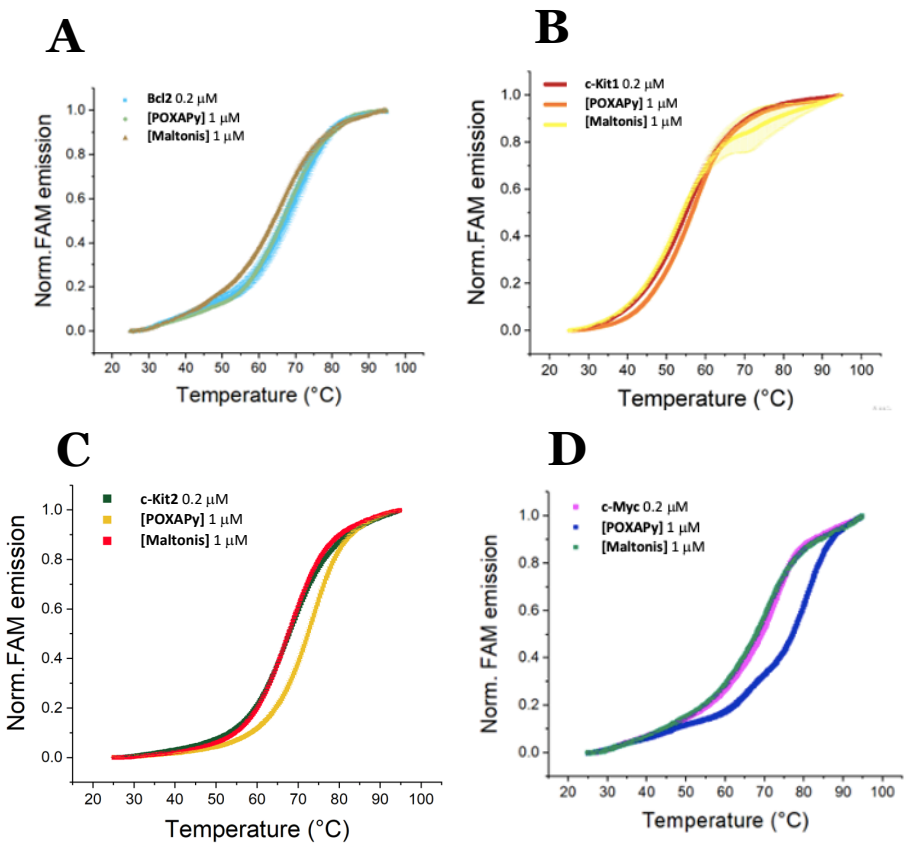

dT (°C)	Ds-DNA	h-Telo	Bcl2	C-Kit1	C-Kit2	SP	C-Myc
POXAPy	-0.02	1.65	-0.81	1.62	**4.54**	-0.71	**7.97**
Maltonis	0.39	0.24	-3.22	-0.85	-0.24	-0.72	-1.25

Figure 26. Thermal denaturation profiles of Bcl-2, c-Kit1, c-Myc e c-Kit2 G-quadruplexes in the presence of POXAPy or Maltonis. POXAPy selectively increases the melting temperature of c-Kit2 and c-Myc, while no interaction is observed with Bcl-2 or c-Kit1 sequences.

3.1 Effect of POXAPy on c-Myc transcript and protein levels

Recent evidence indicates that small molecules and macrocyclic ligands capable of stabilizing G-quadruplex structures can lead to suppression of *c-Myc* expression at the transcriptional and protein levels (Doria et al., 2018; Pomeislová et al., 2020). Therefore, to test whether the binding of POXAPy to the *c-Myc* G4 affects *c-Myc* expression in NB4 cells, we carried out western blot analyses of *c-Myc* protein after treatment with POXAPy.

A marked reduction in Myc transcript levels was detected after 24 h of treatment with POXAPy (Figure 27A). At the sub-lethal concentration of 10 µM, Myc mRNA abundance decreased to 0.33-fold compared to control cells, while a more pronounced reduction was observed at the lethal dose of 17.5 µM, reaching 0.05-fold. Consistently, Myc protein expression was evaluated after 24 h of treatment, showing a clear downregulation at 10 µM and a strongest reduction at 17.5 µM, confirming the dose-dependent effect of POXAPy (Figure 27B).

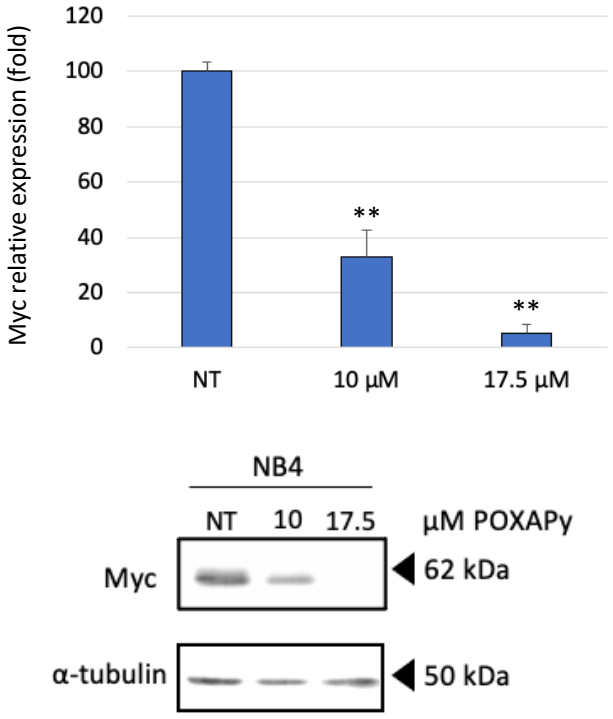

Figure 27. Effect of POXAPy on Myc expression levels in NB4 cells. NB4 cells were treated with increasing concentrations of POXAPy (10 and 17.5 µM) for 24 h. **(A)** Quantitative RT-PCR analysis revealed a reduction in Myc transcript abundance at 10 µM and 17.5 µM. **(B)** Western blot analysis confirmed a dose-dependent decrease in Myc protein levels, with a marked downregulation observed at the lethal dose of 17.5 µM. α-actin was used as a loading control.

3.2 Immunofluorescence with anti-G4 antibody on HeLa cells

Considering the ability of POXAPy to modulate the melting temperature of the c-Myc G-quadruplex motif in cell-free conditions, as well as the observed reduction of both *MYC* transcript and protein levels following treatment, we next performed preliminary experiments to investigate whether such effects could be associated with G4 stabilization at the cellular level.

To this aim, an immunofluorescence (IF) assay was performed in HeLa cells using the anti-G4 antibody BG4 (Merck, MABE917), which specifically recognizes G-quadruplex structures. Pyridostatin (PDS, 10 μM), a well-established G4 stabilizer was included as positive control (Hou et al., 2022; Rodriguez et al., 2008).

As shown in Figure 28, DAPI staining revealed well-defined nuclei in all experimental conditions (NT, PDS, and POXAPy 10 μM). In the FITC channel, corresponding to the BG4 antibody signal, non-treated (NT) cells displayed very weak fluorescence, consistent with the low basal level of stabilized G-quadruplexes in untreated conditions. Upon treatment with PDS, a moderate increase in the nuclear FITC signal was detected, in agreement with its reported ability to stabilize G4 structures. A slight enhancement of the BG4 signal was also observed in cells treated with POXAPy 10 μM compared with NT cells. However, the increase was subtle, and no firm conclusion can be drawn regarding a specific stabilization of G4s by POXAPy under these experimental conditions.

Overall, these preliminary observations suggest that POXAPy treatment may weakly affect G-quadruplex formation or stabilization, although further experiments are required to confirm this potential interaction.

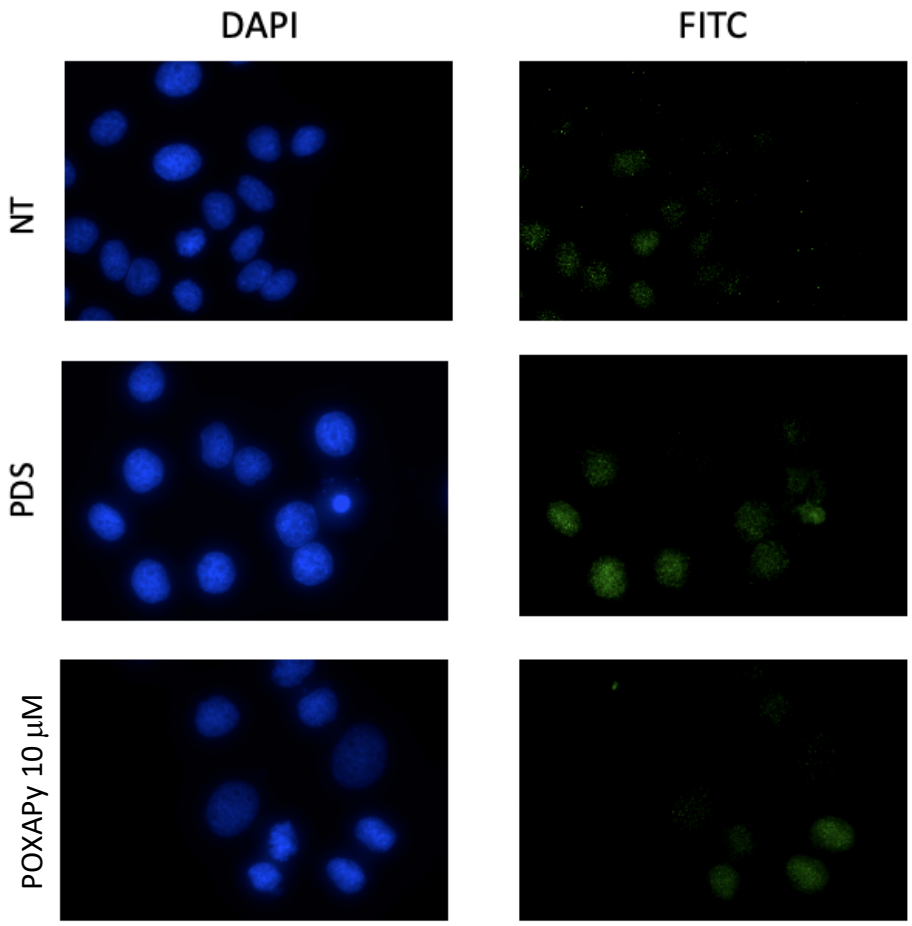

Figure 28. Detection of G-quadruplex structures by immunofluorescence in HeLa cells. Cells were treated for 24 h with POXAPy (10 µM) or with Pyridostatin (PDS, 10 µM) as positive control. Non-treated (NT) cells were used as negative control. Nuclei were stained with DAPI (blue) and G4 structures were detected using the BG4 antibody (FITC channel, green).

DISCUSSION

Macrocyclic polyamines have increasingly gained attention in the field of anticancer drug discovery due to their distinctive structural and physicochemical properties, which can translate into enhanced biological performance. The cyclic arrangement of polyamine chains confers rigidity and preorganization to the molecular scaffold, improving its ability to interact selectively with nucleic acids and metal ions. Moreover, macrocyclic polyamines often display favorable pharmacokinetic profiles, higher cell permeability, and increased stability compared with their linear analogues, making them attractive candidates for therapeutic development (Mallinson & Collins, 2012; Marsault & Peterson, 2011; Song et al., 2023; Yudin, 2015).

In parallel, the incorporation of heterocyclic moieties such as 1,3,4-oxadiazole rings into organic frameworks has emerged as a powerful strategy in medicinal chemistry. Oxadiazole derivatives are known for their planarity, aromaticity, and hydrogen-bonding capacity, properties that facilitate their interaction with diverse biological targets, including DNA, enzymes, and receptors. Numerous studies have reported oxadiazole-containing compounds with antimicrobial, anti-inflammatory, and antitumor activities, suggesting that this heterocycle can act as a key pharmacophoric unit capable of modulating biological functions (Ahsan, 2022; Bajaj et al., 2015; G. Kumar et al., 2024; Vaidya et al., 2021).

The combination of macrocyclic polyamine architecture with oxadiazole functionalities thus represents a promising approach to designing new molecules with multitarget potential. In this context, our work focused on the synthesis and biological characterization of POXAPy, a novel macrocyclic compound bearing oxadiazole rings, with the aim of evaluating its interaction with metal ions, nucleic acid structures, and cellular components potentially involved in cancer-related pathways.

The biological characterization of POXAPy began with the assessment of its antiproliferative potential across a broad panel of human cancer cell lines. To this aim, the compound was first tested within the NCI-60 Human Tumor Cell Line Screen, a standardized assay developed by the Developmental Therapeutics Program (DTP-NCI/NIH) for the identification of novel anticancer agents. This initial screening provided a comprehensive overview of POXAPy activity across different

tumor histotypes, revealing that leukemic and colon carcinoma cell lines were the most sensitive to treatment.

To further deepen this observation, additional in-house experiments were conducted, confirming that among the leukemic models, NB4 cells displayed the highest susceptibility to POXAPy exposure. This cell line, derived from a patient with acute promyelocytic leukemia (APL), represents a well-established model for studying the biological mechanisms underlying this aggressive subtype of acute myeloid leukemia (AML). APL is characterized by the chromosomal translocation *t(15;17)*, which leads to the expression of the oncogenic fusion protein PML-RARα, responsible for the differentiation block of promyelocytes (de Thé et al., 1990; Grignani et al., 1993; Minami et al., 2025; Testa & Pelosi, 2024; Xiao et al., 2024).

Historically, APL was considered one of the most fatal forms of leukemia, until the introduction of all-trans retinoic acid (ATRA) and arsenic trioxide (ATO), which dramatically improved patient survival. Nevertheless, therapy resistance and relapse still occur in a subset of patients, emphasizing the need for alternative or complementary therapeutic strategies (Liang et al., 2021; Rehman & Lübbert, 2025; Yanada, 2024). In this context, the pronounced sensitivity of NB4 cells to POXAPy prompted us to select this model for subsequent molecular and mechanistic investigations.

Time-course and dose-response experiments demonstrated that POXAPy-macrocycle exerts a marked, dose- and time-dependent cytotoxic activity in NB4 cells, confirming the results obtained in the NCI-60 screening and supporting its potential as an antiproliferative agent. This pattern is consistent with the behavior of other macrocyclic or heterocyclic derivatives reported to exert cytostatic or cytotoxic effects through the alteration of DNA or protein functions critical for cell division (Al-Jumaili et al., 2025; Hamad, 2025; Ireson & Kelland, 2006; Negi & Kwatra, 2024).

Importantly, the kinetic profile of POXAPy-macrocycle suggests that its biological activity requires time to manifest fully, possibly due to cellular uptake kinetics or to the progressive induction of DNA structural alterations, which eventually compromise cell proliferation. The stronger effect at higher concentrations might reflect the progressive saturation of molecular targets or the transition from a cytostatic to a cytotoxic mechanism.

Flow cytometric analysis of cell cycle distribution revealed that POXAPy-macrocycle alters the normal cell cycle progression in NB4 cells in a concentration-dependent manner, producing distinct

effects at low and high doses. At low concentrations (≤10 μM), POXAPy induced an accumulation of cells in G1 phase and a decrease of S-phase population, indicative of a G1 arrest and a cytostatic-like response. Such G1 arrest is frequently associated with compounds that interfere with DNA synthesis, metabolic checkpoints, or signaling pathways governing cell cycle entry.

At higher concentrations (≥25 μM), the accumulation of cells in G2/M phase, together with an increase in hypodiploid cells, suggests that POXAPy-macrocycle, beyond a certain threshold, induces DNA damage or checkpoint activation, eventually leading to apoptotic commitment. The increase of the hypodiploid fraction is indeed a hallmark of DNA fragmentation and a typical indicator of apoptosis onset.

The dose-dependent dual behavior observed — cytostatic at low concentrations and cytotoxic at higher doses — highlights that POXAPy-macrocycle's action is not merely due to unspecific toxicity, but likely reflects specific molecular interactions whose downstream consequences depend on the extent of target engagement or DNA perturbation.

The DNA laddering assay confirmed the occurrence of internucleosomal fragmentation — a distinctive feature of apoptotic cell death — only at the highest tested concentrations (25 and 50 μM). This evidence supports the notion that POXAPy-induced apoptosis is a secondary event, activated only when the extent of DNA damage or cell cycle disruption surpasses the cellular repair capacity. This threshold-dependent behavior has been observed for various cytotoxic molecules that primarily exert growth-inhibitory effects at low concentrations and promote apoptosis upon prolonged or high-dose exposure (Fulda & Debatin, 2006; Riccardi & Nicoletti, 2006).

To better define the experimental conditions for molecular characterization, we evaluated the long-term effects of POXAPy exposure on NB4 cell proliferation through a washout assay. This approach allowed us to distinguish between reversible growth inhibition and irreversible cytotoxicity, thus providing a clearer indication of the threshold between cytostatic and lethal effects. The results showed that, after drug removal, cells treated with 10 μM POXAPy were able to resume proliferation, although at a reduced rate compared to untreated controls, suggesting that this concentration primarily exerts a reversible growth-suppressive effect. Conversely, treatments at 17.5 μM and higher doses led to a persistent loss of viability, indicating that the damage induced under these conditions was irreversible and consistent with a cytotoxic outcome. Based on these findings, we confirmed 10

μM as the sub-lethal concentration suitable for investigating the early and reversible molecular alterations associated with POXAPy exposure, while 17.5 μM and above were considered lethal doses inducing cell death.

Thus, we decided to further explore the molecular response induced by POXAPy in NB4 cells by integrating transcriptomic and proteomic approaches. To elucidate the molecular mechanisms underlying the cellular response to POXAPy, we focused our attention on the sub-lethal treatment condition (10 μM for 24 h), which allowed us to investigate adaptive rather than degenerative processes. Under these conditions, we integrated transcriptomic and proteomic analyses to obtain a comprehensive overview of the pathways modulated by the molecule in NB4 cells.

Both datasets revealed a strong convergence in the modulation of genes and proteins belonging to the mTOR signaling cascade, which emerged as one of the most significantly enriched pathways. In particular, several components of the mTOR complex and its upstream regulators were found to be downregulated, suggesting that POXAPy may exert an inhibitory effect on the mTOR axis.

To validate these findings at the biochemical level, we evaluated by Western blotting the expression and activation status of mTOR, monitoring both total protein levels and phosphorylation. The results confirmed a marked reduction in total mTOR expression and a concomitant decrease in its phosphorylation levels, further supporting the hypothesis of a functional attenuation of the mTOR pathway upon POXAPy treatment.

The PI3K/AKT/mTOR signaling cascade is a central regulator of multiple cellular functions, including growth, metabolism, motility, angiogenesis, and survival. Aberrant activation of this pathway has been described in a wide range of human malignancies, where it sustains uncontrolled proliferation and resistance to apoptosis (Le Rhun et al., 2017). Furthermore, the PI3K/AKT/mTOR axis has been extensively studied as a negative regulator of autophagy (P. Wu & Hu, 2010). In addition, serving as an antiapoptotic regulator, the hyperactivation of PI3K/AKT/mTOR axis prevents the initiation of intrinsic pathway mediated apoptosis, provoking resistance to apoptotic signals of cancer cells (Degan & Gelman, 2021). Correspondingly, the suppression of PI3K/AKT/mTOR axis exerts antitumor effects in AML and other leukemia models and enhances chemosensitivity through inducing autophagic cell death and apoptosis (Ma et al., 2019; Mitchell et al., 2018; Swords et al., 2015). Therefore, the observed inhibition of this signaling axis suggests that

POXAPy might interfere with key survival pathways, contributing to its antiproliferative activity in NB4 cells.

Another pathway of interest emerging from our omics analyses under the 10 μM POXAPy treatment, albeit less strongly modulated, was the unfolded protein response (UPR). The UPR is classically triggered by endoplasmic reticulum stress (ERS), which arises when misfolded or unfolded proteins accumulate in the ER lumen. Because the mTOR pathway stimulates protein synthesis, its inhibition can reduce the burden on the ER, thereby attenuating UPR activation. Indeed, downregulation of the UPR may thus be a secondary consequence of mTOR inhibition, contributing to restored proteostasis and reduced proteotoxic stress (Senft & Ronai, 2015).

Regarding the G2/M checkpoint, its enrichment among differentially expressed proteins (DEPs) might appear in apparent contrast with the accumulation of cells in G1 we observed at lower POXAPy concentrations. However, it is important to note that many regulators within the G2/M pathway also participate in earlier cell cycle transitions. For instance, proteins such as CDK4, UBE2S, and UCK2 are implicated not only in G2/M control but also in processes governing the G1–S transition or ubiquitin-mediated regulation of the cell cycle. Thus, the enrichment of the G2/M pathway likely reflects a broad dysregulation of cell cycle progression rather than a strict block at G2/M.

Interestingly, the interplay between mTOR signaling, ER stress, and UPR modulation is known to be tightly connected with the induction of autophagic mechanisms. Under stress conditions, mTOR inhibition can promote the activation of autophagy as a compensatory response aimed at maintaining cellular homeostasis and energy balance. In line with this hypothesis, we next investigated whether POXAPy treatment could activate an autophagic response in NB4 cells, by monitoring key autophagic markers and by performing ultrastructural analysis through transmission electron microscopy (TEM).

Autophagy is a finely regulated catabolic process that allows cells to degrade and recycle cytoplasmic components through the formation of double-membraned vesicles known as autophagosomes. To confirm the activation of autophagy, we monitored the levels of LC3B, a ubiquitin-like protein belonging to the ATG8 family, which plays a key role in autophagosome formation and elongation. LC3B is widely recognized as one of the main molecular markers of autophagy (Gubas & Dikic, 2022). Western blot analysis revealed a progressive accumulation of LC3B in NB4 cells exposed to POXAPy,

starting from the early time points and reaching a marked induction after 24 h of treatment, thus corroborating the activation of an autophagic response.

Autophagy plays a role in stabilizing the internal environment, to promote cancer cell survival, but its induction by external stimuli is considered a promising anticancer strategy (Onorati et al., 2018).

In addition to the mTOR signaling, several nodes of the PI3K/AKT/mTOR cascade are known to be shared or tightly interconnected with another major intracellular pathway, the RAF/MEK/ERK signaling axis. These two pathways are among the most frequently dysregulated in cancer and are involved in the regulation of overlapping cellular processes such as proliferation, survival, differentiation, and stress adaptation. Numerous studies have demonstrated that crosstalk between mTOR and RAF/MEK/ERK allows tumor cells to sustain growth and evade cell death, even in the presence of inhibitory stimuli. Consequently, the dual blockade of both pathways has been proposed as a promising therapeutic approach capable of enhancing anticancer efficacy (Britten, 2013). In this context, the inhibition of mTOR signaling observed upon POXAPy exposure, together with the modulation of ERK detected by proteomic analysis, prompted us to further investigate this pathway at the biochemical level. Western blot analyses confirmed a reduction in total ERK protein levels, accompanied by a decrease in its phosphorylation status, supporting the concomitant inhibition of the RAF/MEK/ERK pathway. Importantly, since mTOR represents a major negative regulator of autophagy, its downregulation by POXAPy provides a plausible mechanistic explanation for the autophagy activation observed in NB4 cells, as evidenced by LC3B accumulation and ultrastructural analyses. Therefore, the data collectively suggest that POXAPy may exert a dual inhibitory effect on two fundamental oncogenic signaling axes—PI3K/AKT/mTOR and RAF/MEK/ERK—culminating in cell growth arrest and the induction of autophagic processes.

Consistent with proteomic findings and LC3B accumulation detected by Western blotting, transmission electron microscopy (TEM) analyses further confirmed the activation of autophagy in NB4 cells exposed to POXAPy. TEM micrographs revealed a marked increase in double-membrane autophagosomes, indicating the onset of a well-organized autophagic process. In addition, the ultrastructural evaluation identified mitochondrial degeneration as one of the major alterations induced by POXAPy treatment. Treated cells exhibited swollen mitochondria with disrupted or lost cristae, frequently enclosed within double-membrane vesicles resembling autophagosomes, strongly

suggesting the engulfment of mitochondria by autophagic membranes and, consequently, the activation of mitophagy. Mitochondrial quality control through mitophagy is a crucial cellular mechanism for maintaining homeostasis under stress conditions. Dysregulated mitochondria can produce excessive mitochondrial reactive oxygen species (mtROS), which act as both signaling molecules and potential sources of oxidative damage. Indeed, mtROS elevation has been associated with mitophagy induction, in line with the observed increase in ROS levels in POXAPy-treated cells (Schofield & Schafer, 2021). These findings corroborate the hypothesis that POXAPy induces mitochondrial stress, leading to the activation of compensatory mitophagic mechanisms.

The involvement of mitochondria as a potential cellular target of POXAPy is further supported by mounting evidence from the literature indicating that targeting bioenergetic metabolism with mitochondria-directed agents can trigger mitophagy and suppress tumor cell proliferation (Boyle et al., 2018; Chourasia et al., 2015; Guan et al., 2021; Kulikov et al., 2017). This approach is particularly promising, as mitochondria are emerging as central hubs in oncogenic transformation and therapy resistance, integrating both energetic and signaling functions crucial for tumor progression. Therefore, the observation that POXAPy induces mitochondrial dysfunction and mitophagy supports the hypothesis that mitochondria may represent a preferential and functionally relevant target of its anticancer activity (Zorova et al., 2024).

Given the known propensity of several macrocyclic compounds to interact with nucleic acids and, in particular, with non-canonical DNA secondary structures such as G-quadruplexes (G4), we preliminarily explored whether POXAPy might share this property. G4 structures, which can form in guanine-rich regions of the genome such as oncogene promoters, telomeres, and replication origins, are increasingly considered potential regulatory elements involved in transcription, replication, and genome stability. Their stabilization by small molecules—often referred to as G4 ligands—has been associated with promising anticancer activities, mainly through transcriptional repression of oncogenes such as *MYC*, *KRAS*, and *BCL2* (Andréasson et al., 2022; Monchaud et al., 2010; Teulade-Fichou et al., 2003).

Through cell-free biophysical assays, we observed that POXAPy displays a selective affinity toward specific G4-forming sequences, including the well-characterized G4 motif within the c-MYC

promoter. Although these findings cannot yet establish a definitive mechanism of action, they suggest that POXAPy might, at least in part, interact with these non-canonical structures.

To assess whether such interaction could have biological consequences, we analyzed the effects of POXAPy on MYC expression at both transcript and protein levels. The results showed a dose-dependent downregulation of *MYC*, with a moderate reduction after exposure to the sub-lethal concentration of 10 μM and a marked suppression at 17.5 μM, the lowest dose associated with cytotoxic effects. Specifically, quantitative PCR analysis revealed a decrease in *MYC* mRNA abundance (approximately 0.33-fold at 10 μM and 0.05-fold at 17.5 μM after 24 h), while Western blotting confirmed a parallel reduction in MYC protein levels, particularly evident at the higher concentration.

It is worth noting, however, that transcriptomic and proteomic analyses performed under sub-lethal conditions (10 μM) did not indicate any significant enrichment of MYC-regulated pathways, suggesting that the downregulation of MYC observed at higher concentrations could be part of a secondary or downstream cellular response, rather than a direct consequence of G4 stabilization. Therefore, although the in vitro assays hint at a possible molecular interaction between POXAPy and G4-forming DNA regions, further studies are required to validate whether this binding occurs in the cellular context and whether it contributes to the overall biological effects observed.

In this respect, the hypothesis of a G4-mediated mechanism of action remains an intriguing but speculative interpretation, which might coexist or synergize with other molecular processes—such as mTOR inhibition, ER stress modulation, or mitophagy induction—collectively contributing to the antitumor activity profile of POXAPy.

In a preliminary attempt to validate the interaction between POXAPy and G4-forming sequences within the cellular environment, immunofluorescence (IF) analysis was performed using a specific anti-G4 antibody (clone BG4). However, this approach did not confirm any significant increase in G4 signal in POXAPy-treated cells compared to the untreated control, in contrast to the positive control represented by cells exposed to pyridostatin (PDS, 10 μM), a well-known G4 stabilizer.

This lack of evidence questions the possibility that the G4–POXAPy interaction observed in cell-free conditions effectively occurs in living cells, suggesting that the downregulation of MYC might instead result from the inhibition of upstream signaling pathways found affected by the molecule—namely

the RAF/MEK/ERK and PI3K/AKT/mTOR axes—both of which are known to regulate *MYC* expression at the transcriptional and post-translational levels (Kerkhoff et al., 1998).

Moreover, no clear connection currently links G4 stabilization with the mitophagic process identified in POXAPy-treated NB4 cells. While some recent studies have reported an increase of mitochondrial G4 structures during mitophagy (She et al., 2022; B. Zhang et al., 2024), the evidence that G4-binding molecules could directly trigger mitophagy remains extremely limited (Karatayeva et al., 2025). Thus, it appears more plausible that the mitochondrial alterations and autophagy activation observed upon POXAPy treatment reflect independent or parallel events, possibly driven by metabolic stress and the inhibition of mTOR signaling.

In conclusion, POXAPy-macrocycle exerts a marked biological impact on NB4 cells, as evidenced by its ability to suppress the PI3K/AKT/mTOR and RAF/MEK/ERK signaling pathways and to induce an autophagic/mitophagic response. The ultrastructural and biochemical alterations observed suggest that the mitochondrion represents a major target of POXAPy activity, consistent with the metabolic and signaling perturbations highlighted by the integrated omics analyses.

Although additional studies will be required to clarify the precise molecular mechanisms underlying the observed effects, the results presented here provide a solid rationale for considering POXAPy as a promising anticancer candidate, endowed with the ability to interfere with key regulatory pathways of cell survival and energy homeostasis.

BIBLIOGRAPHY

Ahsan, M. J. (2022). 1,3,4-Oxadiazole Containing Compounds As Therapeutic Targets For Cancer Therapy. *Mini-Reviews in Medicinal Chemistry*, *22*(1), 164–197. https://doi.org/10.2174/1389557521666210226145837

Al-Jumaili, M. H. A., Bakr, E. A., Huessien, M. A., Hamed, A. S., & Muhaidi, M. J. (2025). Development of heterocyclic-based anticancer agents: A comprehensive review. *Heterocyclic Communications*, *31*(1). https://doi.org/10.1515/hc-2022-0179

Amatori, S., Persico, G., Cantatore, F., Rusin, M., Formica, M., Giorgi, L., Macedi, E., Casciaro, F., Errico Provenzano, A., Gambardella, S., Noberini, R., Bonaldi, T., Fusi, V., Giorgio, M., & Fanelli, M. (2023). Small molecule-induced epigenomic reprogramming of APL blasts leading to antiviral-like response and c-MYC downregulation. *Cancer Gene Therapy*, *30*(5), 671–682. https://doi.org/10.1038/s41417-022-00576-w

Ambrosi, G., Fanelli, M., Paoli, P., Formica, M., Paderni, D., Rossi, P., Micheloni, M., Giorgi, L., & Fusi, V. (2020). Zn(II) detection and biological activity of a macrocycle containing a bis(oxadiazole)pyridine derivative as fluorophore. *Dalton Transactions*, *49*(22), 7496–7506. https://doi.org/10.1039/C9DT03910D

Amrhein, J. A., Beyett, T. S., Feng, W. W., Krämer, A., Weckesser, J., Schaeffner, I. K., Rana, J. K., Jänne, P. A., Eck, M. J., Knapp, S., & Hanke, T. (2022). Macrocyclization of Quinazoline-Based EGFR Inhibitors Leads to Exclusive Mutant Selectivity for EGFR L858R and Del19. *Journal of Medicinal Chemistry*, *65*(23), 15679–15697. https://doi.org/10.1021/acs.jmedchem.2c01041

Andréasson, M., Bhuma, N., Pemberton, N., & Chorell, E. (2022). Using Macrocyclic G-Quadruplex Ligands to Decipher the Interactions Between Small Molecules and G-Quadruplex DNA. *Chemistry – A European Journal*, *28*(65). https://doi.org/10.1002/chem.202202020

Bajaj, S., Asati, V., Singh, J., & Roy, P. P. (2015). 1,3,4-Oxadiazoles: An emerging scaffold to target growth factors, enzymes and kinases as anticancer agents. *European Journal of Medicinal Chemistry*, *97*, 124–141. https://doi.org/10.1016/j.ejmech.2015.04.051

Bandara, S., & Raveendran, S. (2025). Current Landscape and Future Directions in Cancer Immunotherapy: Therapies, Trials, and Challenges. *Cancers*, *17*(5), 821. https://doi.org/10.3390/cancers17050821

Bedard, P. L., Hyman, D. M., Davids, M. S., & Siu, L. L. (2020). Small molecules, big impact: 20 years of targeted therapy in oncology. *The Lancet*, *395*(10229), 1078–1088. https://doi.org/10.1016/S0140-6736(20)30164-1

Bispo, J. A. B., Pinheiro, P. S., & Kobetz, E. K. (2020). Epidemiology and Etiology of Leukemia and Lymphoma. *Cold Spring Harbor Perspectives in Medicine*, *10*(6), a034819. https://doi.org/10.1101/cshperspect.a034819

Bizuayehu, H. M., Ahmed, K. Y., Kibret, G. D., Dadi, A. F., Belachew, S. A., Bagade, T., Tegegne, T. K., Venchiarutti, R. L., Kibret, K. T., Hailegebireal, A. H., Assefa, Y., Khan, M. N., Abajobir, A., Alene, K. A., Mengesha, Z., Erku, D., Enquobahrie, D. A., Minas, T. Z., Misgan, E., & Ross, A. G. (2024). Global Disparities of Cancer and Its Projected Burden in 2050. *JAMA Network Open*, *7*(11), e2443198. https://doi.org/10.1001/jamanetworkopen.2024.43198

Bondarev, A. D., Attwood, M. M., Jonsson, J., Chubarev, V. N., Tarasov, V. V., & Schiöth, H. B. (2021). Recent developments of HDAC inhibitors: Emerging indications and novel molecules.

British Journal of Clinical Pharmacology, *87*(12), 4577–4597. https://doi.org/10.1111/bcp.14889

Bonora, B. M., Palano, M. T., Testa, G., Fadini, G. P., Sangalli, E., Madotto, F., Persico, G., Casciaro, F., Vono, R., Colpani, O., Scavello, F., Cappellari, R., Abete, P., Orlando, P., Carnelli, F., Berardi, A. G., De Servi, S., Raucci, A., Giorgio, M., … Spinetti, G. (2022). Hematopoietic progenitor cell liabilities and alarmins S100A8/A9-related inflammaging associate with frailty and predict poor cardiovascular outcomes in older adults. *Aging Cell*, *21*(3). https://doi.org/10.1111/acel.13545

Boström, J., Hogner, A., Llinàs, A., Wellner, E., & Plowright, A. T. (2012). Oxadiazoles in Medicinal Chemistry. *Journal of Medicinal Chemistry*, *55*(5), 1817–1830. https://doi.org/10.1021/jm2013248

Boyle, K. A., Van Wickle, J., Hill, R. B., Marchese, A., Kalyanaraman, B., & Dwinell, M. B. (2018). Mitochondria-targeted drugs stimulate mitophagy and abrogate colon cancer cell proliferation. *Journal of Biological Chemistry*, *293*(38), 14891–14904. https://doi.org/10.1074/jbc.RA117.001469

Bray, F., Laversanne, M., Sung, H., Ferlay, J., Siegel, R. L., Soerjomataram, I., & Jemal, A. (2024). Global cancer statistics 2022: GLOBOCAN estimates of incidence and mortality worldwide for 36 cancers in 185 countries. *CA: A Cancer Journal for Clinicians*, *74*(3), 229–263. https://doi.org/10.3322/caac.21834

Breitman, T., Collins, S., & Keene, B. (1981). Terminal differentiation of human promyelocytic leukemic cells in primary culture in response to retinoic acid. *Blood*, *57*(6), 1000–1004. https://doi.org/10.1182/blood.V57.6.1000.1000

Britten, C. D. (2013). PI3K and MEK inhibitor combinations: examining the evidence in selected tumor types. *Cancer Chemotherapy and Pharmacology*, *71*(6), 1395–1409. https://doi.org/10.1007/s00280-013-2121-1

Chamcheu, J., Roy, T., Uddin, M., Banang-Mbeumi, S., Chamcheu, R.-C., Walker, A., Liu, Y.-Y., & Huang, S. (2019). Role and Therapeutic Targeting of the PI3K/Akt/mTOR Signaling Pathway in Skin Cancer: A Review of Current Status and Future Trends on Natural and Synthetic Agents Therapy. *Cells*, *8*(8), 803. https://doi.org/10.3390/cells8080803

Chen, R., Tsai, J., Thompson, P. A., Chen, Y., Xiong, P., Liu, C., Burrows, F., Sivina, M., Burger, J. A., Keating, M. J., Wierda, W. G., & Plunkett, W. (2021). The multi-kinase inhibitor TG02 induces apoptosis and blocks B-cell receptor signaling in chronic lymphocytic leukemia through dual mechanisms of action. *Blood Cancer Journal*, *11*(3), 57. https://doi.org/10.1038/s41408-021-00436-0

Chen, X., Tsvetkov, A. S., Shen, H.-M., Isidoro, C., Ktistakis, N. T., Linkermann, A., Koopman, W. J. H., Simon, H.-U., Galluzzi, L., Luo, S., Xu, D., Gu, W., Peulen, O., Cai, Q., Rubinsztein, D. C., Chi, J.-T., Zhang, D. D., Li, C., Toyokuni, S., … Tang, D. (2024). International consensus guidelines for the definition, detection, and interpretation of autophagy-dependent ferroptosis. *Autophagy*, *20*(6), 1213–1246. https://doi.org/10.1080/15548627.2024.2319901

Chourasia, A. H., Boland, M. L., & Macleod, K. F. (2015). Mitophagy and cancer. *Cancer & Metabolism*, *3*(1), 4. https://doi.org/10.1186/s40170-015-0130-8

Daltveit, D. S., Morgan, E., Colombet, M., Steliarova-Foucher, E., Bendahhou, K., Marcos-Gragera, R., Rongshou, Z., Smith, A., Wei, H., & Soerjomataram, I. (2025). Global patterns of leukemia

by subtype, age, and sex in 185 countries in 2022. *Leukemia*, *39*(2), 412–419. https://doi.org/10.1038/s41375-024-02452-y

Das, A. (2023). The emerging role of microplastics in systemic toxicity: Involvement of reactive oxygen species (ROS). *Science of The Total Environment*, *895*, 165076. https://doi.org/10.1016/j.scitotenv.2023.165076

de Thé, H., Chomienne, C., Lanotte, M., Degos, L., & Dejean, A. (1990). The t(15;17) translocation of acute promyelocytic leukaemia fuses the retinoic acid receptor α gene to a novel transcribed locus. *Nature*, *347*(6293), 558–561. https://doi.org/10.1038/347558a0

Degan, S. E., & Gelman, I. H. (2021). Emerging Roles for AKT Isoform Preference in Cancer Progression Pathways. *Molecular Cancer Research*, *19*(8), 1251–1257. https://doi.org/10.1158/1541-7786.MCR-20-1066

Dhameliya, T. M., Chudasma, S. J., Patel, T. M., & Dave, B. P. (2022). A review on synthetic account of 1,2,4-oxadiazoles as anti-infective agents. *Molecular Diversity*, *26*(5), 2967–2980. https://doi.org/10.1007/s11030-021-10375-4

Diepstraten, S. T., Yuan, Y., La Marca, J. E., Young, S., Chang, C., Whelan, L., Ross, A. M., Fischer, K. C., Pomilio, G., Morris, R., Georgiou, A., Litalien, V., Brown, F. C., Roberts, A. W., Strasser, A., Wei, A. H., & Kelly, G. L. (2024). Putting the STING back into BH3-mimetic drugs for TP53-mutant blood cancers. *Cancer Cell*, *42*(5), 850-868.e9. https://doi.org/10.1016/j.ccell.2024.04.004

Doria, F., Pirota, V., Petenzi, M., Teulade-Fichou, M.-P., Verga, D., & Freccero, M. (2018). Oxadiazole/Pyridine-Based Ligands: A Structural Tuning for Enhancing G-Quadruplex Binding. *Molecules*, *23*(9), 2162. https://doi.org/10.3390/molecules23092162

Dougherty, P. G., Sahni, A., & Pei, D. (2019). Understanding Cell Penetration of Cyclic Peptides. *Chemical Reviews*, *119*(17), 10241–10287. https://doi.org/10.1021/acs.chemrev.9b00008

Driggers, E. M., Hale, S. P., Lee, J., & Terrett, N. K. (2008). The exploration of macrocycles for drug discovery — an underexploited structural class. *Nature Reviews Drug Discovery*, *7*(7), 608–624. https://doi.org/10.1038/nrd2590

Fairlie DP, Abbenante, G., & March DR. (1994). *Current medicinal chemistry*.

Falchi, L., Ma, H., Klein, S., Lue, J. K., Montanari, F., Marchi, E., Deng, C., Kim, H. A., Rada, A., Jacob, A. T., Kinahan, C., Francescone, M. M., Soderquist, C. R., Park, D. C., Bhagat, G., Nandakumar, R., Menezes, D., Scotto, L., Sokol, L., … O'Connor, O. A. (2021). Combined oral 5-azacytidine and romidepsin are highly effective in patients with PTCL: a multicenter phase 2 study. *Blood*, *137*(16), 2161–2170. https://doi.org/10.1182/blood.2020009004

Fanelli, M., Caprodossi, S., Ricci-Vitiani, L., Porcellini, A., Tomassoni-Ardori, F., Amatori, S., Andreoni, F., Magnani, M., De Maria, R., Santoni, A., Minucci, S., & Pelicci, P. G. (2008). Loss of pericentromeric DNA methylation pattern in human glioblastoma is associated with altered DNA methyltransferases expression and involves the stem cell compartment. *Oncogene*, *27*(3), 358–365. https://doi.org/10.1038/sj.onc.1210642

Fulda, S., & Debatin, K.-M. (2006). Extrinsic versus intrinsic apoptosis pathways in anticancer chemotherapy. *Oncogene*, *25*(34), 4798–4811. https://doi.org/10.1038/sj.onc.1209608

Garcia Jimenez, D., Poongavanam, V., & Kihlberg, J. (2023). Macrocycles in Drug Discovery—Learning from the Past for the Future. *Journal of Medicinal Chemistry*, *66*(8), 5377–5396. https://doi.org/10.1021/acs.jmedchem.3c00134

González, L., Díaz, M. E., Miquet, J. G., Sotelo, A. I., & Dominici, F. P. (2021). Growth Hormone Modulation of Hepatic Epidermal Growth Factor Receptor Signaling. *Trends in Endocrinology & Metabolism*, *32*(6), 403–414. https://doi.org/10.1016/j.tem.2021.03.004

Grignani, F., Ferrucci, P. F., Testa, U., Talamo, G., Fagioli, M., Alcalay, M., Mencarelli, A., Grignani, F., Peschle, C., Nicoletti, I., & Pelicci, P. G. (1993). The acute promyelocytic leukemia-specific PML-RARα fusion protein inhibits differentiation and promotes survival of myeloid precursor cells. *Cell*, *74*(3), 423–431. https://doi.org/10.1016/0092-8674(93)80044-F

Guan, Y., Wang, Y., Li, B., Shen, K., Li, Q., Ni, Y., & Huang, L. (2021). Mitophagy in carcinogenesis, drug resistance and anticancer therapeutics. *Cancer Cell International*, *21*(1), 350. https://doi.org/10.1186/s12935-021-02065-w

Gubas, A., & Dikic, I. (2022). A guide to the regulation of selective autophagy receptors. *The FEBS Journal*, *289*(1), 75–89. https://doi.org/10.1111/febs.15824

Gupta, A. A., Xue, W., Harrison, D. J., Hawkins, D. S., Dasgupta, R., Wolden, S., Shulkin, B., Qumseya, A., Routh, J. C., MacDonald, T., Feinberg, S., Crompton, B., Rudzinski, E. R., Arnold, M., & Venkatramani, R. (2024). Addition of temsirolimus to chemotherapy in children, adolescents, and young adults with intermediate-risk rhabdomyosarcoma (ARST1431): a randomised, open-label, phase 3 trial from the Children's Oncology Group. *The Lancet Oncology*, *25*(7), 912–921. https://doi.org/10.1016/S1470-2045(24)00255-9

Hajdu, S. I. (2005). 2000 years of chemotherapy of tumors. *Cancer*, *103*(6), 1097–1102. https://doi.org/10.1002/cncr.20908

Hamad, H. T. (2025). The anti-cancer effectiveness of some heterocyclic compounds containing sulfur atom. *Results in Chemistry*, *15*, 102182. https://doi.org/10.1016/j.rechem.2025.102182

Hamilton-Miller, J. M. (1973). Chemistry and biology of the polyene macrolide antibiotics. *Bacteriological Reviews*, *37*(2), 166–196. https://doi.org/10.1128/br.37.2.166-196.1973

Hanahan, D. (2022). Hallmarks of Cancer: New Dimensions. *Cancer Discovery*, *12*(1), 31–46. https://doi.org/10.1158/2159-8290.CD-21-1059

Hanahan, D., & Weinberg, R. A. (2011). Hallmarks of Cancer: The Next Generation. *Cell*, *144*(5), 646–674. https://doi.org/10.1016/j.cell.2011.02.013

Hart, S., Goh, K. C., Novotny-Diermayr, V., Tan, Y. C., Madan, B., Amalini, C., Ong, L. C., Kheng, B., Cheong, A., Zhou, J., Chng, W. J., & Wood, J. M. (2011). Pacritinib (SB1518), a JAK2/FLT3 inhibitor for the treatment of acute myeloid leukemia. *Blood Cancer Journal*, *1*(11), e44–e44. https://doi.org/10.1038/bcj.2011.43

Hou, Y., Gan, T., Fang, T., Zhao, Y., Luo, Q., Liu, X., Qi, L., Zhang, Y., Jia, F., Han, J., Li, S., Wang, S., & Wang, F. (2022). G-quadruplex inducer/stabilizer pyridostatin targets SUB1 to promote cytotoxicity of a transplatinum complex. *Nucleic Acids Research*, *50*(6), 3070–3082. https://doi.org/10.1093/nar/gkac151

Ireson, C. R., & Kelland, L. R. (2006). Discovery and development of anticancer aptamers. *Molecular Cancer Therapeutics*, *5*(12), 2957–2962. https://doi.org/10.1158/1535-7163.MCT-06-0172

Juan, C. A., Pérez de la Lastra, J. M., Plou, F. J., & Pérez-Lebeña, E. (2021). The Chemistry of Reactive Oxygen Species (ROS) Revisited: Outlining Their Role in Biological Macromolecules (DNA, Lipids and Proteins) and Induced Pathologies. *International Journal of Molecular Sciences*, *22*(9), 4642. https://doi.org/10.3390/ijms22094642

Kansal, R. (2025). Research Progress in Hematological Malignancies: A Molecular Genetics Perspective. *Genes*, *16*(6), 663. https://doi.org/10.3390/genes16060663

Karami Fath, M., Akhavan Masouleh, R., Afifi, N., Loghmani, S., Tamimi, P., Fazeli, A., Mousavian, S. A., Falsafi, M. M., & Barati, G. (2023). PI3K/AKT/mTOR signaling pathway modulation by circular RNAs in breast cancer progression. *Pathology - Research and Practice*, *241*, 154279. https://doi.org/10.1016/j.prp.2022.154279

Karatayeva, N., Hegedus, L., Bhattacharjee, A., Nemeth, E., Poti, A., Pongor, L., Juhasz, G., Szuts, D., & Burkovics, P. (2025). The effect of prolonged G-quadruplex stabilization on the functions of human cells. *Scientific Reports*, *15*(1), 19699. https://doi.org/10.1038/s41598-025-04791-x

Karati, D., Mahadik, K. R., Trivedi, P., & Kumar, D. (2022). Alkylating Agents, the Road Less Traversed, Changing Anticancer Therapy. *Anti-Cancer Agents in Medicinal Chemistry*, *22*(8), 1478–1495. https://doi.org/10.2174/1871520621666210811105344

Kerkhoff, E., Houben, R., Löffler, S., Troppmair, J., Lee, J.-E., & Rapp, U. R. (1998). Regulation of c-myc expression by Ras/Raf signalling. *Oncogene*, *16*(2), 211–216. https://doi.org/10.1038/sj.onc.1201520

Khadka, D. B., & Cho, W.-J. (2013). Topoisomerase inhibitors as anticancer agents: a patent update. *Expert Opinion on Therapeutic Patents*, *23*(8), 1033–1056. https://doi.org/10.1517/13543776.2013.790958

Khan, I., Ibrar, A., & Abbas, N. (2014). Oxadiazoles as Privileged Motifs for Promising Anticancer Leads: Recent Advances and Future Prospects. *Archiv Der Pharmazie*, *347*(1), 1–20. https://doi.org/10.1002/ardp.201300231

Kulikov, A. V., Luchkina, E. A., Gogvadze, V., & Zhivotovsky, B. (2017). Mitophagy: Link to cancer development and therapy. *Biochemical and Biophysical Research Communications*, *482*(3), 432–439. https://doi.org/10.1016/j.bbrc.2016.10.088

Kumar, G., Kumar, R., Mazumder, A., Salahuddin, & Kumar, U. (2024). 1,3,4-Oxadiazoles as Anticancer Agents: A Review. *Recent Patents on Anti-Cancer Drug Discovery*, *19*(3), 257–267. https://doi.org/10.2174/1574892818666230727102928

Kumar, V., Swati, & Wadhwa, P. (2025). Oxadiazole Derivatives as Multifunctional Anticancer Agents: Targeting EGFR, PI3K/Akt/mTOR, and p53 Pathways for Enhanced Therapeutic Efficacy. *ChemistrySelect*, *10*(33). https://doi.org/10.1002/slct.202500899

Lamb, Y. N. (2022). Pacritinib: First Approval. *Drugs*, *82*(7), 831–838. https://doi.org/10.1007/s40265-022-01718-y

Langer, R., Neppl, C., Keller, M. D., Schmid, R. A., Tschan, M. P., & Berezowska, S. (2018). Expression Analysis of Autophagy Related Markers LC3B, p62 and HMGB1 Indicate an Autophagy-Independent Negative Prognostic Impact of High p62 Expression in Pulmonary Squamous Cell Carcinomas. *Cancers*, *10*(9), 281. https://doi.org/10.3390/cancers10090281

Le Rhun, E., Bertrand, N., Dumont, A., Tresch, E., Le Deley, M.-C., Mailliez, A., Preusser, M., Weller, M., Revillion, F., & Bonneterre, J. (2017). Identification of single nucleotide polymorphisms of

the PI3K-AKT-mTOR pathway as a risk factor of central nervous system metastasis in metastatic breast cancer. *European Journal of Cancer*, *87*, 189–198. https://doi.org/10.1016/j.ejca.2017.10.006

Lee, S., & Schmitt, C. A. (2019). The dynamic nature of senescence in cancer. *Nature Cell Biology*, *21*(1), 94–101. https://doi.org/10.1038/s41556-018-0249-2

Lee, S., Son, J.-Y., Lee, J., & Cheong, H. (2023). Unraveling the Intricacies of Autophagy and Mitophagy: Implications in Cancer Biology. *Cells*, *12*(23), 2742. https://doi.org/10.3390/cells12232742

Li, Q., Li, Z., Luo, T., & Shi, H. (2022). Targeting the PI3K/AKT/mTOR and RAF/MEK/ERK pathways for cancer therapy. *Molecular Biomedicine*, *3*(1), 47. https://doi.org/10.1186/s43556-022-00110-2

Liang, C., Qiao, G., Liu, Y., Tian, L., Hui, N., Li, J., Ma, Y., Li, H., Zhao, Q., Cao, W., Liu, H., & Ren, X. (2021). Overview of all-trans-retinoic acid (ATRA) and its analogues: Structures, activities, and mechanisms in acute promyelocytic leukaemia. *European Journal of Medicinal Chemistry*, *220*, 113451. https://doi.org/10.1016/j.ejmech.2021.113451

Liu, L., Li, Y., Chen, G., & Chen, Q. (2023). Crosstalk between mitochondrial biogenesis and mitophagy to maintain mitochondrial homeostasis. *Journal of Biomedical Science*, *30*(1), 86. https://doi.org/10.1186/s12929-023-00975-7

Liu, Y., & Zheng, Z. (2024). Understanding the global cancer statistics 2022: growing cancer burden. *Science China Life Sciences*, *67*(10), 2274–2276. https://doi.org/10.1007/s11427-024-2657-y

London, M., & Gallo, E. (2020). Epidermal growth factor receptor (EGFR) involvement in epithelial-derived cancers and its current antibody-based immunotherapies. *Cell Biology International*, *44*(6), 1267–1282. https://doi.org/10.1002/cbin.11340

Lucke-Wold, B., Rangwala, B. S., Shafique, M. A., Siddiq, M. A., Mustafa, M. S., Danish, F., Nasrullah, R. M. U., Zainab, N., & Haseeb, A. (2024). Focus on current and emerging treatment options for glioma: A comprehensive review. *World Journal of Clinical Oncology*, *15*(4), 482–495. https://doi.org/10.5306/wjco.v15.i4.482

Ma, Y., Jin, Z., Yu, K., & Liu, Q. (2019). NVP-BEZ235-induced autophagy as a potential therapeutic approach for multiple myeloma. *American Journal of Translational Research*, *11*(1), 87–105.

Mallinson, J., & Collins, I. (2012). Macrocycles In New Drug Discovery. *Future Medicinal Chemistry*, *4*(11), 1409–1438. https://doi.org/10.4155/fmc.12.93

Marsault, E., & Peterson, M. L. (2011). Macrocycles Are Great Cycles: Applications, Opportunities, and Challenges of Synthetic Macrocycles in Drug Discovery. *Journal of Medicinal Chemistry*, *54*(7), 1961–2004. https://doi.org/10.1021/jm1012374

Mascarenhas, J. (2022). Pacritinib for the treatment of patients with myelofibrosis and thrombocytopenia. *Expert Review of Hematology*, *15*(8), 671–684. https://doi.org/10.1080/17474086.2022.2112565

Mc Neil, V., & Lee, S. W. (2025). Advancing Cancer Treatment: A Review of Immune Checkpoint Inhibitors and Combination Strategies. *Cancers*, *17*(9), 1408. https://doi.org/10.3390/cancers17091408

McCubrey, J. A., Steelman, L. S., Abrams, S. L., Lee, J. T., Chang, F., Bertrand, F. E., Navolanic, P. M., Terrian, D. M., Franklin, R. A., D'Assoro, A. B., Salisbury, J. L., Mazzarino, M. C., Stivala,

F., & Libra, M. (2006). Roles of the RAF/MEK/ERK and PI3K/PTEN/AKT pathways in malignant transformation and drug resistance. *Advances in Enzyme Regulation*, *46*(1), 249–279. https://doi.org/10.1016/j.advenzreg.2006.01.004

Minami, M., Sakoda, T., Kawano, G., Kochi, Y., Sasaki, K., Sugio, T., Jinnouchi, F., Miyawaki, K., Kunisaki, Y., Kato, K., Miyamoto, T., Akashi, K., & Kikushige, Y. (2025). Distinct leukemogenic mechanism of acute promyelocytic leukemia based on genomic structure of PML::RARα. *Leukemia*, *39*(4), 844–853. https://doi.org/10.1038/s41375-025-02530-9

Miranda-Filho, A., Piñeros, M., Ferlay, J., Soerjomataram, I., Monnereau, A., & Bray, F. (2018). Epidemiological patterns of leukaemia in 184 countries: a population-based study. *The Lancet Haematology*, *5*(1), e14–e24. https://doi.org/10.1016/S2352-3026(17)30232-6

Mishra, A. K., Ali, A., Dutta, S., Banday, S., & Malonia, S. K. (2022). Emerging Trends in Immunotherapy for Cancer. *Diseases*, *10*(3), 60. https://doi.org/10.3390/diseases10030060

Mitchell, R., Hopcroft, L. E. M., Baquero, P., Allan, E. K., Hewit, K., James, D., Hamilton, G., Mukhopadhyay, A., O'Prey, J., Hair, A., Melo, J. V, Chan, E., Ryan, K. M., Maguer-Satta, V., Druker, B. J., Clark, R. E., Mitra, S., Herzyk, P., Nicolini, F. E., … Helgason, G. V. (2018). Targeting BCR-ABL-Independent TKI Resistance in Chronic Myeloid Leukemia by mTOR and Autophagy Inhibition. *JNCI: Journal of the National Cancer Institute*, *110*(5), 467–478. https://doi.org/10.1093/jnci/djx236

Monchaud, D., Granzhan, A., Saettel, N., Guédin, A., Mergny, J.-L., & Teulade-Fichou, M.-P. (2010). "One Ring to Bind Them All"—Part I: The Efficiency of the Macrocyclic Scaffold for G-Quadruplex DNA Recognition. *Journal of Nucleic Acids*, *2010*(1). https://doi.org/10.4061/2010/525862

Mortensen, K. T., Osberger, T. J., King, T. A., Sore, H. F., & Spring, D. R. (2019). Strategies for the Diversity-Oriented Synthesis of Macrocycles. *Chemical Reviews*, *119*(17), 10288–10317. https://doi.org/10.1021/acs.chemrev.9b00084

Negi, B., & Kwatra, A. (2024). A Review of Recent Progress on the Anticancer Activity of Heterocyclic Compounds. *SynOpen*, *08*(03), 185–210. https://doi.org/10.1055/s-0040-1720125

Okumura, S., Konishi, Y., Narukawa, M., Sugiura, Y., Yoshimoto, S., Arai, Y., Sato, S., Yoshida, Y., Tsuji, S., Uemura, K., Wakita, M., Matsudaira, T., Matsumoto, T., Kawamoto, S., Takahashi, A., Itatani, Y., Miki, H., Takamatsu, M., Obama, K., … Hara, E. (2021). Gut bacteria identified in colorectal cancer patients promote tumourigenesis via butyrate secretion. *Nature Communications*, *12*(1), 5674. https://doi.org/10.1038/s41467-021-25965-x

Onishi, M., Yamano, K., Sato, M., Matsuda, N., & Okamoto, K. (2021). Molecular mechanisms and physiological functions of mitophagy. *The EMBO Journal*, *40*(3). https://doi.org/10.15252/embj.2020104705

Onorati, A. V., Dyczynski, M., Ojha, R., & Amaravadi, R. K. (2018). Targeting autophagy in cancer. *Cancer*, *124*(16), 3307–3318. https://doi.org/10.1002/cncr.31335

Oybek Kizi, R. F., Theodore Armand, T. P., & Kim, H.-C. (2025). A Review of Deep Learning Techniques for Leukemia Cancer Classification Based on Blood Smear Images. *Applied Biosciences*, *4*(1), 9. https://doi.org/10.3390/applbiosci4010009

Palombo, R., Passacantilli, I., Terracciano, F., Capone, A., Matteocci, A., Tournier, S., Alberdi, A., Chiurchiù, V., Volpe, E., & Paronetto, M. P. (2023). Inhibition of the PI3K/AKT/mTOR

signaling promotes an M1 macrophage switch by repressing the ATF3-CXCL8 axis in Ewing sarcoma. *Cancer Letters*, *555*, 216042. https://doi.org/10.1016/j.canlet.2022.216042

Parker, W. B. (2009). Enzymology of Purine and Pyrimidine Antimetabolites Used in the Treatment of Cancer. *Chemical Reviews*, *109*(7), 2880–2893. https://doi.org/10.1021/cr900028p

Pojani, E., & Barlocco, D. (2021). Romidepsin (FK228), A Histone Deacetylase Inhibitor and its Analogues in Cancer Chemotherapy. *Current Medicinal Chemistry*, *28*(7), 1290–1303. https://doi.org/10.2174/0929867327666200203113926

Pomeislová, A., Vrzal, L., Kozák, J., Dobiaš, J., Hubálek, M., Dvořáková, H., Reyes-Gutiérrez, P. E., Teplý, F., & Veverka, V. (2020). Kinetic Target-Guided Synthesis of Small-Molecule G-Quadruplex Stabilizers. *ChemistryOpen*, *9*(12), 1236–1250. https://doi.org/10.1002/open.202000261

Rajendran, P., Sekar, R., Dhayasankar, P. S., Ali, E. M., Abdelsalam, S. A., Balaraman, S., Chellappan, B. V., Metwally, A. M., & Abdallah, B. M. (2024). PI3K/AKT Signaling Pathway Mediated Autophagy in Oral Carcinoma - A Comprehensive Review. *International Journal of Medical Sciences*, *21*(6), 1165–1175. https://doi.org/10.7150/ijms.94566

Rehman, U.-U., & Lübbert, M. (2025). All-trans retinoic acid beyond acute promyelocytic leukemia. *Cancer Cell*, *43*(6), 998–1000. https://doi.org/10.1016/j.ccell.2025.03.008

Riccardi, C., & Nicoletti, I. (2006). Analysis of apoptosis by propidium iodide staining and flow cytometry. *Nature Protocols*, *1*(3), 1458–1461. https://doi.org/10.1038/nprot.2006.238

Rodriguez, R., Müller, S., Yeoman, J. A., Trentesaux, C., Riou, J.-F., & Balasubramanian, S. (2008). A Novel Small Molecule That Alters Shelterin Integrity and Triggers a DNA-Damage Response at Telomeres. *Journal of the American Chemical Society*, *130*(47), 15758–15759. https://doi.org/10.1021/ja805615w

Salahuddin, Mazumder, A., Yar, M. S., Mazumder, R., Chakraborthy, G. S., Ahsan, M. J., & Rahman, M. U. (2017). Updates on synthesis and biological activities of 1,3,4-oxadiazole: A review. *Synthetic Communications*, *47*(20), 1805–1847. https://doi.org/10.1080/00397911.2017.1360911

Salassa, G., & Terenzi, A. (2019). Metal Complexes of Oxadiazole Ligands: An Overview. *International Journal of Molecular Sciences*, *20*(14), 3483. https://doi.org/10.3390/ijms20143483

SchlÃ¤fli, A. M., Berezowska, S., Adams, O., Langer, R., & Tschan, M. P. (2015). Reliable LC3 and p62 autophagy marker detection in formalin fixed paraffin embedded human tissue by immunohistochemistry. *European Journal of Histochemistry*, *59*(2). https://doi.org/10.4081/ejh.2015.2481

Schofield, J. H., & Schafer, Z. T. (2021). Mitochondrial Reactive Oxygen Species and Mitophagy: A Complex and Nuanced Relationship. *Antioxidants & Redox Signaling*, *34*(7), 517–530. https://doi.org/10.1089/ars.2020.8058

Senft, D., & Ronai, Z. A. (2015). UPR, autophagy, and mitochondria crosstalk underlies the ER stress response. *Trends in Biochemical Sciences*, *40*(3), 141–148. https://doi.org/10.1016/j.tibs.2015.01.002

Sethi G, Ashrafizadeh M, & Ebrahimi N. (2024). *Prostate Cancer: Molecular Events and Therapeutic Modalities* (G. Sethi, M. Ashrafizadeh, & N. Ebrahimi, Eds.). Springer Nature Singapore. https://doi.org/10.1007/978-981-97-4612-5

Sharma, D., Salahuddin, Sharma, V., Kumar, R., Joshi, S., Kumari, S., Saxena, S., Mazumder, A., Yar, M. S., & Ahsan, M. J. (2021). 1,3,4-Oxadiazoles as Potential Pharmacophore for Cytotoxic Potentiality: A Comprehensive Review. *Current Topics in Medicinal Chemistry*, *21*(15), 1377–1397. https://doi.org/10.2174/1568026621666210612031144

She, M.-T., Yang, J.-W., Zheng, B.-X., Long, W., Huang, X.-H., Luo, J.-R., Chen, Z.-X., Liu, A.-L., Cai, D.-P., Wong, W.-L., & Lu, Y.-J. (2022). Design mitochondria-specific fluorescent turn-on probes targeting G-quadruplexes for live cell imaging and mitophagy monitoring study. *Chemical Engineering Journal*, *446*, 136947. https://doi.org/10.1016/j.cej.2022.136947

Shi, Y., Fu, Y., Zhang, X., Zhao, G., Yao, Y., Guo, Y., Ma, G., Bai, S., & Li, H. (2021). Romidepsin (FK228) regulates the expression of the immune checkpoint ligand PD-L1 and suppresses cellular immune functions in colon cancer. *Cancer Immunology, Immunotherapy*, *70*(1), 61–73. https://doi.org/10.1007/s00262-020-02653-1

Song, X., Wu, Y., Qu, X., & Jiang, B. (2023). Applications of macrocyclic molecules in cancer therapy: Target cancer development or overcome drug resistance. *MedComm – Oncology*, *2*(3). https://doi.org/10.1002/mog2.50

Soto-Avellaneda, A., & Morrison, B. E. (2020). Signaling and other functions of lipids in autophagy: a review. *Lipids in Health and Disease*, *19*(1), 214. https://doi.org/10.1186/s12944-020-01389-2

Sung, H., Ferlay, J., Siegel, R. L., Laversanne, M., Soerjomataram, I., Jemal, A., & Bray, F. (2021). Global Cancer Statistics 2020: GLOBOCAN Estimates of Incidence and Mortality Worldwide for 36 Cancers in 185 Countries. *CA: A Cancer Journal for Clinicians*, *71*(3), 209–249. https://doi.org/10.3322/caac.21660

Swords, R. T., Schenk, T., Stengel, S., Gil, V. S., Petrie, K. R., Perez, A., Ana, R., Watts, J. M., Vargas, F., Elias, R., & Zelent, A. (2015). Inhibition of the PI3K/AKT/mTOR Pathway Leads to Down-Regulation of c-Myc and Overcomes Resistance to ATRA in Acute Myeloid Leukemia. *Blood*, *126*(23), 1363–1363. https://doi.org/10.1182/blood.V126.23.1363.1363

Testa, U., & Pelosi, E. (2024). *Function of PML-RARA in Acute Promyelocytic Leukemia* (pp. 321–339). https://doi.org/10.1007/978-3-031-62731-6_14

Teulade-Fichou, M.-P., Carrasco, C., Guittat, L., Bailly, C., Alberti, P., Mergny, J.-L., David, A., Lehn, J.-M., & Wilson, W. D. (2003). Selective Recognition of G-Quadruplex Telomeric DNA by a Bis(quinacridine) Macrocycle. *Journal of the American Chemical Society*, *125*(16), 4732–4740. https://doi.org/10.1021/ja021299j

Trallero, J., Sanvisens, A., Almela Vich, F., Jeghalef El Karoni, N., Saez Lloret, I., Díaz-del-Campo, C., Marcos-Navarro, A. I., Aizpurua Atxega, A., Sancho Uriarte, P., De-la-Cruz Ortega, M., Sánchez, M. J., Perucha, J., Franch, P., Chirlaque, M. D., Guevara, M., Ameijide, A., Galceran, J., Ramírez, C., Camblor, M. R., … Marcos-Gragera, R. (2023). Incidence and time trends of childhood hematological neoplasms: a 36-year population-based study in the southern European context, 1983–2018. *Frontiers in Oncology*, *13*. https://doi.org/10.3389/fonc.2023.1197850

Urruticoechea, A., Alemany, R., Balart, J., Villanueva, A., Vinals, F., & Capella, G. (2010). Recent Advances in Cancer Therapy: An Overview. *Current Pharmaceutical Design*, *16*(1), 3–10. https://doi.org/10.2174/138161210789941847

Vaidya, A., Jain, S., Jain, P., Jain, P., Tiwari, N., Jain, R., Jain, R., K. Jain, A., & K. Agrawal, R. (2016). Synthesis and Biological Activities of Oxadiazole Derivatives: A Review. *Mini-Reviews in Medicinal Chemistry*, *16*(10), 825–845. https://doi.org/10.2174/1389557516666160211120835

Vaidya, A., Pathak, D., & Shah, K. (2021). 1,3,4-oxadiazole and its derivatives: A review on recent progress in anticancer activities. *Chemical Biology & Drug Design*, *97*(3), 572–591. https://doi.org/10.1111/cbdd.13795

Wagner, A. J., Ravi, V., Riedel, R. F., Ganjoo, K., Van Tine, B. A., Chugh, R., Cranmer, L., Gordon, E. M., Hornick, J. L., Du, H., Grigorian, B., Schmid, A. N., Hou, S., Harris, K., Kwiatkowski, D. J., Desai, N. P., & Dickson, M. A. (2021). *nab* -Sirolimus for Patients With Malignant Perivascular Epithelioid Cell Tumors. *Journal of Clinical Oncology*, *39*(33), 3660–3670. https://doi.org/10.1200/JCO.21.01728

Washington, J. A., & Wilson, W. R. (1985). Erythromycin: A Microbial and Clinical Perspective After 30 Years of Clinical Use (Second of Two Parts). *Mayo Clinic Proceedings*, *60*(4), 271–278. https://doi.org/10.1016/S0025-6196(12)60322-X

Westin, G. F., Perez, C. A., Wang, E., & Glück, S. (2013). Biologic Impact and Clinical Implication of mTOR Inhibition in Metastatic Breast Cancer. *The International Journal of Biological Markers*, *28*(3), 233–241. https://doi.org/10.5301/JBM.5000040

Whiteley, A. E., Price, T. T., Cantelli, G., & Sipkins, D. A. (2021). Leukaemia: a model metastatic disease. *Nature Reviews Cancer*, *21*(7), 461–475. https://doi.org/10.1038/s41568-021-00355-z

Wu, P., & Hu, Y.-Z. (2010). PI3K/Akt/mTOR Pathway Inhibitors in Cancer: A Perspective on Clinical Progress. *Current Medicinal Chemistry*, *17*(35), 4326–4341. https://doi.org/10.2174/092986710793361234

Wu, S., Powers, S., Zhu, W., & Hannun, Y. A. (2016). Substantial contribution of extrinsic risk factors to cancer development. *Nature*, *529*(7584), 43–47. https://doi.org/10.1038/nature16166

Wu, W., Wu, M.-Y., Dai, T., Ke, L.-N., Shi, Y., Hu, J., & Wang, Q. (2024). Terphenyllin induces CASP3-dependent apoptosis and pyroptosis in A375 cells through upregulation of p53. *Cell Communication and Signaling*, *22*(1), 409. https://doi.org/10.1186/s12964-024-01784-7

Xiao, W., Nardi, V., Stein, E., & Hasserjian, R. P. (2024). A practical approach on the classifications of myeloid neoplasms and acute leukemia: WHO and ICC. *Journal of Hematology & Oncology*, *17*(1), 56. https://doi.org/10.1186/s13045-024-01571-4

Yanada, M. (2024). Leucocytosis during all- *trans* retinoic acid and arsenic trioxide treatment in acute promyelocytic leukaemia. *British Journal of Haematology*, *205*(5), 1672–1673. https://doi.org/10.1111/bjh.19763

Yudin, A. K. (2015). Macrocycles: lessons from the distant past, recent developments, and future directions. *Chemical Science*, *6*(1), 30–49. https://doi.org/10.1039/C4SC03089C

Zafar, A., Khatoon, S., Khan, M. J., Abu, J., & Naeem, A. (2025). Advancements and limitations in traditional anti-cancer therapies: a comprehensive review of surgery, chemotherapy, radiation

therapy, and hormonal therapy. *Discover Oncology*, *16*(1), 607. https://doi.org/10.1007/s12672-025-02198-8

Zhang, B., Sun, R., Bai, R., Sun, Z., Liu, R., Li, W., Yao, L., Sun, H., & Tang, Y. (2024). G-quadruplex in mitochondria as a possible biomarker for mitophagy detection. *International Journal of Biological Macromolecules*, *259*, 129337. https://doi.org/10.1016/j.ijbiomac.2024.129337

Zhang, J., Xiang, Q., Wu, M., Lao, Y.-Z., Xian, Y.-F., Xu, H.-X., & Lin, Z.-X. (2023). Autophagy Regulators in Cancer. *International Journal of Molecular Sciences*, *24*(13), 10944. https://doi.org/10.3390/ijms241310944

Zhang, M., Wang, J., Guo, Y., Yue, H., & Zhang, L. (2023). Activation of PI3K/AKT/mTOR signaling axis by UBE2S inhibits autophagy leading to cisplatin resistance in ovarian cancer. *Journal of Ovarian Research*, *16*(1), 240. https://doi.org/10.1186/s13048-023-01314-y

Zhao, X., Ma, D., Yang, B., Wang, Y., & Zhang, L. (2024). Research progress of T cell autophagy in autoimmune diseases. *Frontiers in Immunology*, *15*. https://doi.org/10.3389/fimmu.2024.1425443

Zhong, L., Li, Y., Xiong, L., Wang, W., Wu, M., Yuan, T., Yang, W., Tian, C., Miao, Z., Wang, T., & Yang, S. (2021). Small molecules in targeted cancer therapy: advances, challenges, and future perspectives. *Signal Transduction and Targeted Therapy*, *6*(1), 201. https://doi.org/10.1038/s41392-021-00572-w

Zorova, L. D., Abramicheva, P. A., Andrianova, N. V., Babenko, V. A., Zorov, S. D., Pevzner, I. B., Popkov, V. A., Semenovich, D. S., Yakupova, E. I., Silachev, D. N., Plotnikov, E. Y., Sukhikh, G. T., & Zorov, D. B. (2024). Targeting Mitochondria for Cancer Treatment. *Pharmaceutics*, *16*(4), 444. https://doi.org/10.3390/pharmaceutics16040444